MICROCOPY RESOLUTION TEST CHART

AD-A179 608

## REPORT DOCUMENTATION PAGE

| 1a. REPORT SECURITY CLASSIFICATION | 1b. RESTRICTIVE MARKINGS |
|---|---|
| UNCLASSIFIED | N/A |
| 2a. SECURITY CLASSIFICATION AUTHORITY | 3. DISTRIBUTION/AVAILABILITY OF REPORT |
| N/A | Approved for public release; |
| 2b. DECLASSIFICATION/DOWNGRADING SCHEDULE | distribution unlimited |
| N/A | |

| 4. PERFORMING ORGANIZATION REPORT NUMBER(S) | 5. MONITORING ORGANIZATION REPORT NUMBER(S) |
|---|---|
| CAR-TR-254 | |
| CS-TR-1759 | N/A |

| 6a. NAME OF PERFORMING ORGANIZATION | 6b. OFFICE SYMBOL (If applicable) | 7a. NAME OF MONITORING ORGANIZATION |
|---|---|---|
| University of Maryland | N/A | Defense Mapping Agency |

| 6c. ADDRESS (City, State and ZIP Code) | 7b. ADDRESS (City, State and ZIP Code) |
|---|---|
| Center for Automation Research | DMA SPOEM TID, ATTN: W. Alford |
| College Park, MD 20742-3411 | 8301 Greensboro Dr., Suite 800 |
| | McLean, VA 22102-3692 |

| 8a. NAME OF FUNDING/SPONSORING ORGANIZATION | 8b. OFFICE SYMBOL (If applicable) | 9. PROCUREMENT INSTRUMENT IDENTIFICATION NUMBER |
|---|---|---|
| N/A | N/A | DMA800-85-C-0007 |

| 8c. ADDRESS (City, State and ZIP Code) | 10. SOURCE OF FUNDING NOS. | | | |
|---|---|---|---|---|
| | PROGRAM ELEMENT NO. | PROJECT NO. | TASK NO. | WORK UNIT NO. |
| N/A | | | | |

11. TITLE (Include Security Classification)

Mask Matching for Linear Feature Detection

12. PERSONAL AUTHOR(S)

Nathan S. Netanyahu and Azriel Rosenfeld

| 13a. TYPE OF REPORT | 13b. TIME COVERED | 14. DATE OF REPORT (Yr., Mo., Day) | 15. PAGE COUNT |
|---|---|---|---|
| Technical | FROM _____ TO N/A | January 1987 | 78 |

16. SUPPLEMENTARY NOTATION

| 17. | COSATI CODES | | 18. SUBJECT TERMS (Continue on reverse if necessary and identify by block number) |
|---|---|---|---|
| FIELD | GROUP | SUB. GR. | |
| | | | |
| | | | |

19. ABSTRACT (Continue on reverse if necessary and identify by block number)

This paper describes a set of masks that can be used in extracting thin linear features from images. A probabilistic analysis of mask matching for "white noise" images is given, and results of some experimental studies are also presented.

DTIC
ELECTE
S
APR 21 1987
D
E

| 20. DISTRIBUTION/AVAILABILITY OF ABSTRACT | 21. ABSTRACT SECURITY CLASSIFICATION |
|---|---|
| UNCLASSIFIED/UNLIMITED ☒ SAME AS RPT. ☐ DTIC USERS ☐ | UNCLASSIFIED |

| 22a. NAME OF RESPONSIBLE INDIVIDUAL | 22b. TELEPHONE NUMBER (Include Area Code) | 22c. OFFICE SYMBOL |
|---|---|---|
| | | |

**DD FORM 1473, 83 APR**  EDITION OF 1 JAN 73 IS OBSOLETE.  **UNCLASSIFIED**

CAR-TR-254
CS-TR-1759

DMA800-85-C-0007
January 1987

# MASK MATCHING FOR
# LINEAR FEATURE DETECTION

Nathan S. Netanyahu
Azriel Rosenfeld

Computer Vision Laboratory
Center for Automation Research
University of Maryland
College Park, MD. 20742

## ABSTRACT

This paper describes a set of masks that can be used in extracting thin linear features from images. A probabilistic analysis of mask matching for "white noise" images is given, and results of some experimental studies are also presented.

Accession For

| NTIS GRA&I | X |
| DTIC TAB | |
| Unannounced | |
| Justification | |

QUALITY
INSPECTED
1

By

Distribution/

Availability Codes

| Dist | Avail and/or Special |
| A-1 | |

87 1759

## 1. Introduction

Mask matching is a well known procedure [1] in which the detection of specific features in an image is carried out by matching a set of templates or "masks" with the neighborhood of each pixel in the image.

This paper describes a set of $3 \times 3$ binary masks that can be used to extract linear features from an image. The masks are used to assign various labels to each pixel (each label corresponding to a particular mask), and to associate with each label a set of confidence measures based on the homogeneity of the foreground and background in the mask, and the difference between them. The idea of this approach is to record a large set of useful information at the pixel level, in order to efficiently make use of it at the later stages of the linear feature detection process.

In Section 2, we introduce the set of masks and the confidence measures. In Section 3, the data structures and the algorithm used for the implementation of the masks are discussed.

Section 4 contains empirical results obtained by applying the masks to several image samples. The principal conclusion drawn from these results is that it is difficult to decide which matched masks are part of a linear feature by simple thresholding of the confidence measures. However, it is shown in a companion report [2] that by using compatibility relations between masks at neighboring pixels, good linear feature extraction performance can be obtained.

1

Section 5 gives a probabilistic analysis of the frequency of matches and their expected "robustness" for specific masks and classes of masks in "white noise" images. These results may help indicate whether or not a given image region should be considered "interesting", as regards frequency of occurrence of "line-like" masks, for example.

## 2. The Masks and the Confidence Measures

### 2.1. Preliminary Remarks

By applying "mask matching" to an image, we mean finding those $N \times N$ image neighborhoods that match specific masks. The matching procedure is described later in more detail, but basically, matching occurs when there exists a threshold dividing the $N^2$ pixels into two groups, called dark and bright, such that the pattern of black and white pixels is exactly the same as a given mask.

Our goal is to extract "thin" linear features (1-2 pixels wide) from an image. For this task, masks having $N = 1$ or $N = 2$ are obviously too small. On the other hand, higher values of N result in much too large a set of masks. $N = 5$, for example, implies a set of $2^{25} = 32M$ possible binary masks, so even if only about 20% of these were selected as the subset of linear feature masks, the number of cases would still be far beyond practical levels. Even $N = 4$ implies $2^{16} = 64K$ masks, which is still very large. We have used $N = 3$ to reduce the set of masks to a reasonable size: $2^9 = 512$ .

A representation for a 3 × 3 neighborhood is shown in Figure 1a. Note that except for the center pixel (referred to as CP hereafter), the number assigned to each pixel is the angle it forms with the CP (measured counterclockwise from the positive $x$-axis) divided by $45^0$.



(a)  (b)
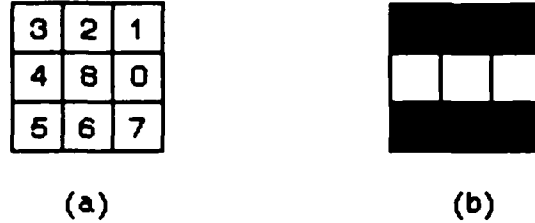
Figure 1. Representation for a 3 × 3 neighborhood. (a) Ordinal numbers of pixels. (b) The mask with *mask_number* = 273.

Each of the possible $2^9 = 512$ binary masks is assigned a mask number according to the formula

$$mask\_number = \sum_{i=0}^{8} b_i\, 2^i$$

where the value of $b_i$ for the $i^{th}$ pixel is either 0 (dark) or 1 (bright). (See Figure 1b, for example.) Note that we have *mask_number* $\geq$ 256 iff the mask has a bright CP. Moreover,

$$mask\_number(bright\ CP) + mask\_number(dark\ CP) = 511$$

holds for all pairs of "complementary" masks (i.e., masks having the same pattern but with dark and bright exchanged).

A list of all possible 3 × 3 binary masks (in increasing order of their mask numbers) appears in Appendix A.

## 2.2. The Linear Feature Masks

We now introduce a set of masks corresponding to various possible configurations that could occur in a $3 \times 3$ neighborhood that intersects a linear feature. The masks are grouped into the following classes:

Edge, Line, Wide-Line, Right-Angle, Acute-Angle, End-Point, Corner, L-Line, T-Junction, X-Junction , and Y-Junction.

The dark CP masks belonging to each class are shown in Figure 2. The remaining dark CP masks in the set are obtained by rotating each of the masks shown in Figure 2 by $90^0$, $180^0$ and $270^0$ .
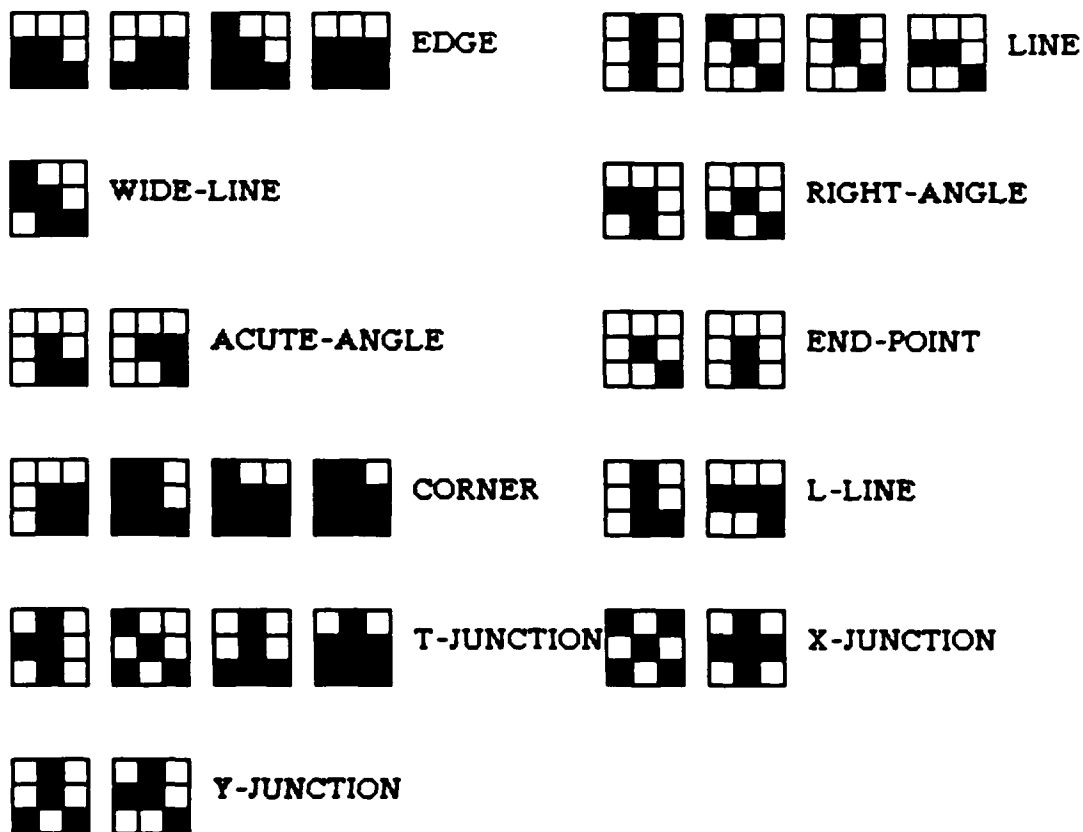
**Figure 2. The dark CP linear feature masks.**

Each mask defines a partition of the $3 \times 3$ neighborhood of the CP into dark and bright pixels. If the CP is dark, we will call the set of dark pixels the *foreground* and the set of bright pixels the *background*.

Table 1 shows the $\{f, 9 - f\}$ partition types for each class of masks, (where $f$ and $9 - f$ denote the numbers of foreground and background pixels respectively) and gives the number of masks of each partition type.

| Table 1 – No. of Masks in each Class and Partition Type | | | | |
|---|---|---|---|---|
| Type No. | Class | Partition Types | No. of Masks | Total |
| 1 | Edge | $\{5,4\}$, $\{6,3\}$ | 8, 8 | 16 |
| 2 | Line | $\{3,6\}$ | 12 | 12 |
| 3 | Wide–Line | $\{5,4\}$ | 4 | 4 |
| 4 | Right–Angle | $\{3,6\}$ | 8 | 8 |
| 5 | Acute–Angle | $\{3,6\}$ | 8 | 8 |
| 6 | End–Point | $\{2,7\}$ | 8 | 8 |
| 7 | Corner | $\{4,5\}$, $\{7,2\}$, $\{8,1\}$ | 4, 8, 4 | 16 |
| 8 | L–Line | $\{4,5\}$ | 8 | 8 |
| 9 | T–Junction | $\{4,5\}$, $\{5,4\}$, $\{7,2\}$ | 8, 4, 4 | 16 |
| 10 | X–Junction | $\{5,4\}$ | 2 | 2 |
| 11 | Y–Junction | $\{4,5\}$ | 8 | 8 |

Table 1 counts dark or bright CP masks only; to count both, the numbers should

be doubled. The total number of masks is $2 \cdot 106 = 212$.

In a given $3 \times 3$ pixel neighborhood, let the nine pixel gray levels be $z_1 \leq \ldots \leq z_9$. Depending on how many of the z's are equal, there can be up to 8 partitions of the nine pixels into $k$ dark pixels and $9 - k$ bright pixels, where $0 < k < 9$, obtained by choosing a threshold between $z_k$ and $z_{k+1}$ (if they are not equal). Thus any pixel neighborhood can match up to 8 masks (not all of which, however, will be linear feature masks).

## 2.3. The Confidence Measures

We shall use the following "confidence measures" to characterize the match of a given pixel neighborhood with a given mask:

(1) *Robustness*, defined by the width of the thresholding interval, i.e. the difference between the minimum gray level of a bright pixel and the maximum gray level value of a dark pixel. Note that robustness $> 0$ is a necessary precondition for mask matching to occur.

(2) *Contrast*, defined as the difference between the average gray levels of the dark and bright pixels. [A more informative measure can be obtained by regarding the background region as consisting of connected components; for example, in line masks there are two background components. In this situation we can consider separately the difference between the average gray level of the foreground pixels and the pixels belonging to each background component.]

(3)  *Fisher distance* (see [1], Section 10.2.3), defined by $|\mu_1 - \mu_2|/(\sigma_1^2 + \sigma_2^2)$ , where $\mu_1$, $\mu_2$ are the average gray levels in the foreground and background, and $\sigma_1$, $\sigma_2$ are the corresponding standard deviations. In Section 4 we explain on what basis this measure was applied to *all* the matched masks even though in principle it should have been used only for single background component masks (edge type masks, for instance).

(4)  *Homogeneity* of the foreground and each of the background connected components. "X-homogeneity" (where X stands for any connected component of pixels) may be defined as $1 - var(X) / var_{max}(X)$ where $var(X)$ and $var_{max}(X)$ denote the gray level variance and the maximum possible gray level variance for the X-set of pixels, respectively. Assuming the gray level in the image takes on values between 0 and $glv_{max}$ , it can easily be shown that

$$
var_{max}(X) = \begin{cases} 1/4 \ glv_{max}^2 & \|X\| \text{ even} \\ \dfrac{\|X\|^2 - 1}{\|X\|^2} \ 1/4 \ glv_{max}^2 & \text{otherwise} \end{cases}
$$

where $\|X\|$ denotes the cardinality of the $X$-set of pixels.

(5)  *Foreground road similarity*, defined by the negative of the distance between the average foreground gray level and a given "expected gray level" interval.

The measures have been defined here for single-band images, but they can easily be extended to multi-band images.

## 3. Data Structures and Algorithm

For several reasons, including ease of modifiability and the availability of a diverse software environment, Lisp was the programming language chosen for the implementation of the proposed system. The Lisp-based data structures used and the algorithm are described in the following subsections.

### 3.1. Data Types and Structures

Using the extended Franz Lisp environment at the University of Maryland [3], we define an image as an abstract data type (or Lisp *"flavor"*) with the following *"instance variables"* or characteristics:

*Width, height, number_of_bands, band_descriptions, data_type, ranges, row_scale, col_scale* and *data*.

*Band_description* is a list of character strings giving a short description of the contents of the band, one for each of the *number_of_bands* bands.

*Data_type* describes the type of data in the image arrays (e.g., eight bit integer, list, etc.). All bands have the same type.

*Ranges* is a list of lists that specify the range of data in each band. For a gray level image, each element of the *ranges* list is a list of two fixnums indicating the extrema of the corresponding band (i.e., the min and max gray level value). For a label image, each element is a list of the possible labels occurring in that band.

*Row_scale* and *col_scale* are the numbers of meters per pixel in the row and column dimensions, respectively. The scale factors are flonums that are negative if unknown.

*Data* is the three dimensional array (band row column) of data. The first row of data is the uppermost row of the image.

One of the operations that can be performed on an image (i.e., one of the image flavor *methods*) is extracting a $3 \times 3$ neighborhood centered around a point at *row, col.*: (*get_3 $\times$ 3_neighborhood row col.*) The value returned is an ordered list (*center* 0 1 2 3 4 5 6 7) of nine elements, where each element is bound to a sublist consisting of the gray level values of the corresponding numbered pixel (See Fig. 1a), in the different bands of the image.

A look-up table for the labels assigned to all possible binary masks is stored in a 512-entry *mask_set* array, where each element is bound either to one of the mask classes or to nil, depending on the corresponding entry (or *mask_number*).

The desired output of the mask matching procedure is an image (*out_image* instance) of the same size as the input image in which each non-border pixel is labeled. For every labeled pixel, the following Lisp structure is stored:

*((label (mask_number robustness (min_threshold) contrast*

    *foreground_homogeneity min_background_homogeneity*

    *fisher_distance foreground_road_similarity)*

    *...)*

  *...)*

Note that several labels may be associated with each labeled pixel.

## 3.2. Algorithm Outline

To better understand the algorithm, let us first explain the mask matching procedure in somewhat more detail. As indicated earlier, matching occurs when there exists a threshold dividing the pixels of the $3 \times 3$ neighborhood into two groups, dark and bright, such that the pattern of dark and bright is the same as one of the masks.

To find such thresholds, we sort the 9 pixel gray levels in the neighborhood. These 9 sorted values define up to 8 intervals where a threshold can be placed to separate the neighborhood into two non-empty groups of pixels, the foreground and the background. If two or more pixels in the neighborhood have the same gray level, there will be fewer than 8 intervals in which to place the threshold. (Robustness must be strictly positive.) Each threshold may give rise to a match, and thus each pixel may receive several labels.

To allow easy modification while experimenting with various data samples, the following control parameters (in addition to the *input_image* instance and the 512-entry *mask_set* of labels) are provided:

- *Sub_image* to examine, namely a list of the following form: ($x0$ $y0$ *ncols* *nrows*), where ($x0$, $y0$) denotes the upper left pixel coordinates of the *sub_image*, and *ncols*, *nrows* are the number of columns and rows. The *sub_image* passed to the algorithm should not include border pixels of the *input_image*. Thus if the *input_image* size is $N \times N$, the *sub_image* and the resulting label image should never exceed $(N - 2) \times (N - 2)$.

- Minimum acceptable robustness for any given threshold. The default value for this parameter was chosen as zero. However, higher values should help eliminate "weakly matched" masks.

- Expected road gray level interval.

The algorithm can now be outlined as follows:

(0) **[Initialization]**

Set $xn \leftarrow (x0 + ncols)$, $yn \leftarrow (y0 + nrows)$, $x \leftarrow x0$, $y \leftarrow y0$, $t \leftarrow 0$ and $label \leftarrow$ nil, $mask\_info \leftarrow$ nil.

(1) **[Read 3 $\times$ 3 Neighborhood]**

Read the gray levels of the 3 $\times$ 3 neighborhood centered at ( $x$ $y$ ).

Set $n \leftarrow (c \ n0 \ n1 \ n2 \ n3 \ n4 \ n5 \ n6 \ n7)$.

(2) **[Sort the Neighborhood Gray Levels]**

Sort the $n$ list in increasing order.

Set $sn \leftarrow (sn0 \ sn1 \ sn2 \ sn3 \ sn4 \ sn5 \ sn6 \ sn7 \ sn8)$.

(3) **[Threshold]**

If $snt < sn(t+1)$, partition the 3 $\times$ 3 neighborhood with respect to the $t^{\text{th}}$ threshold, assigning binary coefficients to each of the 9 pixels (for $i=0,1,...,8$ $b_i \leftarrow 0$ if $glv(p_i) \leq snt$, otherwise $b_i \leftarrow 1$).

Otherwise, goto step (6).

(4) **[Evaluate Mask No. and Reference Array]**

Evaluate the corresponding $mask\_number$.

Reference the *mask_set* array; if $label(mask\_number)$=nil, goto step (6).

Otherwise, set $label \leftarrow mask\_set[mask\_number]$.

**(5) [Collect Information]**

Compute all confidence measures associated with the matched masks, namely robustness, contrast, foreground/background homogeneities, Fisher distance, etc.

Insert the above information into the *mask_info* list associated with the $(x, y)$ element of the *out_image* array.

**(6) [Increment Threshold]**

Set $t \leftarrow t+1$; if $t < 8$, return to step (3). Otherwise, set $t \leftarrow 0$.

**(7) [Scan the Image]**

Set $y \leftarrow y+1$; if $y \leq yn$, return to step (1).

Otherwise, set $y \leftarrow y0$, $x \leftarrow x+1$. If $x \leq xn$, return to step (1).

**(8) [Terminate]**

An output example, generated by the algorithm for a $10 \times 10$ *sub_image*, is illustrated in the following figures. Figures 3a and 3b show the bright CP masks in the corresponding $8 \times 8$ sub-image and (respectively) the robustness and contrast values associated with each mask. (The number at the center of each pixel denotes its gray level value.)

In [2], criteria for the consistency of pairs of masks centered at adjacent pixels are defined. Figure 3c shows the consistent pairs of masks in Figures 3a-b, linked by lines. By tracing along the links, we see that the image contains a
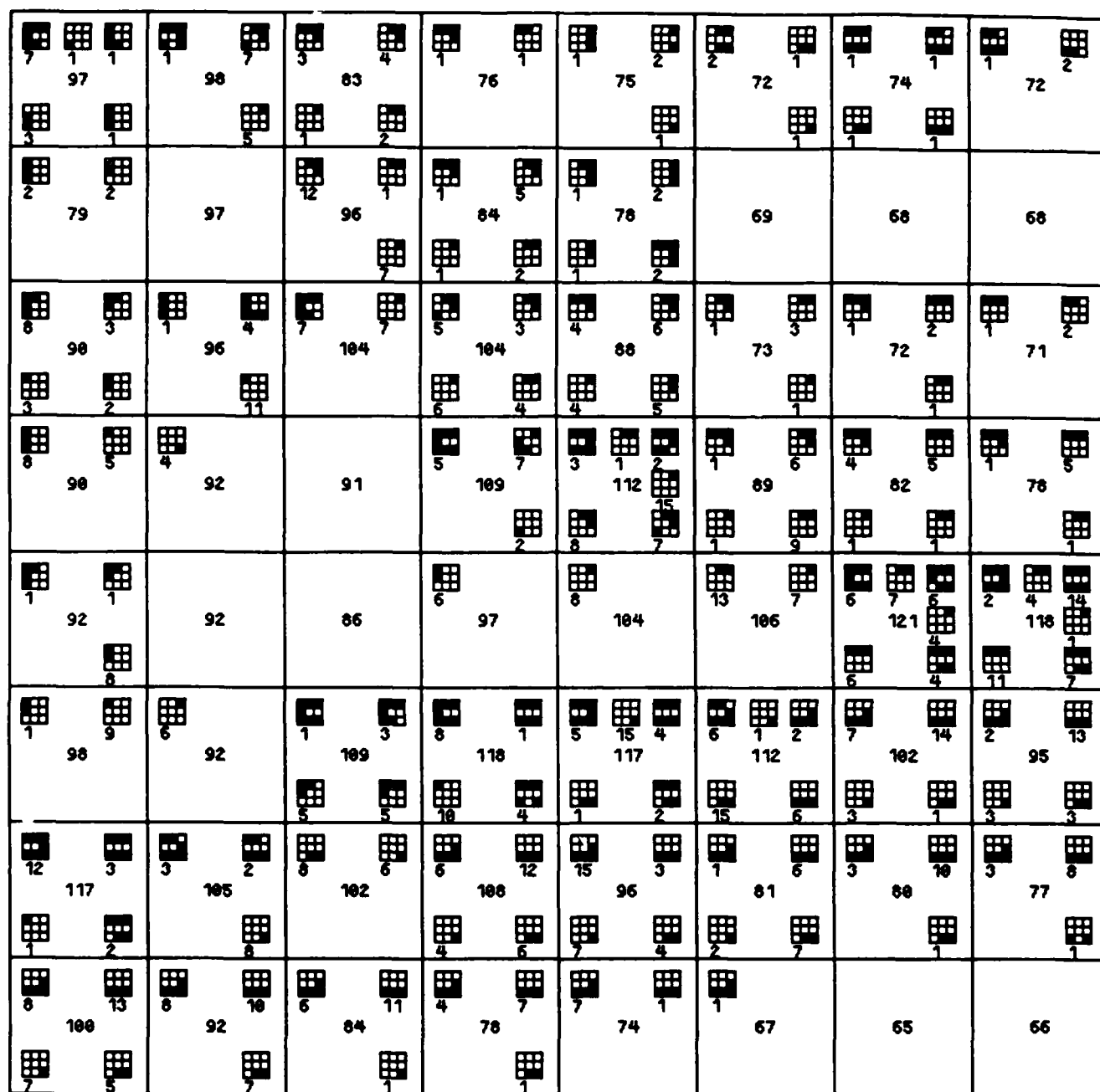
Figure 3a. An example of 8 × 8 bright CP mask output with associated robustness values.
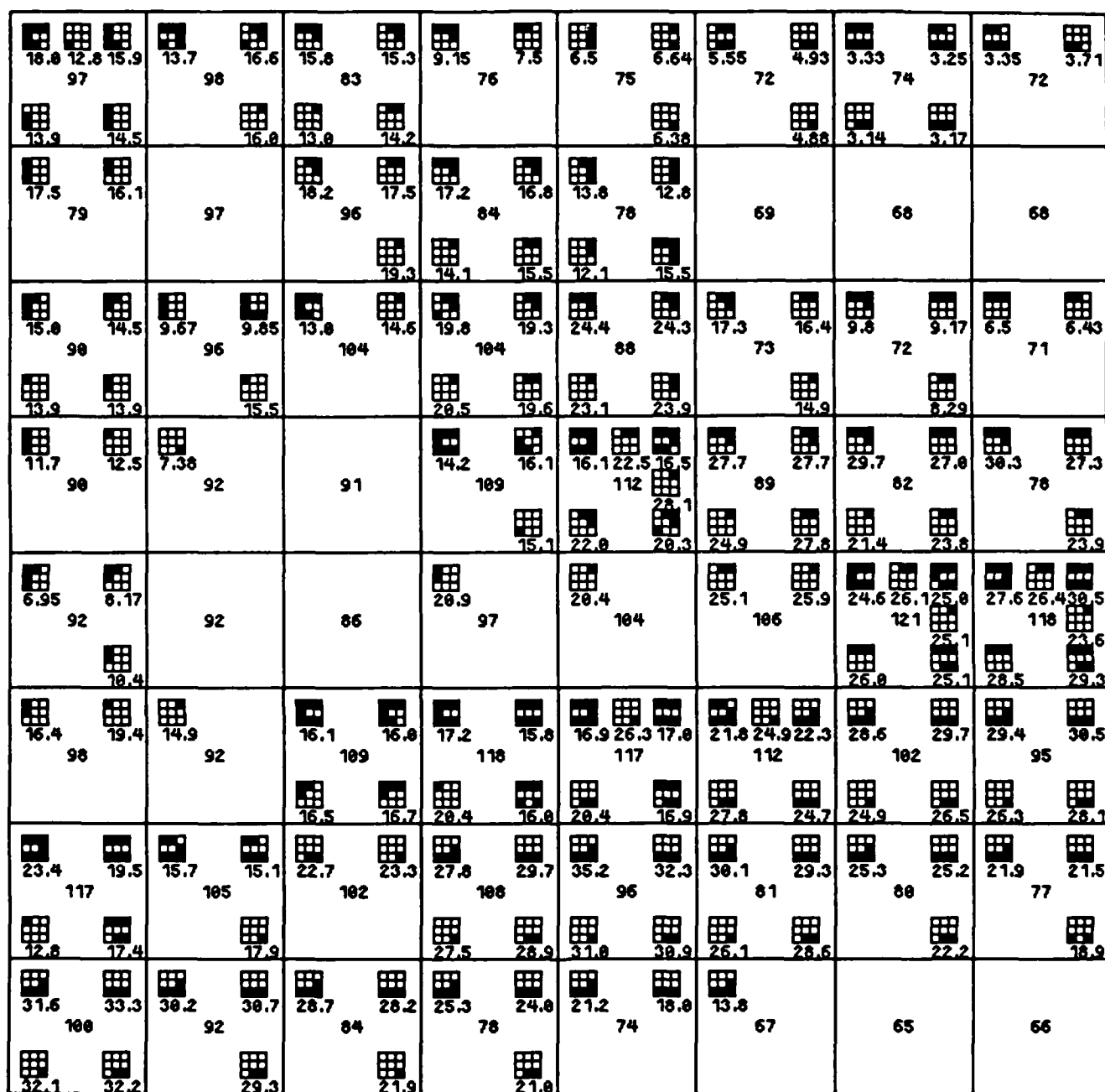
Figure 3b. An example of 8 × 8 bright CP mask output with associated contrast values.
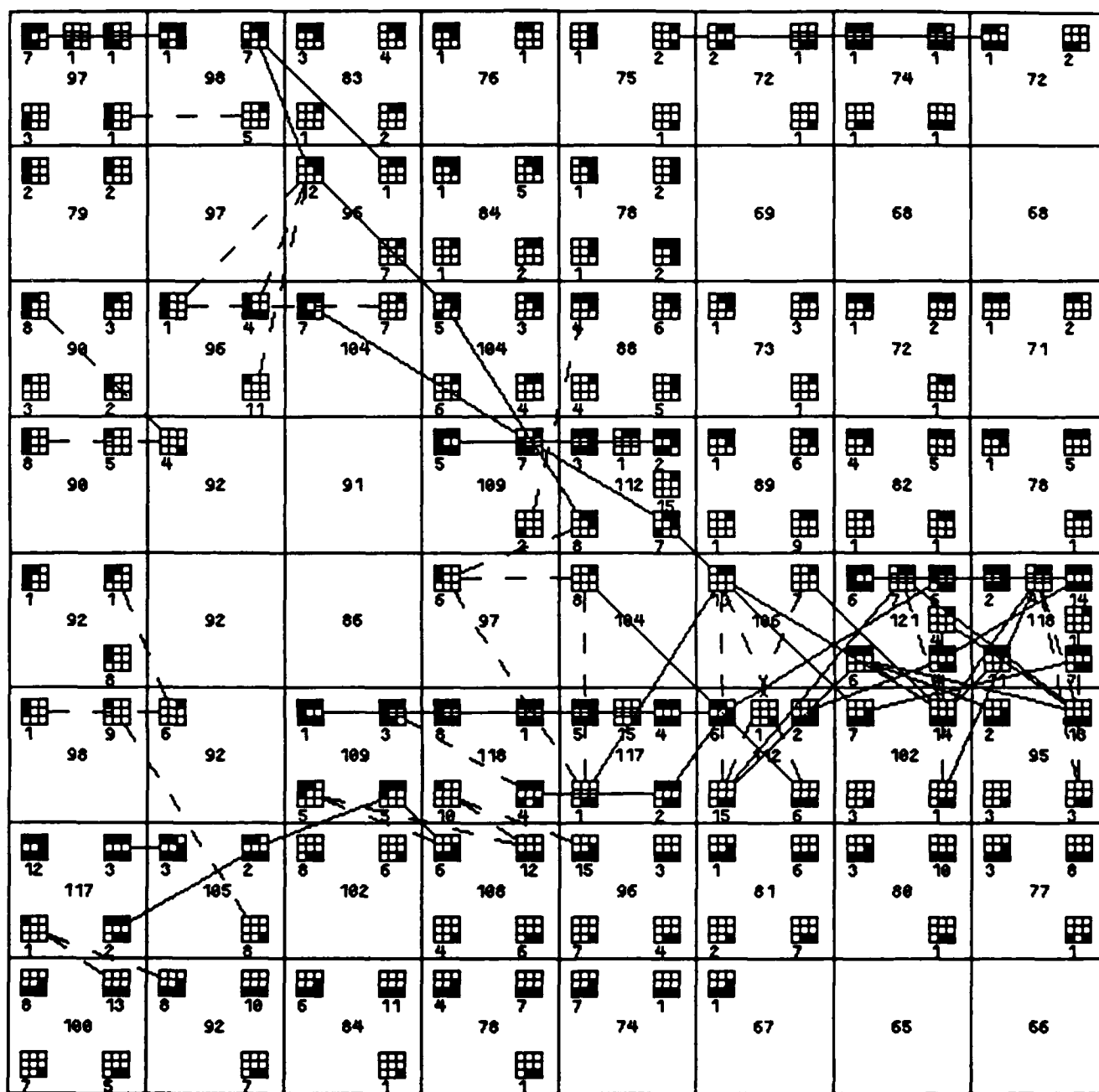
Figure 3c. Consistency links found for the bright CP masks.

15

branching linear feature, with one branch, roughly horizontal, just below the center of the image, and the other, roughly diagonal, extending upward and leftward from the center.

### 3.3. Suppressing "Weak" Masks

One might think that it is not necessary to make use of all the masks that match the neighborhood of each pixel, but only of the "strongest" ones, say those having the highest robustness or contrast values. A simple experiment shows, however, that this is not true. Figures 4-8 show, respectively, the consistency links obtained when we keep, at each pixel, only the mask(s) having

(1) Highest robustness value.

(2) Two highest robustness values.

(3) Highest contrast value.

(4) Two highest contrast values.

(5) Highest robustness or highest contrast.

(In cases of tied values, all the masks involved are included.) We see that when this is done, the results are very poor, especially for methods (1), (3), and (5). Note that the results obtained using methods (1), (3), and (5) are very similar, indicating that generally, a mask having the highest robustness value at a pixel also has the highest contrast value, and vice versa.

Even the somewhat better results obtained using methods (2) and (4) show that elimination of masks leads to loss of information. (See Figures 5 and 7.)
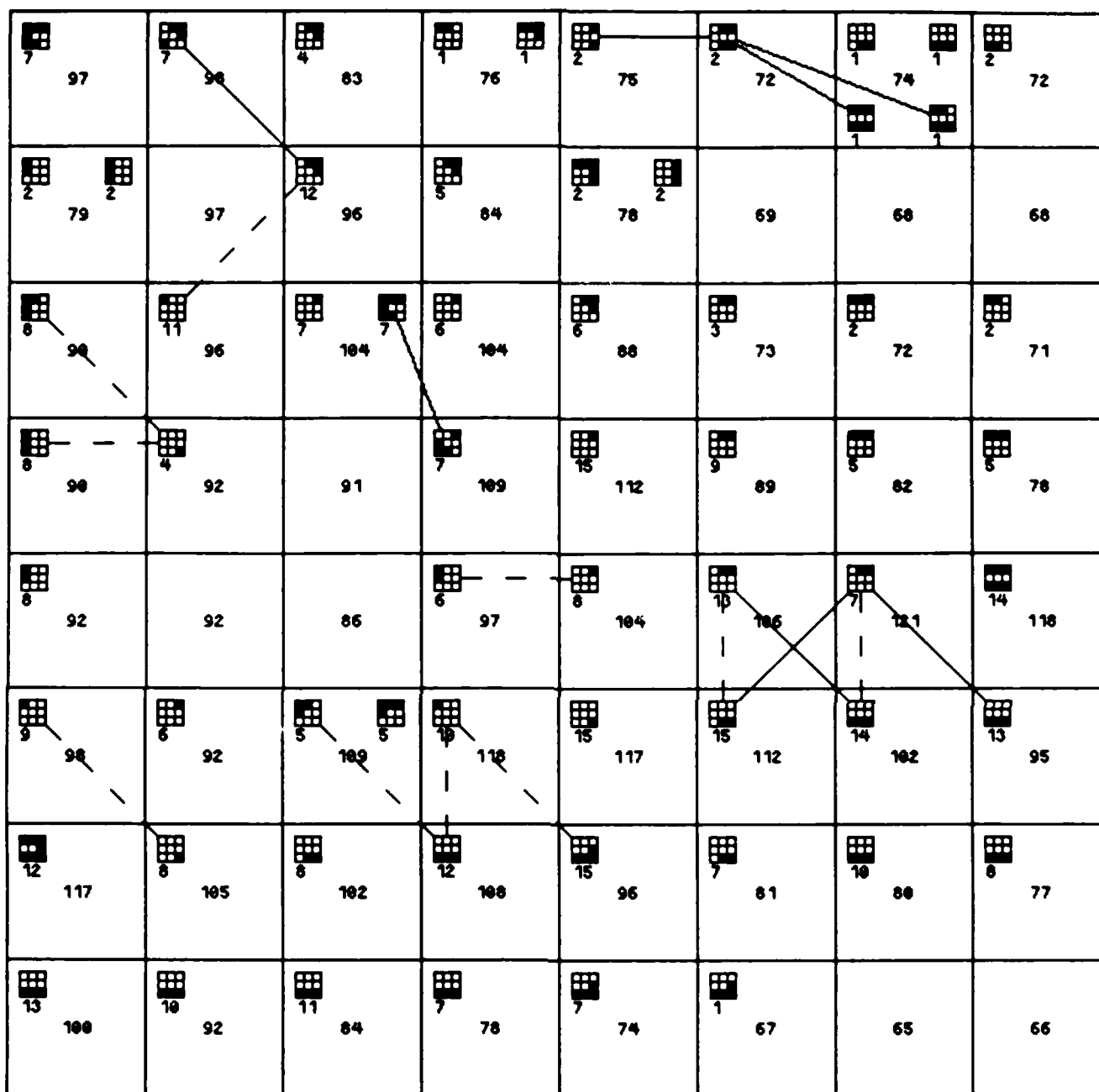
Figure 4. Consistency links found for bright CP masks having the highest robustness values.
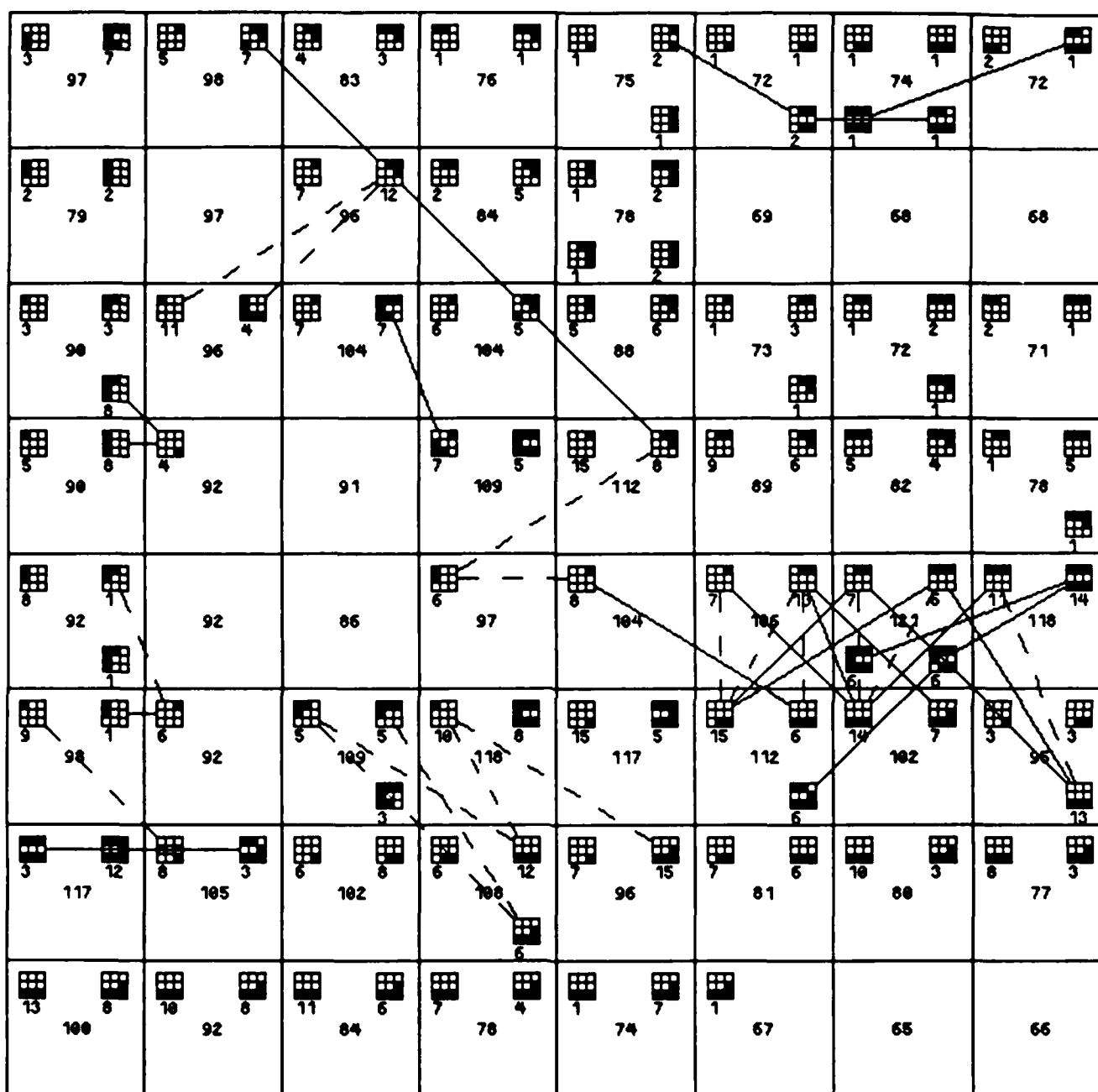
Figure 5. Consistency links found for bright CP masks having the two highest robustness values.

Figure 6. Consistency links found for bright CP masks having the highest contrast values.
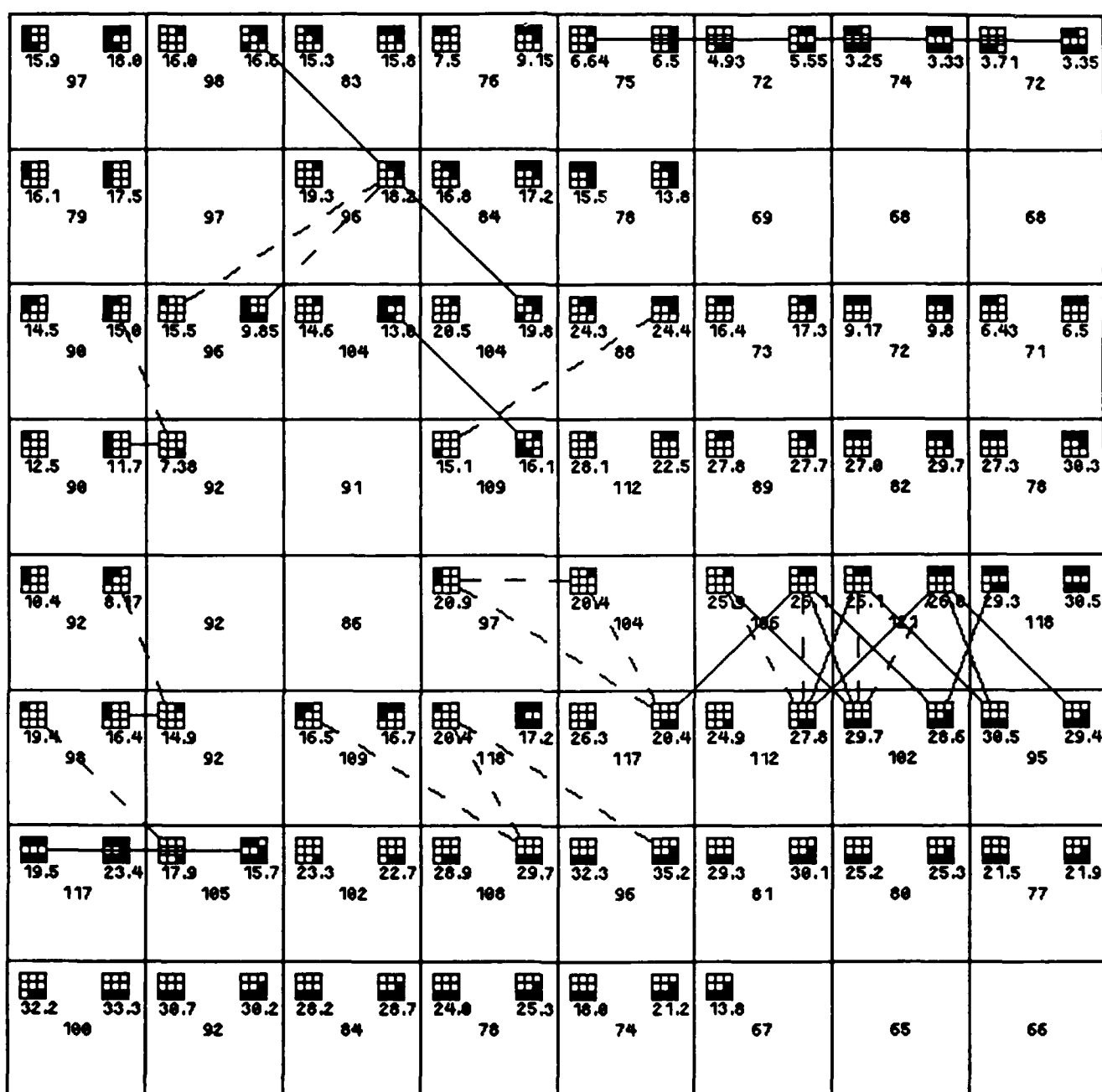
Figure 7. Consistency links found for bright CP masks having the two highest contrast values.
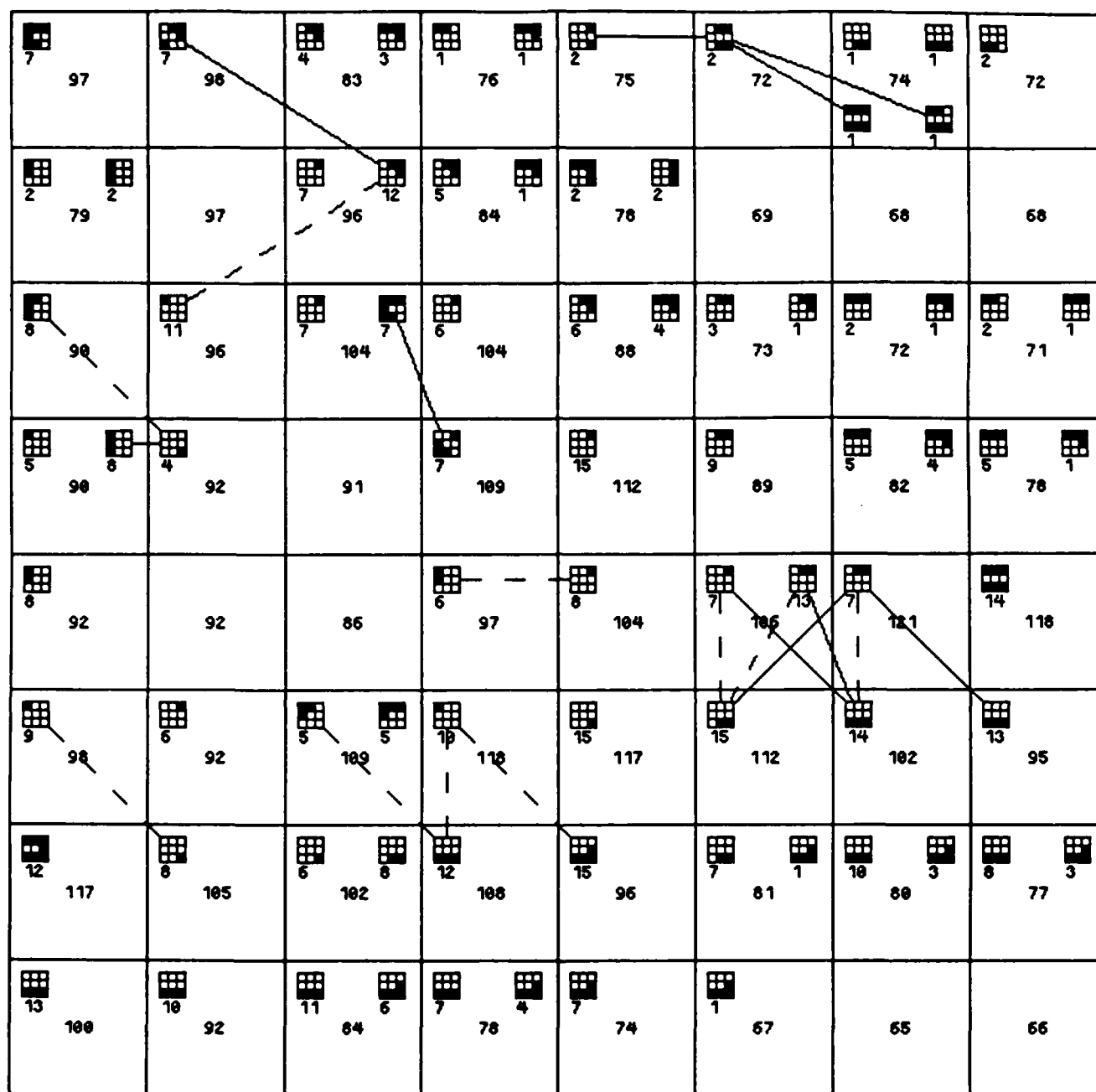
Figure 8. Consistency links found for bright CP masks having either highest robustness or highest contrast. (Robustness values are associated with each mask.)

Thus, it is not desirable to suppress any masks at this stage, in order to maintain all available information at the pixel level for use in the linear feature extraction process.

## 4. Statistical Studies

It is of interest to study statistical properties of the confidence measures and other parameters associated with the mask matching process. The purpose of these studies is to investigate to what extent it would be useful to make use of statistical properties in the linear feature detection process. The studies performed treat the following issues:

- Evaluation of the frequency of occurrence of classes of matched masks in a given image.

- Computation of the distribution of the various confidence measures associated with the matched masks (e.g., robustness, contrast, Fisher distance, etc.), and of the corresponding statistical parameters (i.e., the maximum, mean, median, and variance values), as functions of the class of matched masks.

- Comparison between the statistical results obtained for the dark CP masks and those for the bright CP masks, as a function of the class of matched masks.

- Comparison between confidence measures evaluated for matched masks at pixels where a non-linear line detector (described in Section 10.3.2 of [1] and referred to as NLD hereafter) responds, and the same measures evaluated at

22

pixels where the above non-linear detector does not respond.

In repeating the above studies for various image instances, we want to find out whether or not there exists a correlation between the experimental results obtained and the presence of an extensive road network in a given image. For example, it would be of interest to establish that the higher the frequency of occurrence of line-like masks in a certain image is, the more likely road segments are to be found in that image.

## 4.1. Classification of Image Types

The statistical results given in the following subsections were obtained for the sub-images shown in Figures 9a-b and for 64 $\times$ 64 "white noise" images generated using [4] (for $\mu = 127$, and $\sigma = 5$, 10, 15, 20, 25, 30, 35). Figures 9a-b show 128 $\times$ 128 and 256 $\times$ 475 gray level images respectively, with four selected window overlays in each (denoted by w1, w2, ..., w8.). The image of Figure 9a (called "Greenbelt1") is a sub-image of the image shown in Figure 9b (called "Green-belt"), which was digitized from an aerial photograph of the Greenbelt, Maryland area. The quadrants of Figure 9a will be referred to below as "upper-left", "upper-right", etc.

In order to relate the statistical properties to the presence of roads in an image, we have classified the sub-images into the following three categories:

- "suburban" and "highway" images – e.g., windows 4, 7, and 8.

- "homogeneous" images – e.g., windows 1, 2, 3, 5, and 6.

23
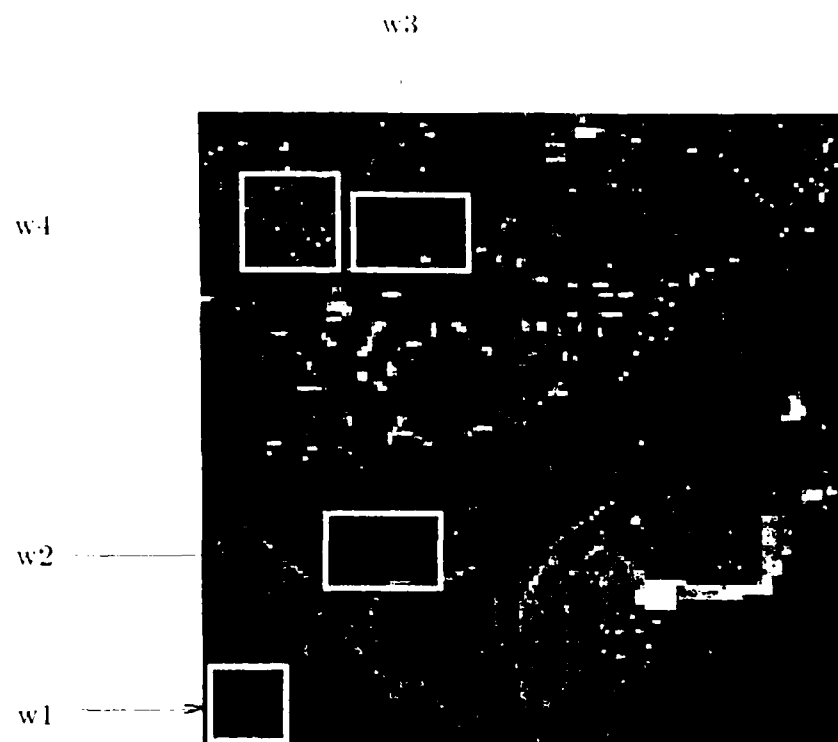
Figure 9a. "Greenbelt1" Image (128 × 128)
with four selected windows.
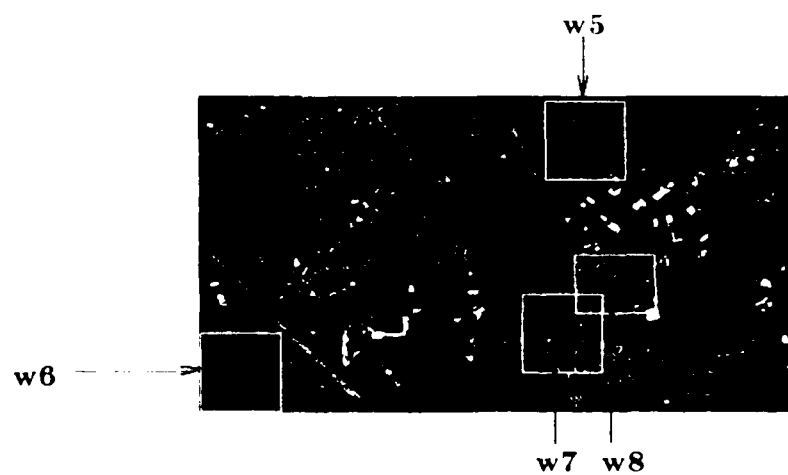


Figure 9b. "Greenbelt" Image (256 × 475)
with four selected windows.

- "white noise" images.

Figure 10 gives the gray level histograms of several 64 × 64 sub-images of the Greenbelt area images and of two white noise images. Notice the general resemblance of the histograms of images of the same class. We did not attempt, however, to develop a method of automatically classifying the sub-images by analyzing their histograms.

## 4.2. Statistical Results

### 4.2.1. Frequency of Occurrence of Classes of Masks

The histograms of frequencies of occurrence of the classes of bright CP masks (in the images referred to in Figure 10) are shown in Figure 11. Again, the distributions obtained for images of the same type are characteristic. Moreover, the common characteristics of this distribution for images of different types (e.g., the common general shape and the maximal frequency obtained for Corner masks) should be noticed. However, the frequencies of occurrence of Edge and Corner masks are significantly lower in the homogeneous and white noise images, compared with the suburban images. (See Tables 3a-b through 10a-b in the next subsection for the exact figures.)

In order to try to differentiate between the various image types in terms more closely related to the presence of roads in a given image, we apply the following test. Let the set of Line, Wide-Line, and L-Line masks be called "line-like" masks. Given 1-2 pixel wide road images, it is of interest to verify, for example, whether the frequency of occurrence of line-like masks increases in

25
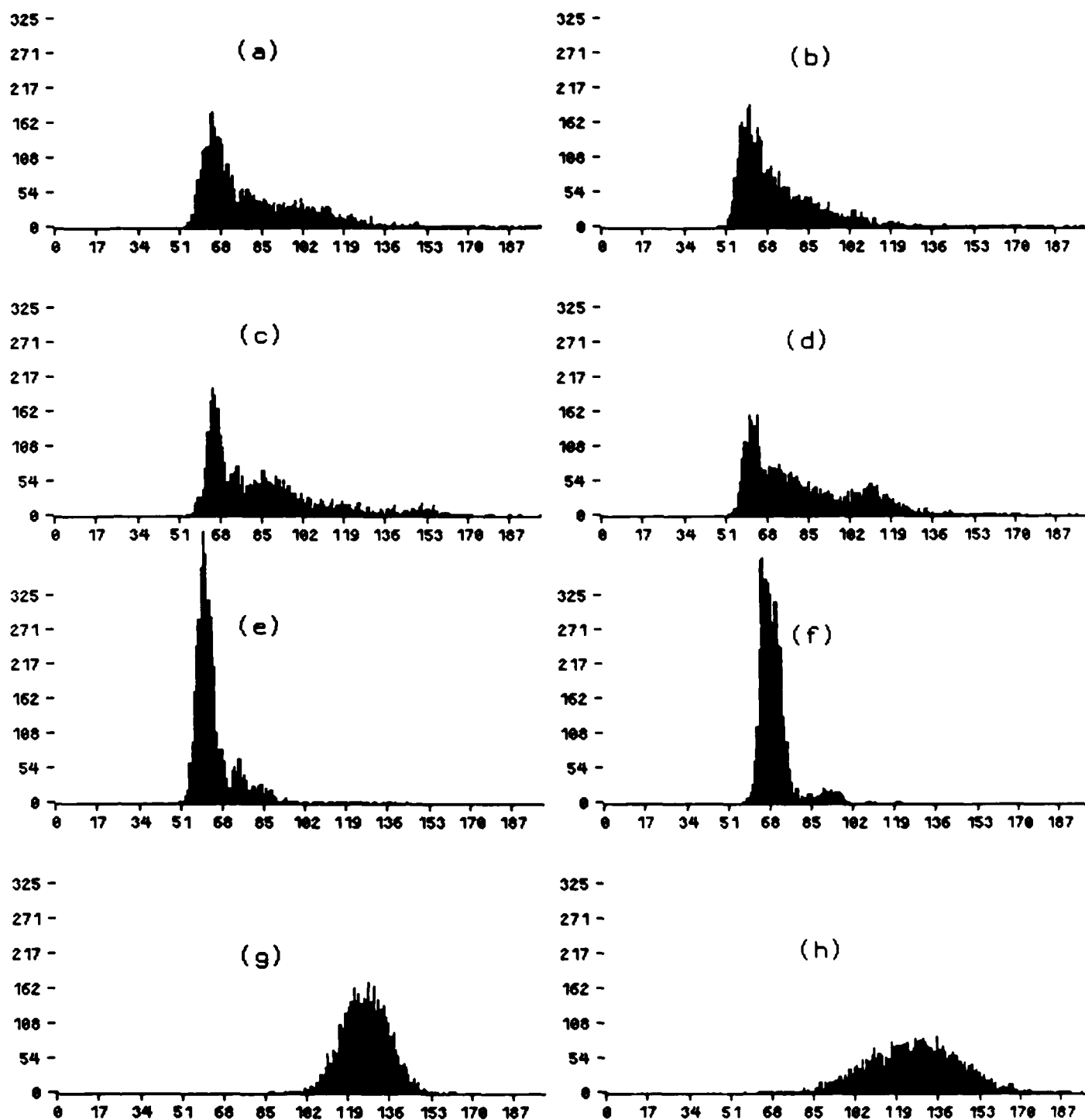
**Figure 10. Gray Level Histograms for 64 × 64 Images.**

(a), (b), (c), (d):  **suburban:** upper-left, upper-right, lower-left. window_7.

(e), (f):  **homogeneous:** window_5, window_6.

(g), (h):  **white noise** with $\sigma = 10$, $\sigma = 20$.

26
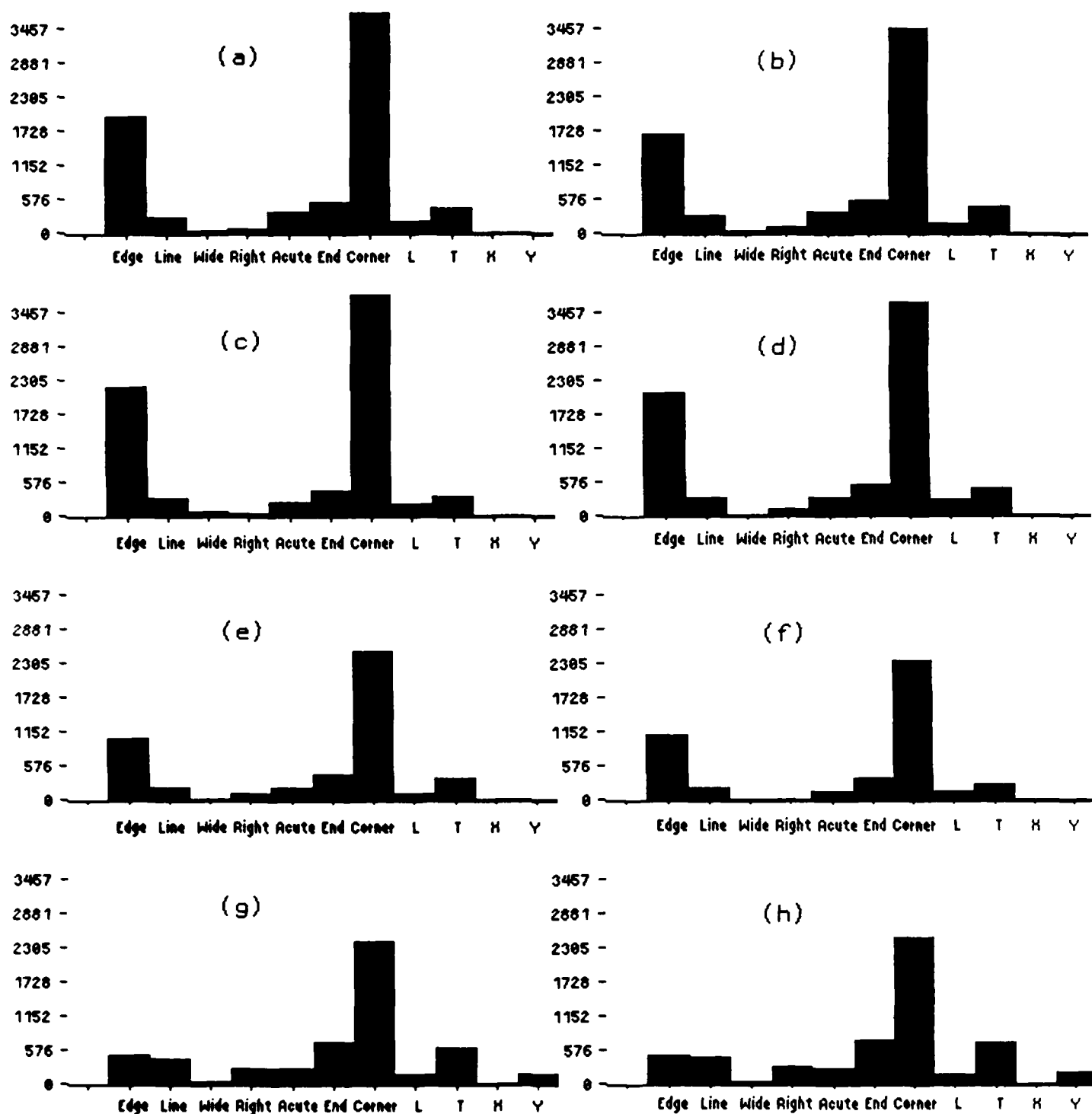
**Figure 11. Bright CP Mask Histograms for 64 × 64 Images.**

(a), (b), (c), (d): **suburban:** upper-left, upper-right, lower-left, window_7.

(e), (f): **homogeneous:** window_5, window_6.

(g), (h): **white noise** with $\sigma=10$, $\sigma=20$.

27

| Table 2 – Frequency of Occurrence of Line–Like Masks in Various Images | | | | | | |
|---|---|---|---|---|---|---|
| Name | Type | Size | % of Dark CP Line–Like Masks | | % of Bright CP Line–Like Masks | |
| | | | 1 Mask per Pixel | Total | 1 Mask per Pixel | Total |
| window_4 | suburban | 20×20 | 18.5 | 24.0 | 18.8 | 26.2 |
| window_8 | suburban | 48×64 | 11.4 | 15.1 | 13.9 | 18.5 |
| window_7 | suburban | 64×64 | 12.5 | 16.3 | 14.4 | 19.7 |
| upper–left | suburban | 64×64 | 13.7 | 17.3 | 13.0 | 16.7 |
| upper–right | suburban | 64×64 | 13.8 | 17.2 | 13.9 | 17.5 |
| lower–left | suburban | 64×64 | 12.5 | 15.2 | 14.1 | 18.1 |
| lower–right | suburban | 64×64 | 12.1 | 15.2 | 12.5 | 16.1 |
| window_1 | homogeneous | 16×16 | 13.2 | 14.3 | 10.7 | 10.7 |
| window_2 | homogeneous | 16×24 | 14.6 | 16.2 | 11.7 | 14.0 |
| window_3 | homogeneous | 16×24 | 10.4 | 11.0 | 10.1 | 12.3 |
| window_5 | homogeneous | 64×64 | 11.6 | 13.7 | 10.5 | 11.8 |
| window_6 | homogeneous | 64×64 | 12.1 | 14.2 | 10.6 | 12.3 |
| $\mu=127, \sigma=5$ | white noise | 64×64 | 14.7 | 17.2 | 15.2 | 17.4 |
| $\mu=127, \sigma=10$ | white noise | 64×64 | 17.7 | 20.7 | 17.8 | 20.8 |
| $\mu=127, \sigma=15$ | white noise | 64×64 | 17.9 | 20.6 | 17.2 | 20.6 |
| $\mu=127, \sigma=20$ | white noise | 64×64 | 19.1 | 22.8 | 18.2 | 21.9 |
| $\mu=127, \sigma=25$ | white noise | 64×64 | 18.3 | 22.2 | 17.8 | 21.6 |
| $\mu=127, \sigma=30$ | white noise | 64×64 | 17.9 | 21.2 | 18.7 | 22.7 |
| $\mu=127, \sigma=35$ | white noise | 64×64 | 19.1 | 23.1 | 19.7 | 23.5 |

suburban images relative to images of other types. The results, summarized in Table 2, reveal that this frequency in fact decreases in the suburban images examined, compared with most of the white noise images. (A theoretical derivation of the frequency of occurrence of masks in white noise images is given in Section 5.) Hence it is impossible to conclude that a given image region is "suburban" based on its frequency of occurrence of line–like masks.

### 4.2.2. Distribution of the Confidence Measures

The study performed next computes the distributions of the mask confidence measures (robustness, contrast, and Fisher distance) and their statistical properties (maximum, mean, variance, and median) for the different classes of masks in various types of images. The numerical results obtained for the set of 64 × 64 images used in the previous subsections are given in Tables 3a-b through 10a-b. (Tables .or additional images are appended to this report.) The robustness, contrast, and Fisher distance histograms for the bright CP Line masks are shown in Figures 12-14. Based on these results, the following observations can be made.

(1) The statistical properties are most similar for images of the same type. (The numerical values obtained for the white noise images differ from one another, but their statistical properties (as functions of the class of masks) are qualitatively similar.)

(2) The mean and median robustness and contrast values of the matched masks of given classes are generally greater in the suburban images than in the homogeneous images. On the other hand, the mean and median Fisher distance values in the homogeneous images are generally slightly greater than in the suburban images. Also, the Fisher distance variance over all matched masks of a given class is usually smaller in the homogeneous images, except in degenerate cases where the Fisher distance is infinite.

(3) The values obtained for the statistical properties in the white noise images strongly depend on $\sigma$. The values obtained for $\sigma=5$, for example, are similar

to the values for the homogeneous images (see Tables B–7a–b, and Tables 7a-b, 8a-b), whereas the results for $\sigma=10$-20 are much closer to those obtained for the suburban images (see Table 10a-b, Tables 3a-b through 6a-b, and Figure 12). Generally, the frequency of occurrence and the mean and median values of robustness and contrast of given classes of masks in white noise images are increasing functions of $\sigma$. (See the theoretical proof of this in Section 5.) The Fisher distance in white noise images seems to vary little, with respect to either $\sigma$ or the class of masks.

(4) The contrast histograms of the bright CP Line masks in the white noise images strongly resemble the gray level distributions in the images themselves (see Figures 10, 13). They differ greatly in shape from the contrast histograms obtained for the suburban images; the contrast of the Line masks in the suburban images is more uniformly distributed. The maximal robustness and contrast values for the suburban images are usually greater than in the white noise images. (See also the robustness and contrast histograms of the bright CP Line masks, shown in Figures 12-14.) These observations might suggest the selection of masks based on robustness/contrast criteria, but the consequences of doing this are unsatisfactory, as illustrated in Section 3.3.

These results may be useful in distinguishing between suburban and homogeneous images, but do not seem to be useful in distinguishing between suburban and white noise images.

**Table 3a – Statistics for Dark Center Pixel Masks in Upper–left Quadrant of Greenbelt1**

| Class | # of Masks | Robustness | | | | Contrast | | | | Fisher distance | | | |
|---|---|---|---|---|---|---|---|---|---|---|---|---|---|
| | | Max | Mean | Var | Med | Max | Mean | Var | Med | Max | Mean | Var | Med |
| Edge | 1976 | 127.0 | 7.6 | 113.9 | 4.0 | 141.7 | 28.4 | 501.9 | 22.8 | 29.7 | 3.5 | 2.8 | 3.1 |
| Line | 315 | 45.0 | 6.1 | 72.3 | 3.0 | 97.2 | 22.8 | 272.5 | 21.3 | 9.5 | 2.6 | 1.9 | 2.2 |
| Wide-Line | 85 | 30.0 | 4.2 | 26.7 | 3.0 | 99.9 | 23.3 | 365.4 | 18.6 | 4.6 | 2.8 | 0.6 | 2.7 |
| Right-Angle | 122 | 14.0 | 2.7 | 7.7 | 1.5 | 71.7 | 17.4 | 176.7 | 14.4 | 3.9 | 2.1 | 0.5 | 2.0 |
| Acute-Angle | 355 | 20.0 | 3.3 | 10.5 | 2.0 | 74.7 | 19.4 | 179.5 | 17.2 | 6.8 | 2.3 | 0.8 | 2.2 |
| End-Point | 518 | 48.0 | 3.6 | 16.7 | 2.0 | 107.1 | 19.5 | 199.6 | 17.1 | 5.3 | 2.0 | 0.6 | 1.8 |
| Corner | 3981 | 133.0 | 12.2 | 246.3 | 6.0 | 158.1 | 31.8 | 699.1 | 24.3 | 47.2 | 3.7 | 6.3 | 3.1 |
| L-Line | 268 | 38.0 | 4.5 | 27.3 | 2.0 | 85.1 | 23.8 | 305.2 | 21.0 | 9.4 | 2.7 | 1.0 | 2.5 |
| T-Junction | 470 | 81.0 | 5.3 | 59.9 | 3.0 | 118.3 | 22.8 | 312.8 | 18.8 | 10.4 | 3.1 | 1.3 | 3.0 |
| X-Junction | 7 | 3.0 | 1.6 | 0.5 | 1.0 | 19.4 | 10.7 | 33.6 | 10.2 | 4.9 | 2.9 | 0.7 | 2.7 |
| Y-Junction | 42 | 19.0 | 3.4 | 14.4 | 2.0 | 51.7 | 19.3 | 170.3 | 16.7 | 5.2 | 2.8 | 0.6 | 2.8 |

**Table 3b – Statistics for Bright Center Pixel Masks in Upper–left Quadrant of Greenbelt1**

| Class | # of Masks | Robustness | | | | Contrast | | | | Fisher distance | | | |
|---|---|---|---|---|---|---|---|---|---|---|---|---|---|
| | | Max | Mean | Var | Med | Max | Mean | Var | Med | Max | Mean | Var | Med |
| Edge | 2009 | 64.0 | 6.3 | 57.2 | 3.0 | 112.4 | 27.9 | 391.3 | 23.8 | 13.2 | 2.8 | 1.5 | 2.5 |
| Line | 315 | 67.0 | 7.6 | 98.8 | 3.0 | 119.7 | 27.2 | 535.1 | 20.7 | 9.4 | 3.3 | 1.6 | 3.0 |
| Wide-Line | 81 | 50.0 | 6.9 | 73.0 | 4.0 | 78.9 | 27.4 | 397.4 | 20.8 | 5.7 | 3.1 | 1.1 | 3.1 |
| Right-Angle | 138 | 34.0 | 6.3 | 49.4 | 3.0 | 103.2 | 30.5 | 437.7 | 25.3 | 6.3 | 3.0 | 0.7 | 3.0 |
| Acute-Angle | 418 | 57.0 | 6.6 | 74.9 | 3.0 | 110.5 | 30.6 | 500.6 | 24.4 | 10.9 | 3.2 | 1.1 | 3.0 |
| End Point | 568 | 104.0 | 9.1 | 148.9 | 4.0 | 137.9 | 31.6 | 637.9 | 24.3 | 13.1 | 3.2 | 2.1 | 2.9 |
| Corner | 3769 | 65.0 | 5.1 | 38.6 | 3.0 | 115.5 | 24.1 | 310.5 | 20.6 | 13.8 | 2.2 | 1.0 | 2.0 |
| L-Line | 246 | 48.0 | 5.4 | 39.4 | 3.0 | 115.7 | 25.6 | 426.7 | 19.7 | 8.9 | 3.1 | 0.9 | 3.0 |
| T-Junction | 482 | 20.0 | 3.2 | 8.8 | 2.0 | 92.4 | 22.2 | 257.2 | 19.0 | 6.5 | 2.2 | 0.7 | 2.1 |
| X-Junction | 4 | 9.0 | 3.8 | 9.2 | 2.0 | 41.8 | 23.5 | 117.7 | 19.2 | 2.8 | 2.3 | 0.1 | 2.1 |
| Y-Junction | 49 | 14.0 | 3.1 | 9.3 | 2.0 | 61.4 | 19.0 | 202.6 | 16.0 | 4.1 | 2.9 | 0.4 | 2.8 |

Table 4a – Statistics for Dark Center Pixel Masks in Upper-right Quadrant of Greenbelt1

| Class | # of Masks | Robustness | | | | Contrast | | | | Fisher distance | | | |
|---|---|---|---|---|---|---|---|---|---|---|---|---|---|
| | | Max | Mean | Var | Med | Max | Mean | Var | Med | Max | Mean | Var | Med |
| Edge | 1773 | 125.0 | 7.5 | 123.0 | 4.0 | 155.0 | 28.0 | 573.7 | 20.8 | 28.8 | 3.5 | 3.0 | 3.1 |
| Line | 326 | 55.0 | 3.2 | 19.2 | 2.0 | 95.5 | 19.2 | 287.1 | 13.4 | 7.5 | 2.3 | 1.0 | 2.0 |
| Wide-Line | 95 | 17.0 | 3.4 | 9.5 | 2.0 | 69.8 | 21.3 | 250.2 | 16.8 | 4.9 | 2.6 | 0.5 | 2.7 |
| Right-Angle | 158 | 20.0 | 2.4 | 6.5 | 2.0 | 66.0 | 15.6 | 151.8 | 12.4 | 7.8 | 2.1 | 0.8 | 2.1 |
| Acute-Angle | 329 | 32.0 | 3.0 | 11.3 | 2.0 | 90.0 | 19.4 | 191.5 | 15.5 | 6.5 | 2.1 | 0.6 | 1.9 |
| End-Point | 521 | 19.0 | 2.9 | 7.6 | 2.0 | 86.4 | 17.0 | 178.6 | 13.1 | 5.8 | 1.9 | 0.7 | 1.7 |
| Corner | 3726 | 161.0 | 13.1 | 323.0 | 6.0 | 185.4 | 31.7 | 844.2 | 22.0 | 36.1 | 4.0 | 7.8 | 3.2 |
| L-Line | 240 | 75.0 | 4.4 | 45.3 | 2.0 | 108.9 | 24.2 | 422.2 | 16.8 | 9.4 | 2.5 | 1.1 | 2.3 |
| T-Junction | 545 | 69.0 | 5.4 | 55.1 | 3.0 | 111.6 | 23.7 | 427.2 | 17.5 | 10.3 | 3.1 | 1.3 | 2.9 |
| X-Junction | 6 | 10.0 | 2.7 | 10.9 | 1.0 | 45.7 | 15.2 | 199.5 | 10.1 | 3.7 | 2.7 | 0.4 | 2.9 |
| Y-Junction | 55 | 14.0 | 2.9 | 10.8 | 1.0 | 62.8 | 15.8 | 196.2 | 9.8 | 6.2 | 2.8 | 0.9 | 2.6 |

Table 4b – Statistics for Bright Center Pixel Masks in Upper-right Quadrant of Greenbelt1

| Class | # of Masks | Robustness | | | | Contrast | | | | Fisher distance | | | |
|---|---|---|---|---|---|---|---|---|---|---|---|---|---|
| | | Max | Mean | Var | Med | Max | Mean | Var | Med | Max | Mean | Var | Med |
| Edge | 1725 | 103.0 | 5.7 | 60.0 | 3.0 | 140.8 | 25.6 | 419.6 | 19.6 | 13.1 | 2.7 | 1.6 | 2.5 |
| Line | 350 | 123.0 | 8.1 | 209.3 | 3.0 | 149.7 | 27.7 | 702.2 | 18.7 | 22.0 | 3.4 | 3.2 | 3.1 |
| Wide-Line | 104 | 18.0 | 3.3 | 12.5 | 2.0 | 61.1 | 18.5 | 127.7 | 15.8 | 5.7 | 2.6 | 0.9 | 2.5 |
| Right-Angle | 166 | 51.0 | 4.9 | 37.3 | 3.0 | 102.5 | 26.0 | 428.5 | 19.7 | 6.8 | 2.9 | 1.0 | 2.8 |
| Acute-Angle | 412 | 64.0 | 5.2 | 51.4 | 3.0 | 118.8 | 26.8 | 495.8 | 19.7 | 9.0 | 3.0 | 0.9 | 2.9 |
| End-Point | 611 | 111.0 | 11.5 | 309.3 | 4.0 | 158.4 | 31.8 | 815.8 | 21.0 | 18.8 | 3.6 | 4.7 | 3.0 |
| Corner | 3504 | 88.0 | 4.7 | 36.6 | 3.0 | 127.6 | 21.8 | 300.2 | 17.4 | 18.3 | 2.1 | 1.3 | 1.9 |
| L-Line | 220 | 45.0 | 4.6 | 27.1 | 3.0 | 114.7 | 27.3 | 445.5 | 22.2 | 6.7 | 2.9 | 1.0 | 2.7 |
| T-Junction | 503 | 26.0 | 3.3 | 12.7 | 2.0 | 117.4 | 22.0 | 347.5 | 16.6 | 7.0 | 2.2 | 0.7 | 2.1 |
| X-Junction | 7 | 9.0 | 3.3 | 6.2 | 2.0 | 71.6 | 31.5 | 326.4 | 26.3 | 2.7 | 2.2 | 0.4 | 2.5 |
| Y-Junction | 72 | 20.0 | 3.6 | 16.2 | 2.0 | 66.4 | 18.7 | 203.7 | 14.8 | 5.0 | 2.8 | 0.7 | 2.7 |

Table 5a – Statistics for Dark Center Pixel Masks in Lower–left Quadrant of Greenbelt1

| Class | # of Masks | Robustness | | | | Contrast | | | | Fisher distance | | | |
|---|---|---|---|---|---|---|---|---|---|---|---|---|---|
| | | Max | Mean | Var | Med | Max | Mean | Var | Med | Max | Mean | Var | Med |
| Edge | 2353 | 78.0 | 8.0 | 101.3 | 4.0 | 95.5 | 24.8 | 273.5 | 21.7 | 48.1 | 4.0 | 7.9 | 3.3 |
| Line | 294 | 34.0 | 3.3 | 16.5 | 2.0 | 56.8 | 15.0 | 137.9 | 11.7 | 17.7 | 2.8 | 2.4 | 2.6 |
| Wide–Line | 96 | 34.0 | 5.0 | 39.3 | 2.0 | 60.4 | 17.9 | 196.3 | 12.2 | 9.3 | 3.3 | 1.6 | 3.1 |
| Right–Angle | 93 | 11.0 | 2.5 | 4.8 | 2.0 | 45.0 | 13.5 | 90.6 | 11.3 | 5.3 | 2.4 | 0.8 | 2.5 |
| Acute–Angle | 284 | 30.0 | 3.1 | 17.9 | 2.0 | 75.5 | 16.3 | 146.1 | 13.0 | 5.7 | 2.3 | 0.8 | 2.2 |
| End–Point | 447 | 27.0 | 2.5 | 7.2 | 2.0 | 49.9 | 13.9 | 106.5 | 11.1 | 6.3 | 2.2 | 0.9 | 2.0 |
| Corner | 4014 | 98.0 | 7.3 | 85.2 | 4.0 | 113.0 | 23.3 | 302.4 | 19.7 | 33.5 | 3.3 | 4.8 | 2.8 |
| L–Line | 196 | 21.0 | 3.4 | 13.5 | 2.0 | 66.7 | 17.0 | 182.2 | 13.2 | 9.9 | 2.9 | 1.2 | 2.7 |
| T–Junction | 345 | 40.0 | 3.3 | 16.1 | 2.0 | 88.7 | 16.2 | 205.6 | 12.2 | 7.9 | 2.9 | 0.9 | 2.8 |
| X–Junction | 3 | 3.0 | 1.7 | 0.9 | 1.0 | 16.4 | 9.4 | 29.9 | 8.7 | 3.9 | 3.1 | 0.3 | 2.8 |
| Y–Junction | 30 | 7.0 | 2.2 | 3.6 | 1.0 | 36.0 | 10.9 | 80.6 | 9.8 | 6.0 | 3.1 | 1.4 | 2.8 |

Table 5b – Statistics for Bright Center Pixel Masks in Lower–left Quadrant of Greenbelt1

| Class | # of Masks | Robustness | | | | Contrast | | | | Fisher distance | | | |
|---|---|---|---|---|---|---|---|---|---|---|---|---|---|
| | | Max | Mean | Var | Med | Max | Mean | Var | Med | Max | Mean | Var | Med |
| Edge | 2241 | 70.0 | 6.4 | 60.2 | 3.0 | 81.8 | 23.5 | 236.1 | 21.0 | 20.5 | 3.2 | 2.7 | 2.9 |
| Line | 338 | 74.0 | 7.6 | 113.6 | 3.0 | 82.0 | 23.1 | 258.6 | 21.3 | 24.1 | 3.5 | 7.5 | 2.9 |
| Wide–Line | 115 | 20.0 | 4.6 | 13.3 | 3.0 | 59.5 | 19.8 | 111.0 | 18.7 | 5.7 | 3.0 | 0.7 | 2.8 |
| Right–Angle | 97 | 19.0 | 3.2 | 11.2 | 2.0 | 65.3 | 18.2 | 178.0 | 15.0 | 4.9 | 2.5 | 0.5 | 2.5 |
| Acute–Angle | 277 | 48.0 | 3.9 | 23.0 | 2.0 | 79.7 | 18.5 | 193.9 | 16.2 | 6.3 | 2.8 | 0.8 | 2.7 |
| End–Point | 464 | 86.0 | 5.0 | 57.6 | 3.0 | 97.6 | 20.8 | 270.2 | 17.4 | 11.0 | 2.7 | 1.2 | 2.5 |
| Corner | 3792 | 47.0 | 4.9 | 37.4 | 3.0 | 75.7 | 20.3 | 208.6 | 17.6 | 14.2 | 2.5 | 1.5 | 2.2 |
| L–Line | 242 | 48.0 | 4.8 | 26.2 | 3.0 | 68.8 | 23.1 | 213.7 | 22.6 | 10.8 | 3.2 | 0.9 | 3.1 |
| T–Junction | 387 | 21.0 | 2.8 | 8.6 | 2.0 | 61.8 | 16.8 | 144.1 | 15.2 | 5.8 | 2.5 | 0.8 | 2.4 |
| X–Junction | 1 | 6.0 | 6.0 | 0.0 | 6.0 | 16.1 | 16.1 | 0.0 | 16.1 | 3.6 | 3.6 | 0.0 | 3.6 |
| Y–Junction | 45 | 13.0 | 3.1 | 6.6 | 2.0 | 43.4 | 15.6 | 129.2 | 13.2 | 6.1 | 2.9 | 0.9 | 2.7 |

Table 6a – Statistics for Dark Center Pixel Masks in window_7 of Greenbelt

| Class | # of Masks | Robustness | | | | Contrast | | | | Fisher distance | | | |
|---|---|---|---|---|---|---|---|---|---|---|---|---|---|
| | | Max | Mean | Var | Med | Max | Mean | Var | Med | Max | Mean | Var | Med |
| Edge | 2240 | 79.0 | 9.0 | 103.5 | 5.0 | 93.3 | 28.5 | 261.4 | 26.9 | 37.3 | 3.9 | 5.2 | 3.3 |
| Line | 311 | 25.0 | 4.1 | 16.0 | 3.0 | 59.3 | 18.8 | 113.6 | 17.5 | 7.7 | 2.5 | 0.9 | 2.3 |
| Wide-Line | 65 | 32.0 | 5.2 | 38.6 | 3.0 | 46.6 | 21.4 | 142.9 | 22.5 | 7.1 | 3.1 | 1.6 | 2.8 |
| Right-Angle | 157 | 21.0 | 3.3 | 10.6 | 2.0 | 49.7 | 18.8 | 132.6 | 18.5 | 8.5 | 2.4 | 0.9 | 2.2 |
| Acute-Angle | 355 | 29.0 | 3.7 | 16.3 | 2.0 | 59.2 | 20.1 | 129.6 | 20.2 | 5.7 | 2.4 | 0.7 | 2.3 |
| End-Point | 510 | 25.0 | 3.5 | 11.6 | 2.0 | 50.8 | 18.4 | 108.6 | 18.1 | 9.2 | 2.1 | 0.7 | 1.9 |
| Corner | 3916 | 87.0 | 9.0 | 107.1 | 5.0 | 131.0 | 27.7 | 310.1 | 25.3 | 26.0 | 3.2 | 3.4 | 2.8 |
| L-Line | 249 | 31.0 | 4.6 | 23.2 | 3.0 | 60.8 | 0.7 | 125.2 | 18.9 | 8.8 | 2.9 | 1.2 | 2.7 |
| T-Junction | 536 | 34.0 | 4.3 | 21.3 | 3.0 | 83.1 | 22.3 | 196.9 | 21.3 | 7.3 | 2.9 | 0.9 | 2.8 |
| X-Junction | 7 | 5.0 | 2.0 | 2.0 | 1.0 | 31.8 | 17.4 | 110.5 | 12.7 | 4.3 | 2.8 | 0.5 | 2.6 |
| Y-Junction | 33 | 8.0 | 2.3 | 3.3 | 1.0 | 41.0 | 14.2 | 101.9 | 11.0 | 4.9 | 2.6 | 0.8 | 2.7 |

Table 6b – Statistics for Bright Center Pixel Masks in window_7 of Greenbelt

| Class | # of Masks | Robustness | | | | Contrast | | | | Fisher distance | | | |
|---|---|---|---|---|---|---|---|---|---|---|---|---|---|
| | | Max | Mean | Var | Med | Max | Mean | Var | Med | Max | Mean | Var | Med |
| Edge | 2159 | 54.0 | 7.4 | 59.9 | 5.0 | 75.5 | 27.7 | 196.1 | 27.3 | 22.2 | 3.2 | 2.4 | 2.8 |
| Line | 367 | 68.0 | 7.0 | 74.9 | 4.0 | 86.2 | 25.8 | 249.5 | 22.3 | 10.2 | 3.2 | 1.8 | 2.9 |
| Wide-Line | 66 | 31.0 | 5.8 | 38.2 | 3.0 | 46.4 | 22.9 | 97.4 | 22.0 | 7.9 | 3.0 | 1.3 | 2.8 |
| Right-Angle | 145 | 23.0 | 4.4 | 21.7 | 3.0 | 73.3 | 24.0 | 242.1 | 21.2 | 5.9 | 2.7 | 0.7 | 2.5 |
| Acute-Angle | 364 | 36.0 | 5.0 | 28.3 | 3.0 | 71.2 | 24.6 | 210.8 | 23.8 | 10.9 | 2.9 | 1.1 | 2.8 |
| End-Point | 560 | 51.0 | 5.6 | 48.0 | 3.0 | 84.9 | 25.4 | 271.3 | 22.5 | 8.6 | 2.7 | 1.1 | 2.5 |
| Corner | 3675 | 43.0 | 5.5 | 33.1 | 3.0 | 67.9 | 24.2 | 162.7 | 23.7 | 12.2 | 2.3 | 1.4 | 2.1 |
| L-Line | 326 | 37.0 | 5.5 | 32.9 | 3.0 | 77.8 | 25.6 | 224.9 | 23.5 | 8.3 | 3.2 | 1.0 | 3.1 |
| T-Junction | 524 | 27.0 | 3.8 | 15.5 | 2.0 | 69.6 | 21.5 | 163.4 | 20.6 | 8.3 | 2.5 | 0.8 | 2.4 |
| X-Junction | 7 | 5.0 | 3.0 | 3.4 | 3.0 | 31.8 | 17.4 | 44.4 | 16.6 | 3.0 | 2.2 | 0.2 | 2.2 |
| Y-Junction | 47 | 12.0 | 2.6 | 6.1 | 2.0 | 43.3 | 15.0 | 90.9 | 15.3 | 7.2 | 2.9 | 1.2 | 2.9 |

Table 7a – Statistics for Dark Center Pixel Masks in window_5 of Greenbelt

| Class | # of Masks | Robustness | | | | Contrast | | | | Fisher distance | | | |
|---|---|---|---|---|---|---|---|---|---|---|---|---|---|
| | | Max | Mean | Var | Med | Max | Mean | Var | Med | Max | Mean | Var | Med |
| Edge | 986 | 24.0 | 2.7 | 7.0 | 2.0 | 40.2 | 8.9 | 39.1 | 7.2 | 13.9 | 3.4 | 1.7 | 3.2 |
| Line | 310 | 6.0 | 1.6 | 1.4 | 1.0 | 16.2 | 5.5 | 12.6 | 4.2 | 7.5 | 3.0 | 0.8 | 2.9 |
| Wide–Line | 40 | 3.0 | 1.1 | 0.2 | 1.0 | 12.8 | 5.1 | 8.2 | 4.2 | 6.1 | 3.1 | 0.6 | 2.8 |
| Right–Angle | 140 | 5.0 | 1.2 | 0.3 | 1.0 | 14.7 | 4.3 | 7.0 | 3.3 | 6.0 | 2.9 | 0.8 | 2.9 |
| Acute–Angle | 190 | 9.0 | 1.4 | 0.9 | 1.0 | 14.3 | 4.8 | 8.2 | 4.0 | 6.9 | 3.0 | 0.8 | 2.9 |
| End–Point | 458 | 7.0 | 1.6 | 1.0 | 1.0 | 16.0 | 5.1 | 9.1 | 4.2 | 7.2 | 2.7 | 0.8 | 2.6 |
| Corner | 2580 | 31.0 | 2.7 | 9.0 | 2.0 | 43.1 | 7.2 | 32.9 | 5.0 | 24.0 | 3.1 | 2.1 | 2.8 |
| L–Line | 178 | 10.0 | 1.8 | 2.6 | 1.0 | 16.8 | 6.1 | 15.0 | 4.6 | 7.4 | 3.3 | 1.2 | 3.2 |
| T–Junction | 395 | 6.0 | 1.5 | 0.9 | 1.0 | 22.8 | 4.8 | 9.2 | 3.9 | 7.2 | 3.0 | 0.8 | 2.9 |
| X–Junction | 14 | 2.0 | 1.1 | 0.1 | 1.0 | 7.4 | 3.4 | 2.0 | 3.3 | 4.6 | 2.9 | 0.5 | 2.8 |
| Y–Junction | 54 | 4.0 | 1.2 | 0.3 | 1.0 | 11.2 | 3.7 | 3.2 | 3.5 | 4.8 | 3.1 | 0.6 | 3.2 |

Table 7b – Statistics for Bright Center Pixel Masks in window_5 of Greenbelt

| Class | # of Masks | Robustness | | | | Contrast | | | | Fisher distance | | | |
|---|---|---|---|---|---|---|---|---|---|---|---|---|---|
| | | Max | Mean | Var | Med | Max | Mean | Var | Med | Max | Mean | Var | Med |
| Edge | 1072 | 18.0 | 2.7 | 7.0 | 2.0 | 36.0 | 9.0 | 37.0 | 7.0 | $\infty$ | $\infty$ | $\infty$ | 3.2 |
| Line | 254 | 8.0 | 1.7 | 1.7 | 1.0 | 20.3 | 4.9 | 10.2 | 3.8 | $\infty$ | $\infty$ | $\infty$ | 3.1 |
| Wide–Line | 50 | 9.0 | 1.5 | 1.5 | 1.0 | 23.5 | 4.8 | 13.6 | 3.9 | 6.6 | 3.1 | 0.8 | 3.0 |
| Right–Angle | 153 | 6.0 | 1.4 | 0.7 | 1.0 | 22.0 | 4.8 | 10.9 | 3.8 | 9.8 | 2.9 | 1.0 | 2.7 |
| Acute–Angle | 241 | 14.0 | 1.6 | 1.7 | 1.0 | 28.0 | 5.9 | 19.1 | 4.3 | 6.1 | 3.0 | 0.8 | 2.9 |
| End–Point | 470 | 20.0 | 1.7 | 2.5 | 1.0 | 29.4 | 5.2 | 14.5 | 4.1 | 10.6 | 2.9 | 1.1 | 2.7 |
| Corner | 2551 | 24.0 | 2.3 | 5.1 | 1.0 | 40.4 | 6.9 | 26.8 | 5.0 | $\infty$ | $\infty$ | $\infty$ | 2.6 |
| L–Line | 148 | 8.0 | 1.3 | 0.7 | 1.0 | 14.8 | 5.2 | 8.8 | 4.4 | 7.1 | 3.2 | 0.9 | 3.1 |
| T–Junction | 411 | 9.0 | 1.4 | 0.7 | 1.0 | 24.4 | 4.9 | 9.7 | 4.0 | 6.2 | 2.9 | 0.8 | 2.8 |
| X–Junction | 5 | 2.0 | 1.2 | 0.2 | 1.0 | 4.1 | 3.6 | 0.3 | 3.7 | 4.4 | 3.1 | 0.6 | 2.8 |
| Y–Junction | 60 | 3.0 | 1.1 | 0.1 | 1.0 | 8.0 | 3.4 | 2.0 | 3.2 | $\infty$ | $\infty$ | $\infty$ | 2.9 |

Table 8a – Statistics for Dark Center Pixel Masks in window_6 of Greenbelt

| Class | # of Masks | Robustness | | | | Contrast | | | | Fisher distance | | | |
|---|---|---|---|---|---|---|---|---|---|---|---|---|---|
| | | Max | Mean | Var | Med | Max | Mean | Var | Med | Max | Mean | Var | Med |
| Edge | 1110 | 26.0 | 2.3 | 6.7 | 1.0 | 37.5 | 6.8 | 32.1 | 4.5 | ∞ | ∞ | ∞ | 3.4 |
| Line | 305 | 8.0 | 1.5 | 0.8 | 1.0 | 16.0 | 4.1 | 6.0 | 3.5 | ∞ | ∞ | ∞ | 3.2 |
| Wide–Line | 38 | 5.0 | 1.3 | 0.6 | 1.0 | 10.1 | 4.0 | 4.5 | 3.5 | 5.0 | 3.2 | 0.5 | 3.1 |
| Right–Angle | 68 | 3.0 | 1.1 | 0.1 | 1.0 | 13.8 | 3.2 | 3.8 | 2.8 | 6.1 | 2.9 | 1.0 | 2.8 |
| Acute–Angle | 175 | 6.0 | 1.2 | 0.4 | 1.0 | 19.5 | 4.0 | 6.5 | 3.3 | 6.5 | 3.0 | 0.8 | 2.9 |
| End–Point | 398 | 7.0 | 1.3 | 0.6 | 1.0 | 20.7 | 3.9 | 5.6 | 3.4 | 6.6 | 2.8 | 0.9 | 2.8 |
| Corner | 2576 | 31.0 | 2.1 | 5.8 | 1.0 | 55.1 | 5.5 | 24.6 | 3.7 | ∞ | ∞ | ∞ | 2.8 |
| L–Line | 201 | 7.0 | 1.4 | 0.6 | 1.0 | 18.2 | 4.2 | 7.3 | 3.4 | ∞ | ∞ | ∞ | 3.3 |
| T–Junction | 310 | 12.0 | 1.4 | 1.3 | 1.0 | 24.1 | 4.3 | 13.2 | 3.1 | ∞ | ∞ | ∞ | 3.0 |
| X–Junction | 3 | 1.0 | 1.0 | 0.0 | 1.0 | 2.1 | 1.7 | 0.1 | 1.7 | 4.5 | 3.1 | 1.0 | 2.5 |
| Y–Junction | 34 | 5.0 | 1.3 | 0.9 | 1.0 | 12.2 | 3.0 | 5.3 | 2.3 | 6.1 | 3.6 | 1.0 | 3.5 |

Table 8b – Statistics for Bright Center Pixel Masks in window_6 of Greenbelt

| Class | # of Masks | Robustness | | | | Contrast | | | | Fisher distance | | | |
|---|---|---|---|---|---|---|---|---|---|---|---|---|---|
| | | Max | Mean | Var | Med | Max | Mean | Var | Med | Max | Mean | Var | Med |
| Edge | 1143 | 25.0 | 2.1 | 3.8 | 1.0 | 39.6 | 6.4 | 24.6 | 4.3 | ∞ | ∞ | ∞ | 3.3 |
| Line | 249 | 23.0 | 1.9 | 6.1 | 1.0 | 26.0 | 4.9 | 20.2 | 3.3 | ∞ | ∞ | ∞ | 3.2 |
| Wide–Line | 42 | 2.0 | 1.1 | 0.1 | 1.0 | 18.2 | 3.9 | 8.6 | 3.0 | 4.1 | 3.0 | 0.3 | 3.1 |
| Right–Angle | 72 | 10.0 | 1.3 | 1.4 | 1.0 | 22.5 | 4.1 | 15.7 | 3.0 | 4.5 | 3.0 | 0.5 | 2.9 |
| Acute–Angle | 190 | 10.0 | 1.2 | 0.7 | 1.0 | 23.2 | 4.2 | 11.1 | 3.1 | 6.1 | 3.0 | 0.6 | 3.0 |
| End–Point | 408 | 24.0 | 1.7 | 4.4 | 1.0 | 36.8 | 4.7 | 19.3 | 3.3 | ∞ | ∞ | ∞ | 2.8 |
| Corner | 2409 | 20.0 | 1.7 | 1.9 | 1.0 | 35.9 | 4.9 | 13.5 | 3.8 | ∞ | ∞ | ∞ | 2.7 |
| L–Line | 180 | 10.0 | 1.6 | 1.2 | 1.0 | 23.8 | 5.1 | 17.1 | 3.6 | 9.9 | 3.5 | 1.3 | 3.3 |
| T–Junction | 324 | 7.0 | 1.3 | 0.5 | 1.0 | 17.6 | 4.5 | 11.2 | 3.1 | 6.4 | 3.0 | 0.8 | 2.9 |
| X–Junction | 8 | 1.0 | 1.0 | 0.0 | 1.0 | 3.8 | 2.3 | 0.5 | 2.1 | 4.4 | 3.3 | 0.6 | 3.0 |
| Y–Junction | 27 | 5.0 | 1.4 | 1.4 | 1.0 | 11.3 | 3.2 | 7.1 | 2.3 | 6.1 | 3.4 | 0.7 | 3.2 |

Table 9a – Statistics for Dark Center Pixel Masks in a 64×64 "White Noise" Image with $\mu=127$, $\sigma=10$

| Class | # of Masks | Robustness | | | | Contrast | | | | Fisher distance | | | |
|---|---|---|---|---|---|---|---|---|---|---|---|---|---|
| | | Max | Mean | Var | Med | Max | Mean | Var | Med | Max | Mean | Var | Med |
| Edge | 529 | 16.0 | 3.4 | 6.4 | 3.0 | 29.8 | 15.0 | 13.5 | 14.9 | 8.0 | 2.9 | 0.7 | 2.8 |
| Line | 461 | 15.0 | 3.3 | 6.1 | 3.0 | 30.2 | 15.0 | 15.7 | 14.8 | 7.5 | 2.8 | 0.7 | 2.7 |
| Wide-Line | 121 | 11.0 | 3.3 | 6.5 | 2.0 | 24.8 | 14.4 | 12.3 | 14.4 | 6.1 | 3.1 | 0.6 | 3.0 |
| Right-Angle | 309 | 15.0 | 3.3 | 6.7 | 2.0 | 55.3 | 15.2 | 21.7 | 14.5 | 10.2 | 2.9 | 0.8 | 2.8 |
| Acute-Angle | 336 | 14.0 | 3.4 | 6.0 | 3.0 | 27.7 | 15.1 | 15.8 | 14.8 | 8.6 | 2.8 | 0.6 | 2.7 |
| End-Point | 754 | 22.0 | 4.0 | 9.5 | 3.0 | 75.1 | 15.7 | 24.2 | 15.1 | 7.5 | 2.7 | 0.7 | 2.6 |
| Corner | 2448 | 28.0 | 5.0 | 16.7 | 4.0 | 40.0 | 16.2 | 24.1 | 15.6 | 21.8 | 2.5 | 0.9 | 2.3 |
| L-Line | 213 | 14.0 | 3.2 | 6.7 | 2.0 | 27.8 | 15.0 | 13.0 | 14.4 | 10.4 | 2.9 | 0.8 | 2.8 |
| T-Junction | 697 | 17.0 | 3.6 | 7.0 | 3.0 | 30.6 | 15.3 | 15.3 | 14.9 | 7.8 | 2.8 | 0.7 | 2.7 |
| X-Junction | 47 | 7.0 | 2.6 | 2.2 | 2.0 | 21.0 | 14.1 | 8.8 | 14.1 | 3.9 | 2.8 | 0.3 | 2.7 |
| Y-Junction | 198 | 13.0 | 3.3 | 6.5 | 2.0 | 29.9 | 14.8 | 12.3 | 14.7 | 8.6 | 3.0 | 0.8 | 2.9 |

Table 9b – Statistics for Bright Center Pixel Masks in a 64×64 "White Noise" Image with $\mu=127$, $\sigma=10$

| Class | # of Masks | Robustness | | | | Contrast | | | | Fisher distance | | | |
|---|---|---|---|---|---|---|---|---|---|---|---|---|---|
| | | Max | Mean | Var | Med | Max | Mean | Var | Med | Max | Mean | Var | Med |
| Edge | 556 | 16.0 | 3.6 | 6.9 | 3.0 | 28.8 | 15.4 | 14.9 | 15.3 | 8.9 | 2.9 | 0.7 | 2.8 |
| Line | 471 | 16.0 | 3.6 | 7.4 | 3.0 | 27.0 | 15.1 | 14.2 | 15.0 | 7.8 | 2.9 | 0.8 | 2.7 |
| Wide-Line | 107 | 9.0 | 3.0 | 4.6 | 2.0 | 21.6 | 14.3 | 11.8 | 14.3 | 6.3 | 2.9 | 0.6 | 2.8 |
| Right-Angle | 323 | 14.0 | 3.3 | 6.9 | 3.0 | 26.5 | 14.9 | 14.2 | 14.5 | 6.0 | 2.8 | 0.6 | 2.7 |
| Acute-Angle | 312 | 13.0 | 3.3 | 6.2 | 3.0 | 27.8 | 15.1 | 14.1 | 14.7 | 12.1 | 2.9 | 0.9 | 2.7 |
| End-Point | 755 | 17.0 | 3.9 | 9.1 | 3.0 | 30.4 | 15.4 | 15.9 | 15.2 | 10.2 | 2.6 | 0.8 | 2.5 |
| Corner | 2466 | 115.0 | 5.2 | 24.5 | 4.0 | 130.4 | 16.4 | 32.9 | 15.7 | 13.3 | 2.5 | 0.9 | 2.3 |
| L-Line | 220 | 19.0 | 3.3 | 7.0 | 2.0 | 27.1 | 15.0 | 15.3 | 14.5 | 11.4 | 3.0 | 1.0 | 2.8 |
| T-Junction | 668 | 16.0 | 3.6 | 7.5 | 3.0 | 33.5 | 15.2 | 17.2 | 14.8 | 10.9 | 2.8 | 0.8 | 2.7 |
| X-Junction | 34 | 8.0 | 3.4 | 4.4 | 3.0 | 27.4 | 15.0 | 15.2 | 14.6 | 4.2 | 2.9 | 0.4 | 2.8 |
| Y-Junction | 219 | 12.0 | 3.1 | 6.5 | 2.0 | 24.2 | 14.8 | 12.5 | 14.4 | 5.8 | 3.0 | 0.6 | 2.9 |

**Table 10a – Statistics for Dark Center Pixel Masks in a 64×64 "White Noise" Image with $\mu=127$, $\sigma=20$**

| Class | # of Masks | Robustness | | | | Contrast | | | | Fisher distance | | | |
|---|---|---|---|---|---|---|---|---|---|---|---|---|---|
| | | Max | Mean | Var | Med | Max | Mean | Var | Med | Max | Mean | Var | Med |
| Edge | 524 | 33.0 | 6.5 | 27.6 | 5.0 | 53.3 | 29.9 | 70.6 | 28.9 | 6.6 | 2.9 | 0.7 | 2.8 |
| Line | 524 | 27.0 | 6.1 | 23.9 | 5.0 | 56.2 | 30.3 | 65.5 | 30.2 | 7.4 | 2.8 | 0.6 | 2.7 |
| Wide-Line | 108 | 27.0 | 5.9 | 21.9 | 4.0 | 54.6 | 29.5 | 73.3 | 28.6 | 5.8 | 2.9 | 0.6 | 2.9 |
| Right-Angle | 339 | 29.0 | 6.0 | 26.2 | 4.0 | 58.8 | 29.8 | 75.3 | 28.8 | 7.4 | 2.8 | 0.6 | 2.7 |
| Acute-Angle | 309 | 27.0 | 6.6 | 31.5 | 5.0 | 54.8 | 30.9 | 75.3 | 30.2 | 11.6 | 2.9 | 1.0 | 2.7 |
| End-Point | 801 | 40.0 | 7.8 | 40.5 | 6.0 | 60.4 | 31.7 | 84.9 | 30.8 | 9.1 | 2.7 | 0.7 | 2.5 |
| Corner | 2574 | 67.0 | 9.6 | 72.0 | 7.0 | 90.6 | 32.3 | 113.8 | 30.9 | 8.3 | 2.5 | 0.8 | 2.3 |
| L-Line | 245 | 28.0 | 6.2 | 24.1 | 5.0 | 50.9 | 30.6 | 64.4 | 30.3 | 6.1 | 2.8 | 0.5 | 2.7 |
| T-Junction | 743 | 39.0 | 6.9 | 35.6 | 5.0 | 65.4 | 30.8 | 78.6 | 30.5 | 7.3 | 2.8 | 0.7 | 2.6 |
| X-Junction | 53 | 15.0 | 6.0 | 15.4 | 5.0 | 44.2 | 27.6 | 48.2 | 27.9 | 5.5 | 2.8 | 0.5 | 2.7 |
| Y-Junction | 239 | 26.0 | 5.8 | 21.3 | 5.0 | 55.7 | 29.4 | 66.7 | 28.7 | 5.3 | 2.9 | 0.5 | 2.7 |

**Table 10b – Statistics for Bright Center Pixel Masks in a 64×64 "White Noise" Image with $\mu=127$, $\sigma=20$**

| Class | # of Masks | Robustness | | | | Contrast | | | | Fisher distance | | | |
|---|---|---|---|---|---|---|---|---|---|---|---|---|---|
| | | Max | Mean | Var | Med | Max | Mean | Var | Med | Max | Mean | Var | Med |
| Edge | 540 | 29.0 | 6.4 | 30.3 | 5.0 | 66.2 | 29.3 | 72.4 | 28.4 | 13.0 | 2.9 | 1.0 | 2.8 |
| Line | 517 | 32.0 | 6.6 | 29.4 | 5.0 | 65.3 | 30.6 | 78.7 | 30.0 | 5.5 | 2.8 | 0.5 | 2.6 |
| Wide-Line | 97 | 32.0 | 6.1 | 28.5 | 4.0 | 50.5 | 29.4 | 54.8 | 29.6 | 5.7 | 2.9 | 0.5 | 2.9 |
| Right-Angle | 345 | 34.0 | 6.5 | 29.6 | 5.0 | 57.3 | 29.7 | 76.8 | 28.5 | 6.6 | 2.8 | 0.7 | 2.6 |
| Acute-Angle | 331 | 22.0 | 6.0 | 18.8 | 5.0 | 55.0 | 29.8 | 62.0 | 28.5 | 5.1 | 2.7 | 0.5 | 2.7 |
| End-Point | 803 | 38.0 | 7.5 | 37.3 | 6.0 | 68.6 | 31.3 | 91.5 | 30.1 | 9.4 | 2.6 | 0.7 | 2.4 |
| Corner | 2535 | 104.0 | 10.2 | 80.5 | 8.0 | 133.3 | 32.8 | 118.7 | 31.8 | 9.9 | 2.5 | 0.9 | 2.3 |
| L-Line | 229 | 26.0 | 5.8 | 20.5 | 4.0 | 56.6 | 29.5 | 62.6 | 29.2 | 7.0 | 2.9 | 0.5 | 2.8 |
| T-Junction | 777 | 30.0 | 6.9 | 31.6 | 5.0 | 61.2 | 30.6 | 81.3 | 29.8 | 6.4 | 2.7 | 0.7 | 2.6 |
| X-Junction | 60 | 24.0 | 5.2 | 22.6 | 3.0 | 54.1 | 29.5 | 91.0 | 27.9 | 4.4 | 2.8 | 0.4 | 2.6 |
| Y-Junction | 247 | 29.0 | 6.0 | 23.5 | 5.0 | 53.7 | 30.1 | 66.1 | 29.9 | 6.5 | 2.9 | 0.6 | 2.8 |
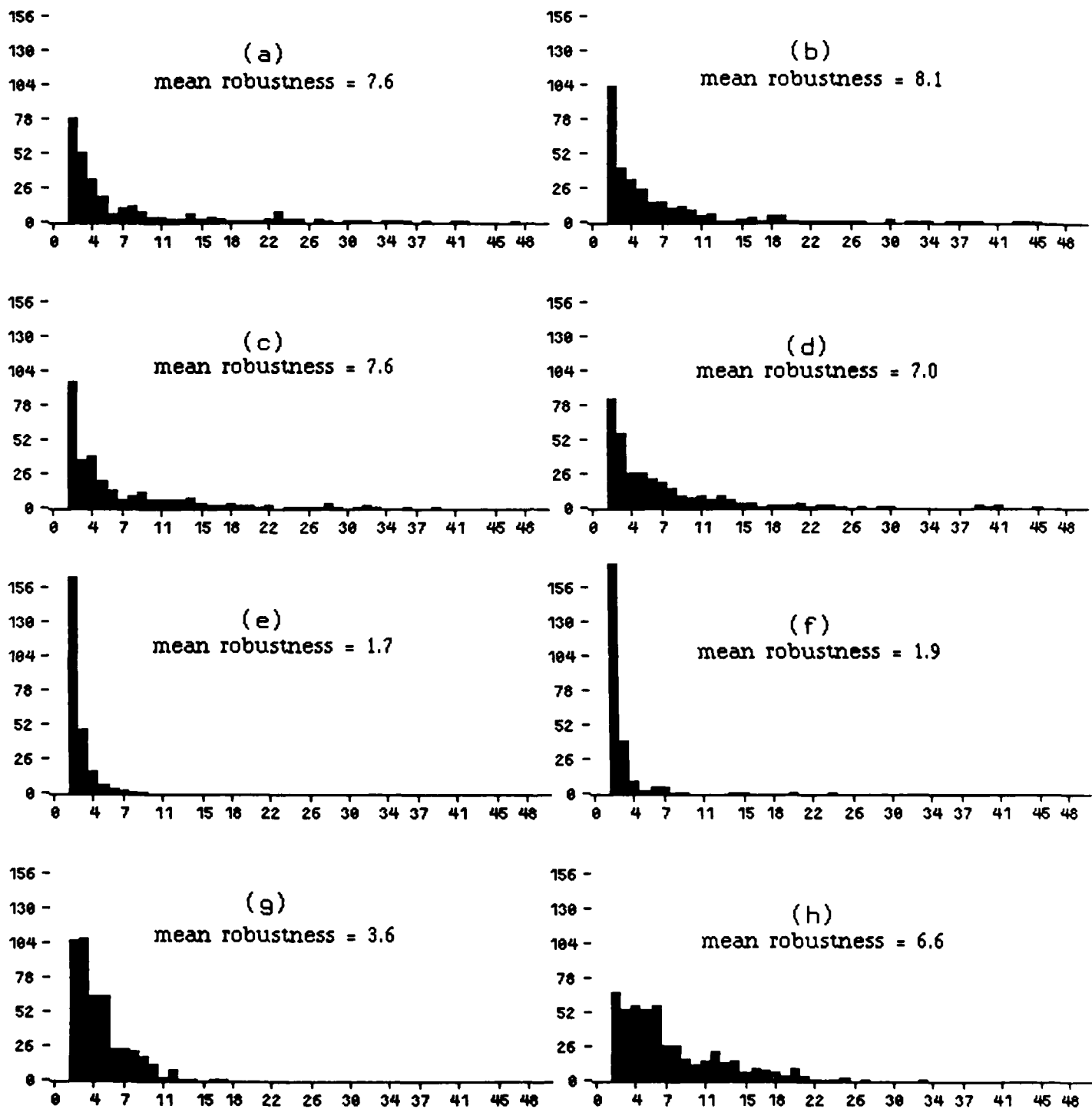
**Figure 12. Robustness Histograms for Bright CP Line Masks in 64 × 64 Images.**

(a), (b), (c), (d):  **suburban:** upper–left, upper–right, lower–left, window_7.

(e), (f):   **homogeneous:** window_5, window_6.

(g), (h):   **white noise** with $\sigma=10$, $\sigma=20$.
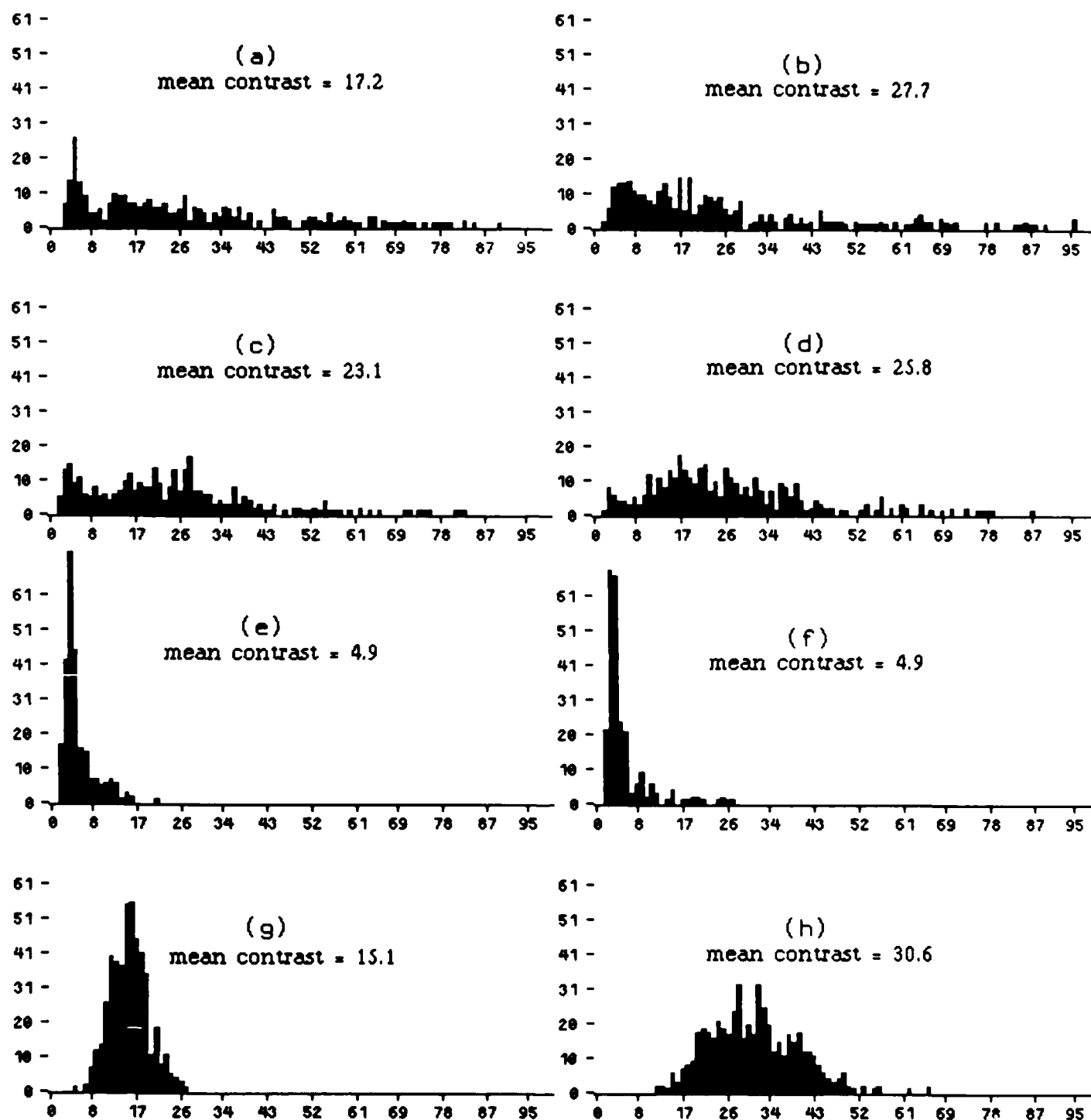
**Figure 13. Contrast Histograms for Bright CP Line Masks in 64 × 64 Images.**

(a), (b), (c), (d):  **suburban:** upper-left, upper-right, lower-left, window_7.

(e), (f):  **homogeneous:** window_5, window_6.

(g), (h):  **white noise** with $\sigma = 10$, $\sigma = 20$.
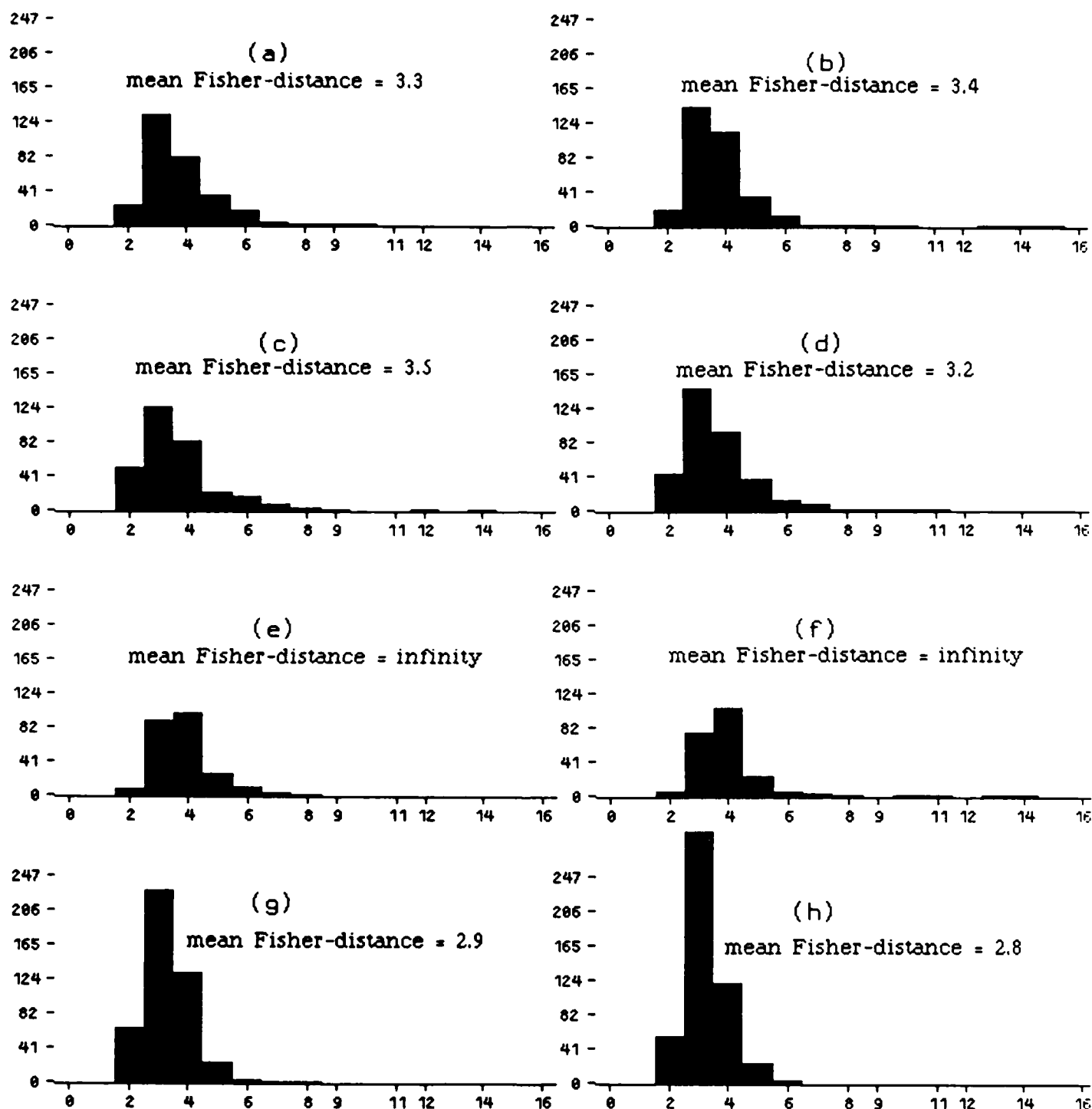
**Figure 14. Fisher–Distance Histograms for Bright CP Line Masks in 64 × 64 Images.**

(a), (b), (c), (d):   **suburban:** upper–left, upper–right, lower–left, window_7.

(e), (f):                   **homogeneous:** window_5, window_6.

(g), (h):                   **white noise** with $\sigma=10$, $\sigma=20$.

41

### 4.2.3. Statistics of Dark vs. Bright CP Masks

Linear features in an image include both bright features on a dark background and dark features on a bright background. It is of interest to compare the statistics obtained for bright and dark CP masks, which should respond to these two types of features.

The results presented in Tables 2 through 10a-b indicate the following facts:

(1) There is no significant difference between the frequencies of occurrence of dark and bright CP masks, even though some of the images seem to contain more bright linear features.

(2) The values of most of the statistical properties are approximately the same for both dark and bright CP masks in the homogeneous and white noise images.

(3) In the suburban images, the mean and median robustness and contrast of the bright CP masks are generally greater than those of the dark CP masks. Since the roads in the Greenbelt images are bright, this would suggest that it might be appropriate to supress weak masks, but we have already seen that this yields poor results. A more interesting suggestion is that if the robustness and contrast values of, say, the bright CP masks are significantly greater than those of the dark CP masks, we have evidence that the image is not homogeneous or white noise, and may contain bright linear features. (This ignores the possibility that an image may contain both dark linear features on a bright background and bright features on a dark background.)

However, even if this assertion is correct, it can only be thought of as an aid in labeling an image region as a whole, but not as a means of detecting individual linear features.

### 4.2.4. Characterization of "Line–Like" Masks at Pixels where the NLD Responds

If we assume that the nonlinear line detector (NLD) provides "image truth" for the location of linear features, it is of interest to compare the statistics obtained for line–like masks at pixels where the NLD responds with those obtained at pixels where it does not respond.

The results, given in Tables 11-12, and the histograms, shown in Figures 15a-c through 17a-c, indicate the following facts. As might be expected, the frequency of occurrence of bright CP line–like masks at pixels where the NLD responds is generally much greater than at pixels where it does not respond. Similarly, for suburban and homogeneous images, the mean robustness and contrast values at pixels where the NLD responds are greater than the values at pixels where it does not respond. (This is not true for white noise images.) These results show, not surprisingly, that the line–like masks tend to be matched at the same pixels at which the NLD responds.

## Table 11 – Statistical Results for Bright CP Line–Like Masks at Pixels where Nonlinear Detector Responds

| Name | Type | Size | % of Masks vs. Magnitude | | | Mean Robustness vs. Magnitude | | | Mean Contrast vs. Magnitude | | | Mean Fisher–distance vs. Magnitude | | |
|---|---|---|---|---|---|---|---|---|---|---|---|---|---|---|
| | | | 1 | 5 | 10 | 1 | 5 | 10 | 1 | 5 | 10 | 1 | 5 | 10 |
| window_4 | suburban | 20×20 | 21.9 | 21.0 | 20.0 | 8.4 | 8.7 | 9.0 | 33.0 | 34.3 | 35.5 | 3.2 | 3.2 | 3.2 |
| window_8 | suburban | 48×64 | 15.8 | 15.1 | 13.5 | 6.1 | 6.3 | 6.8 | 25.5 | 26.5 | 28.7 | 3.2 | 3.2 | 3.2 |
| window_7 | suburban | 64×64 | 16.2 | 15.5 | 14.4 | 6.8 | 7.0 | 7.4 | 27.1 | 28.2 | 29.5 | 3.3 | 3.3 | 3.3 |
| upper–left | suburban | 64×64 | 13.3 | 11.8 | 10.0 | 7.1 | 7.9 | 8.9 | 27.9 | 31.0 | 35.0 | 3.3 | 3.3 | 3.3 |
| upper–right | suburban | 64×64 | 13.6 | 12.9 | 10.6 | 7.2 | 7.5 | 8.7 | 28.8 | 30.3 | 35.1 | 3.3 | 3.3 | 3.3 |
| lower–left | suburban | 64×64 | 14.2 | 12.7 | 11.2 | 6.6 | 7.3 | 7.9 | 23.7 | 26.1 | 28.2 | 3.5 | 3.5 | 3.6 |
| lower–right | suburban | 64×64 | 13.1 | 12.0 | 10.4 | 5.4 | 5.8 | 6.4 | 23.3 | 25.1 | 27.8 | 3.2 | 3.2 | 3.2 |
| window_1 | homogeneous | 16×16 | 9.2 | 0 | 0 | 1.1 | - | - | 2.4 | - | - | 3.7 | - | - |
| window_2 | homogeneous | 16×24 | 11.4 | 7.8 | 5.2 | 5.8 | 7.9 | 11.0 | 23.1 | 32.2 | 45.2 | 3.4 | 3.5 | 3.8 |
| window_3 | homogeneous | 16×24 | 9.7 | 5.8 | 3.2 | 3.1 | 4.4 | 6.4 | 14.5 | 21.4 | 32.7 | 3.1 | 3.0 | 3.1 |
| window_5 | homogeneous | 64×64 | 8.2 | 3.0 | 0.8 | 1.7 | 2.5 | 3.8 | 5.4 | 8.6 | 13.1 | 3.3 | 3.3 | 3.4 |
| window_6 | homogeneous | 64×64 | 8.9 | 2.7 | 1.1 | 1.8 | 3.3 | 5.2 | 5.4 | 10.7 | 16.3 | $\infty$ | 3.8 | 4.3 |
| $\mu=127, \sigma=5$ | white noise | 62×62 | 14.2 | 12.8 | 1.9 | 2.0 | 2.1 | 2.9 | 7.9 | 8.1 | 10.9 | 3.0 | 3.0 | 3.2 |
| $\mu=127, \sigma=10$ | white noise | 62×62 | 17.4 | 17.4 | 15.1 | 3.5 | 3.5 | 3.7 | 15.0 | 15.0 | 15.7 | 2.9 | 2.9 | 2.9 |
| $\mu=127, \sigma=15$ | white noise | 62×62 | 17.2 | 17.2 | 17.0 | 4.7 | 4.7 | 4.7 | 22.9 | 22.9 | 23.0 | 2.8 | 2.8 | 2.8 |
| $\mu=127, \sigma=20$ | white noise | 62×62 | 18.8 | 18.8 | 18.7 | 6.6 | 6.6 | 6.6 | 30.5 | 30.5 | 30.6 | 2.8 | 2.8 | 2.8 |
| $\mu=127, \sigma=25$ | white noise | 62×62 | 18.6 | 18.6 | 18.6 | 7.8 | 7.8 | 7.8 | 38.0 | 38.0 | 38.0 | 2.8 | 2.8 | 2.8 |
| $\mu=127, \sigma=30$ | white noise | 62×62 | 18.9 | 18.9 | 18.9 | 9.1 | 9.1 | 9.1 | 45.7 | 45.7 | 45.7 | 2.8 | 2.8 | 2.8 |
| $\mu=127, \sigma=35$ | white noise | 62×62 | 20.0 | 20.0 | 20.0 | 10.3 | 10.3 | 10.3 | 52.7 | 52.7 | 52.7 | 2.8 | 2.8 | 2.8 |

Table 12 – Statistical Results for Bright CP Line–Like Masks at Pixels where Nonlinear Detector Does Not Respond

| Name | Type | Size | % of Masks vs. Magnitude | | | Mean Robustness vs. Magnitude | | | Mean Contrast vs. Magnitude | | | Mean Fisher-distance vs. Magnitude | | |
|---|---|---|---|---|---|---|---|---|---|---|---|---|---|---|
| | | | 1 | 5 | 10 | 1 | 5 | 10 | 1 | 5 | 10 | 1 | 5 | 10 |
| window_4 | suburban | 20×20 | 4.3 | 5.2 | 6.2 | 4.9 | 4.2 | 3.8 | 23.4 | 19.9 | 18.3 | 2.8 | 2.7 | 2.7 |
| window_8 | suburban | 48×64 | 2.8 | 3.4 | 5.0 | 4.4 | 3.8 | 3.2 | 18.4 | 15.7 | 13.3 | 3.0 | 3.0 | 3.0 |
| window_7 | suburban | 64×64 | 3.6 | 4.3 | 5.3 | 3.9 | 3.5 | 3.2 | 18.0 | 15.7 | 14.5 | 2.9 | 2.9 | 3.0 |
| upper-left | suburban | 64×64 | 3.4 | 4.9 | 6.7 | 4.9 | 3.8 | 3.4 | 21.7 | 16.2 | 14.2 | 3.0 | 3.1 | 3.1 |
| upper-right | suburban | 64×64 | 3.9 | 4.7 | 7.0 | 2.9 | 2.6 | 2.4 | 16.9 | 14.8 | 12.6 | 2.6 | 2.7 | 2.8 |
| lower-left | suburban | 64×64 | 3.9 | 5.4 | 6.8 | 4.2 | 3.3 | 3.1 | 18.4 | 14.3 | 13.3 | 2.8 | 2.9 | 2.9 |
| lower-right | suburban | 64×64 | 3.0 | 4.1 | 5.7 | 3.5 | 2.9 | 2.6 | 17.9 | 14.4 | 12.4 | 2.8 | 2.8 | 2.8 |
| window_1 | homogeneous | 16×16 | 1.5 | 10.7 | 10.7 | 1.0 | 1.0 | 1.0 | 2.6 | 2.5 | 2.5 | 3.7 | 3.7 | 3.7 |
| window_2 | homogeneous | 16×24 | 2.6 | 6.2 | 8.8 | 1.1 | 1.2 | 1.3 | 4.4 | 3.9 | 4.5 | 2.6 | 3.0 | 2.9 |
| window_3 | homogeneous | 16×24 | 2.6 | 6.5 | 9.1 | 2.4 | 1.6 | 1.7 | 7.8 | 5.6 | 6.1 | 3.0 | 3.2 | 3.0 |
| window_5 | homogeneous | 64×64 | 3.5 | 8.8 | 11.0 | 1.2 | 1.2 | 1.4 | 4.1 | 3.7 | 4.4 | ∞ | ∞ | ∞ |
| window_6 | homogeneous | 64×64 | 3.4 | 9.6 | 11.2 | 1.2 | 1.2 | 1.3 | 3.6 | 3.3 | 3.8 | 3.3 | ∞ | ∞ |
| $\mu=127,\ \sigma=5$ | white noise | 62×62 | 3.2 | 4.6 | 15.5 | 1.8 | 1.6 | 1.8 | 7.2 | 6.7 | 7.4 | 2.9 | 2.9 | 2.9 |
| $\mu=127,\ \sigma=10$ | white noise | 62×62 | 3.5 | 3.6 | 5.9 | 3.3 | 3.3 | 2.8 | 14.6 | 14.5 | 12.9 | 3.0 | 3.0 | 2.8 |
| $\mu=127,\ \sigma=15$ | white noise | 62×62 | 3.2 | 3.2 | 3.4 | 4.5 | 4.5 | 4.3 | 22.0 | 22.0 | 21.5 | 2.7 | 2.7 | 2.7 |
| $\mu=127,\ \sigma=20$ | white noise | 62×62 | 3.4 | 3.4 | 3.5 | 5.0 | 5.0 | 5.0 | 27.8 | 27.8 | 27.6 | 2.7 | 2.7 | 2.7 |
| $\mu=127,\ \sigma=25$ | white noise | 62×62 | 3.4 | 3.4 | 3.4 | 7.0 | 7.0 | 7.0 | 35.6 | 35.6 | 35.6 | 2.8 | 2.8 | 2.8 |
| $\mu=127,\ \sigma=30$ | white noise | 62×62 | 3.3 | 3.3 | 3.3 | 8.1 | 8.1 | 8.1 | 40.0 | 40.0 | 40.0 | 2.8 | 2.8 | 2.8 |
| $\mu=127,\ \sigma=35$ | white noise | 62×62 | 3.4 | 3.4 | 3.4 | 7.8 | 7.8 | 7.8 | 47.3 | 47.3 | 47.3 | 2.6 | 2.6 | 2.6 |
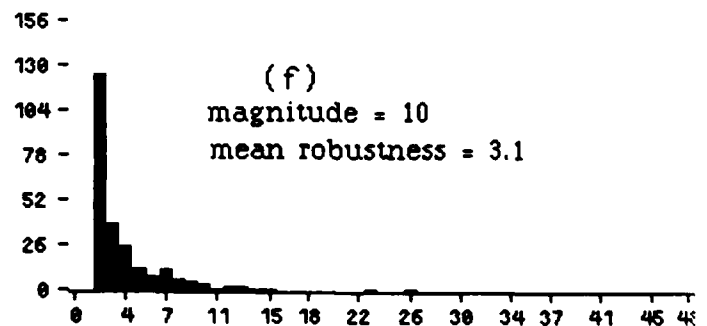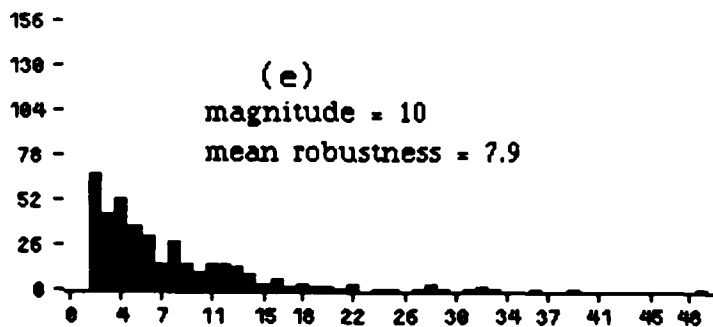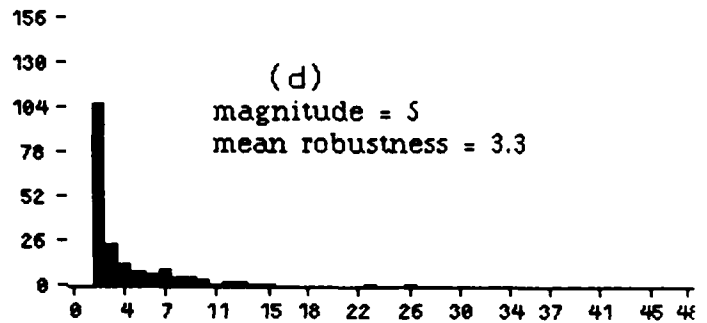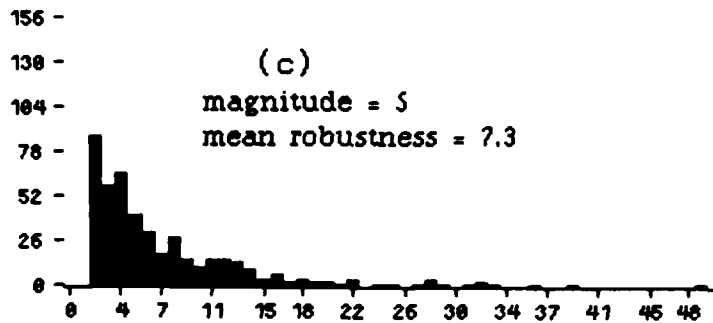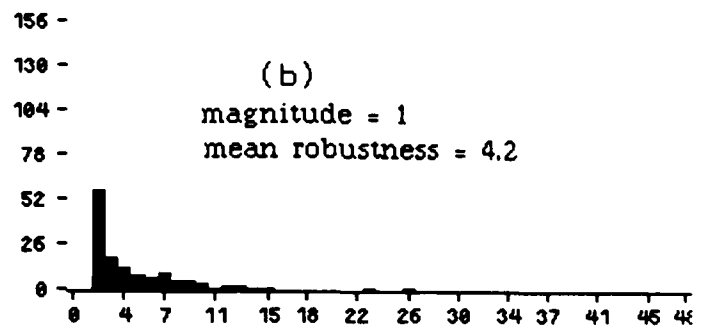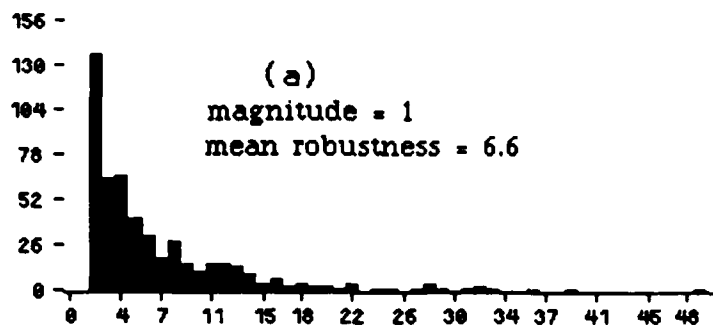
**Figure 15a. Robustness Histograms for Bright CP Line–Like Masks in Lower–left Quadrant.**

(a), (c), (e): at pixels where nonlinear detector responds.

(b), (e), (f): at pixels where nonlinear detector does not respond.
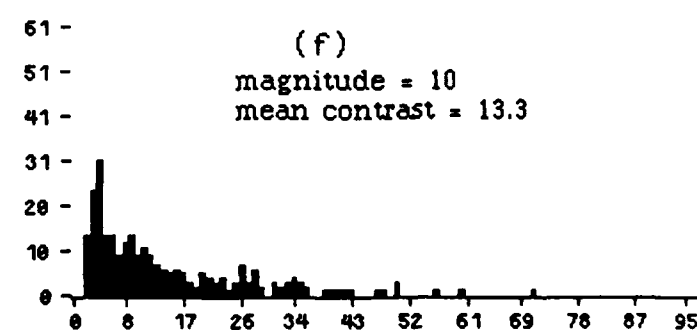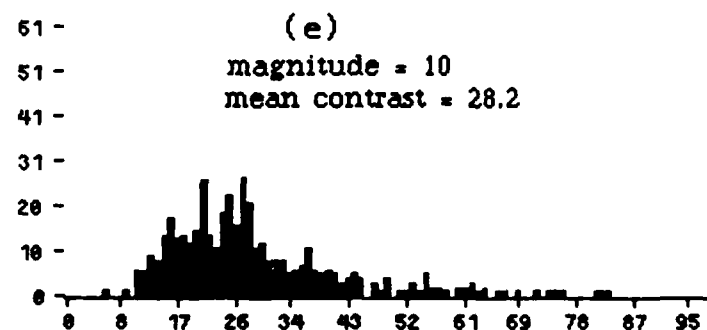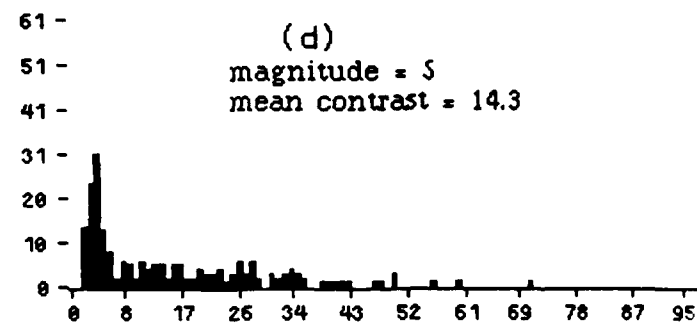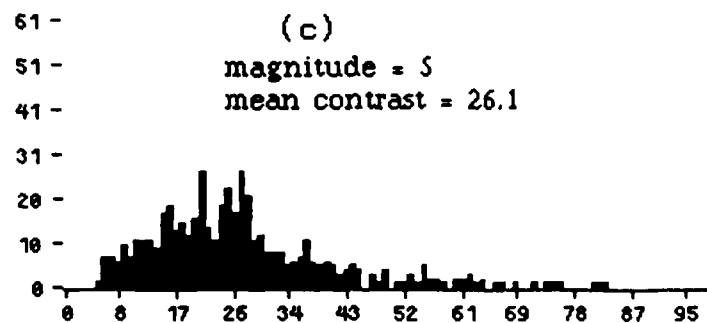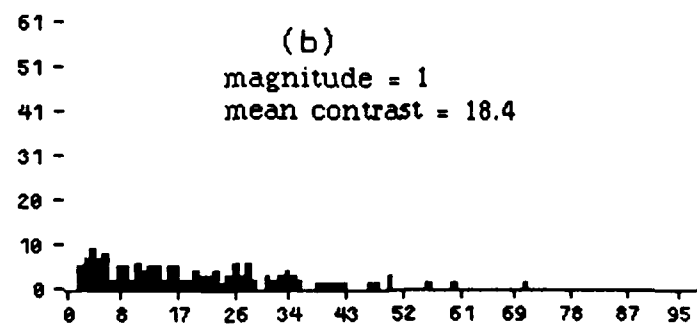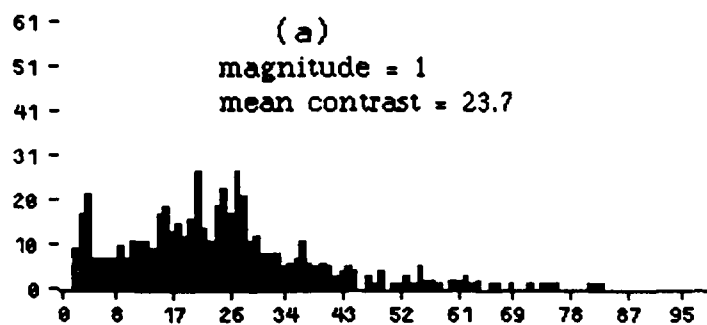
**Figure 15b. Contrast Histograms for Bright CP Line–Like Masks in Lower–left Quadrant.**

(a), (c), (e):  at pixels where nonlinear detector responds.

(b), (e), (f):  at pixels where nonlinear detector does not respond.

247 –
206 –
165 –
124 –
82 –
41 –
0 –
0  2  4  6  8  9  11 12  14  16

(a)
magnitude = 1
mean Fisher-distance = 3.5

247 –
206 –
165 –
124 –
82 –
41 –
0 –
0  2  4  6  8  9  11 12  14  16

(b)
magnitude = 1
mean Fisher-distance = 2.8

247 –
206 –
165 –
124 –
82 –
41 –
0 –
0  2  4  6  8  9  11 12  14  16

(c)
magnitude = 5
mean Fisher-distance = 3.5

247 –
206 –
165 –
124 –
82 –
41 –
0 –
0  2  4  6  8  9  11 12  14  16

(d)
magnitude = 5
mean Fisher-distance = 2.9

247 –
206 –
165 –
124 –
82 –
41 –
0 –
0  2  4  6  8  9  11 12  14  16

(e)
magnitude = 10
mean Fisher-distance = 3.6

247 –
206 –
165 –
124 –
82 –
41 –
0 –
0  2  4  6  8  9  11 12  14  16

(f)
magnitude = 10
mean Fisher-distance = 2.9
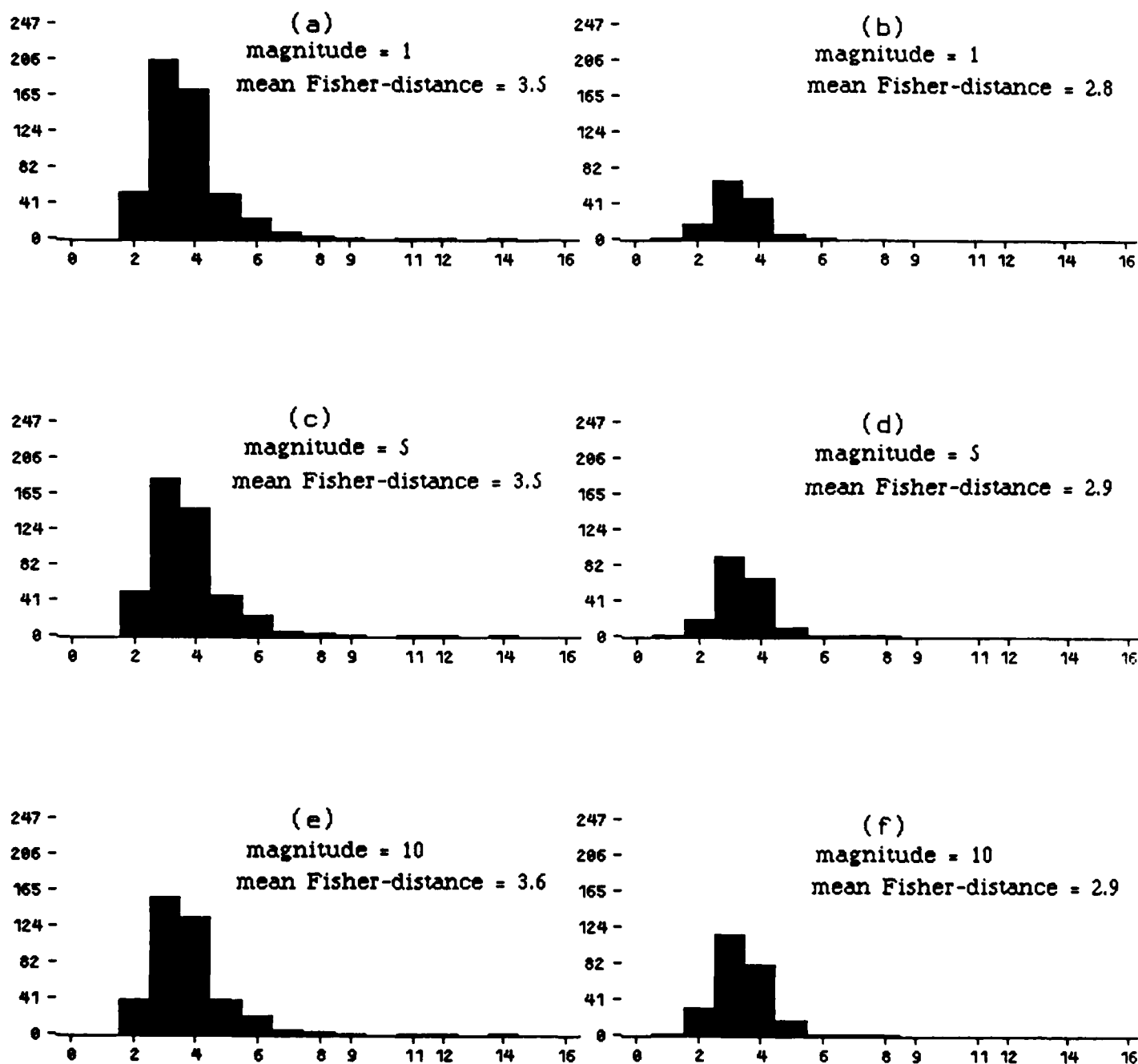
**Figure 15c. Fisher–distance Histograms for Bright CP Line–Like Masks in Lower–left Quadrant.**

(a), (c), (e):  at pixels where nonlinear detector responds.
(b), (e), (f):  at pixels where nonlinear detector does not respond.
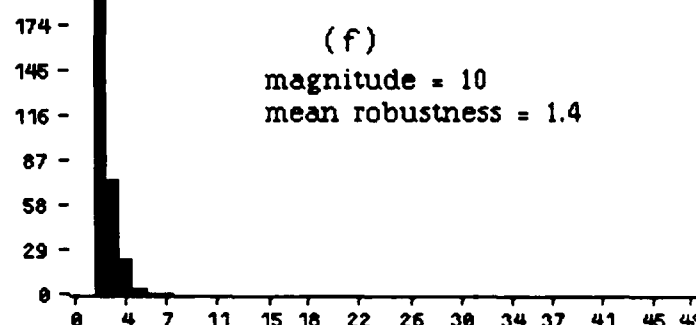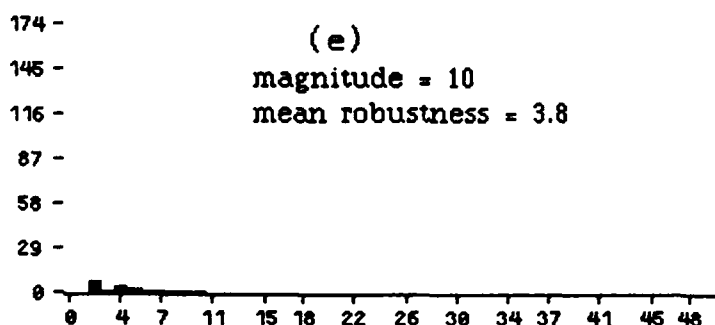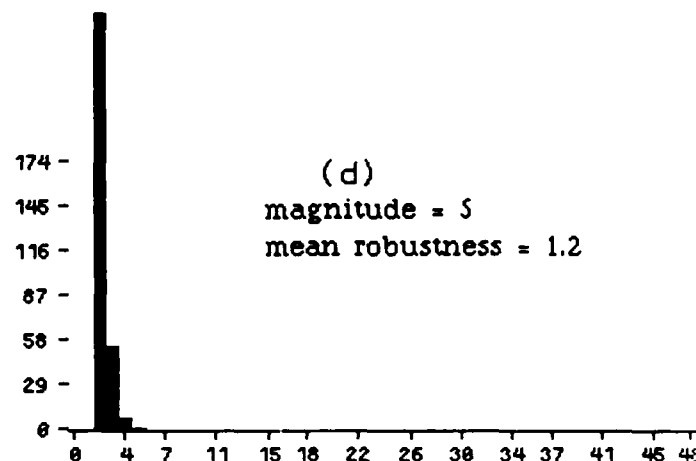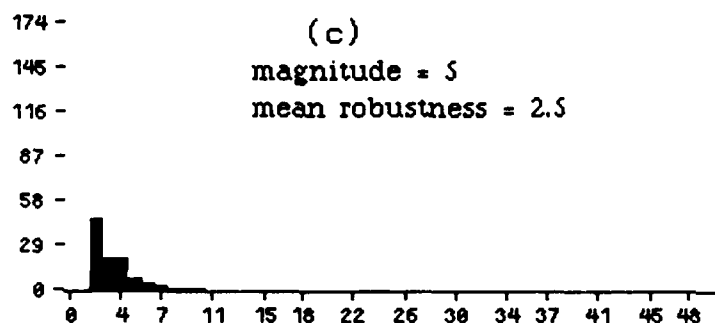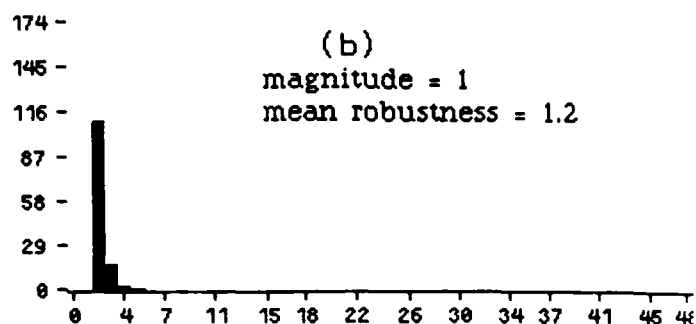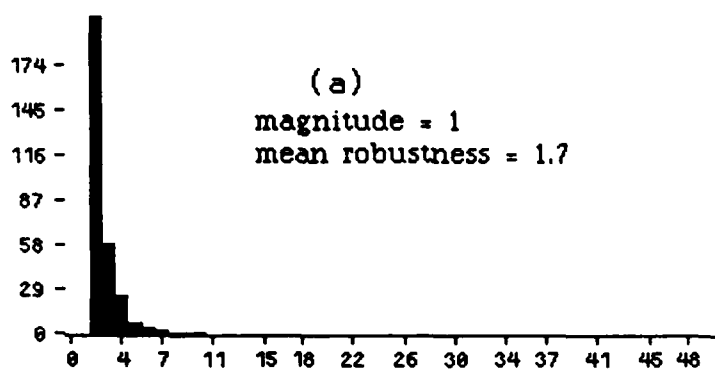
**Figure 16a. Robustness Histograms for Bright CP Line–Like Masks in window_5.**

(a), (c), (e): at pixels where nonlinear detector responds.

(b), (e), (f): at pixels where nonlinear detector does not respond.

49
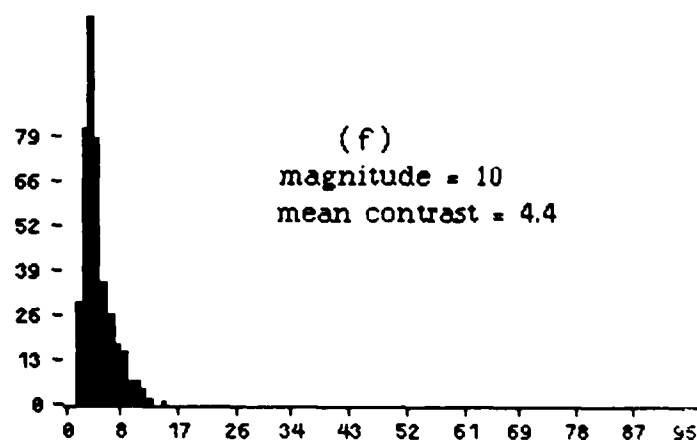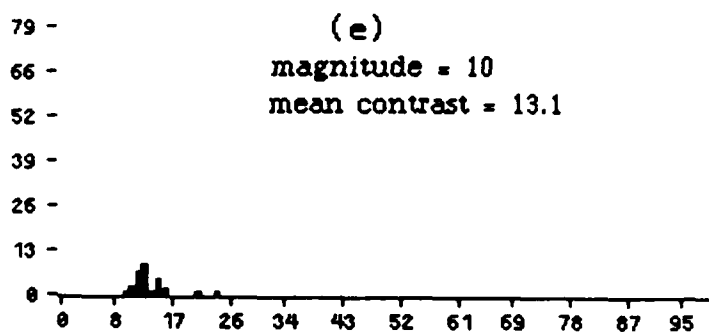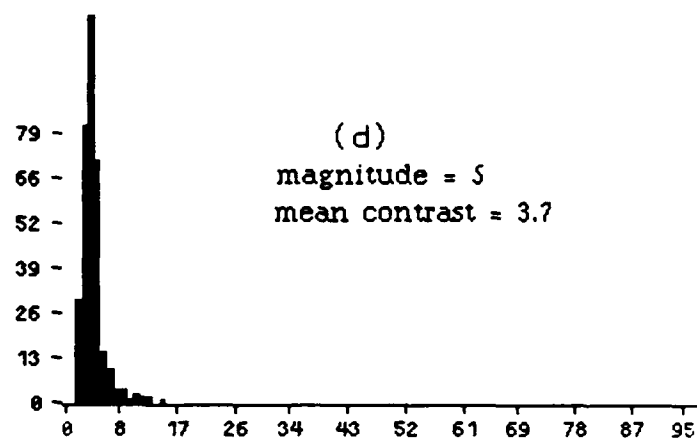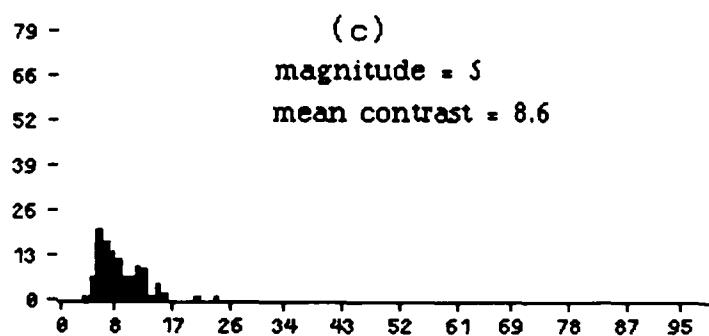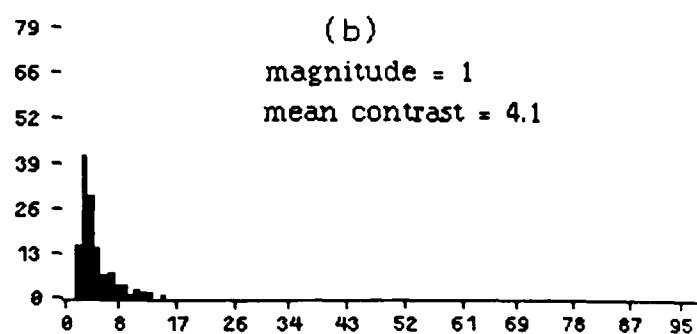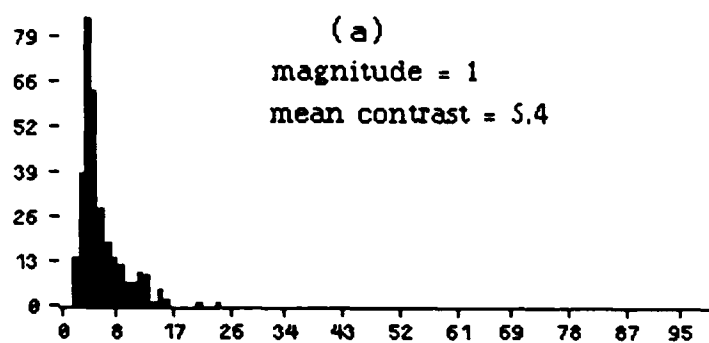
**Figure 16b. Contrast Histograms for Bright CP Line–Like Masks in window_5.**

(a), (c), (e): at pixels where nonlinear detector responds.

(b), (e), (f): at pixels where nonlinear detector does not respond.
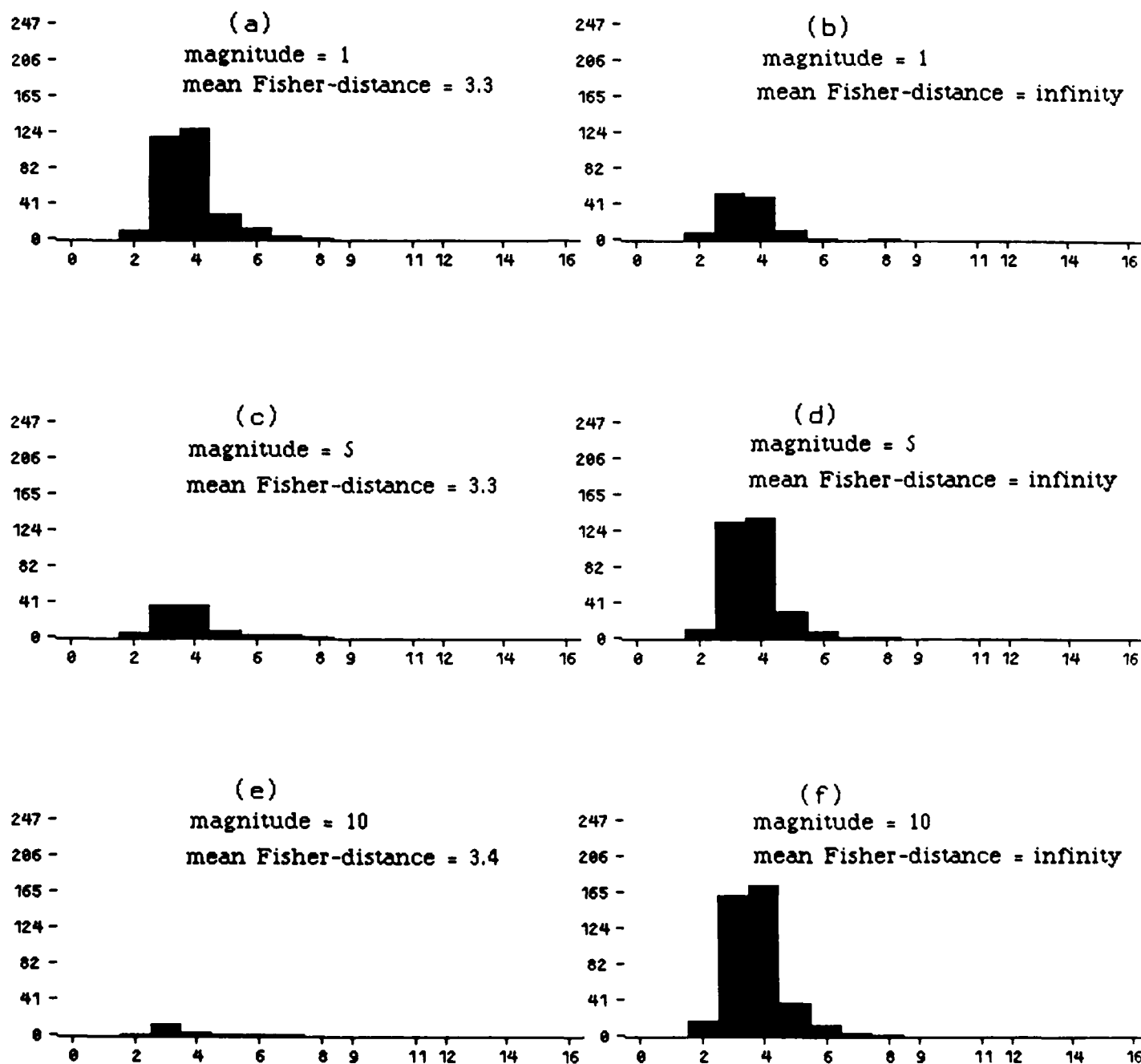
**Figure 16c. Fisher–distance Histograms for Bright CP Line–Like Masks in window_5.**

(a), (c), (e): at pixels where nonlinear detector responds.

(b), (e), (f): at pixels where nonlinear detector does not respond.

51
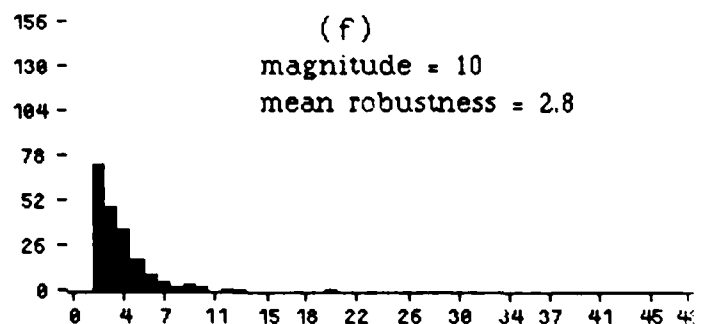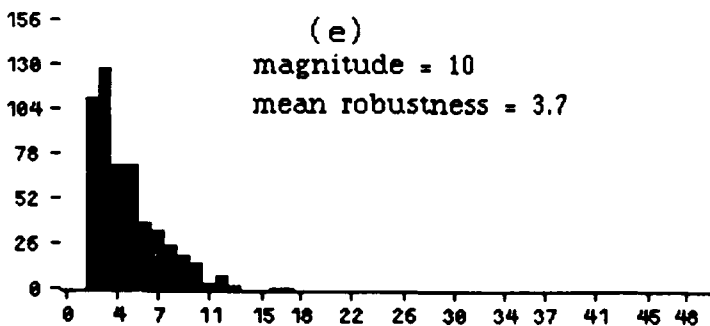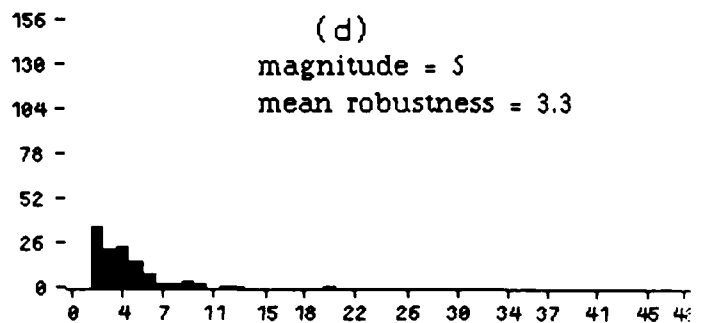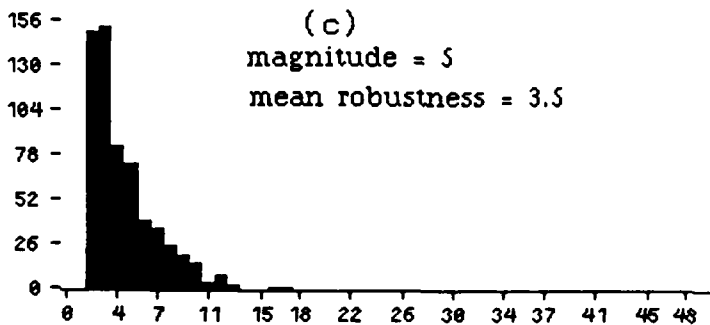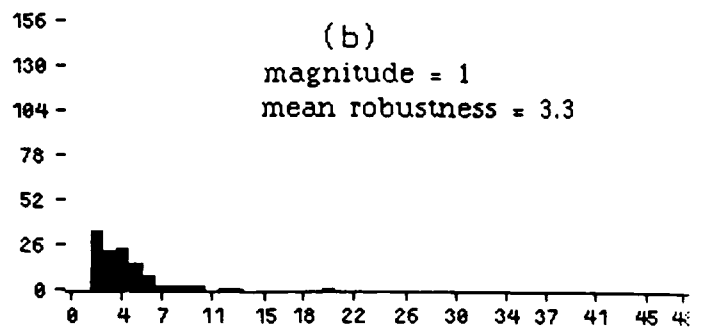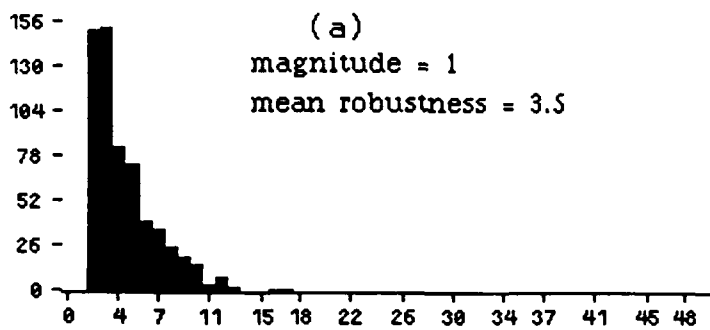
**Figure 17a. Robustness Histograms for Bright CP Line–Like Masks in "White Noise" ($\sigma=10$) Image.**

(a), (c), (e): at pixels where nonlinear detector responds.

(b), (e), (f): at pixels where nonlinear detector does not respond.

52
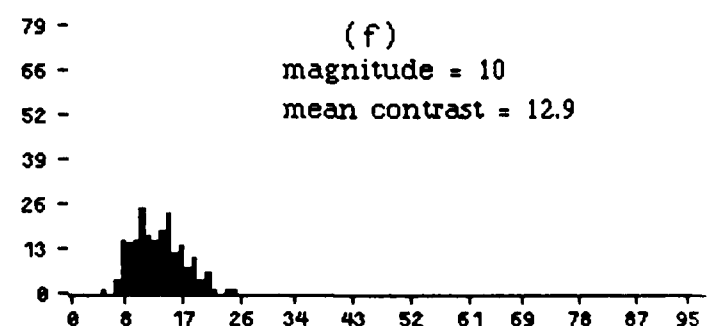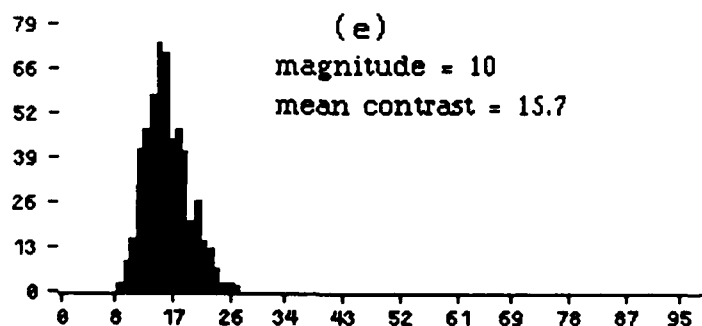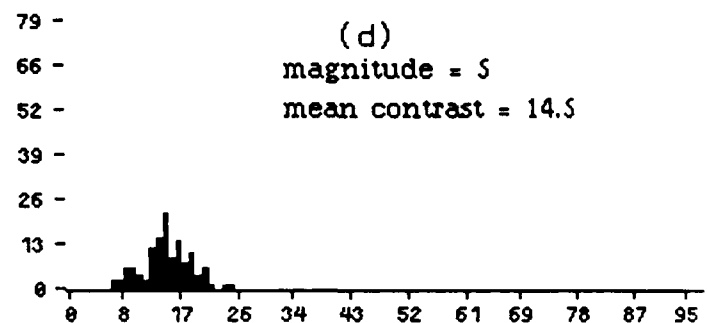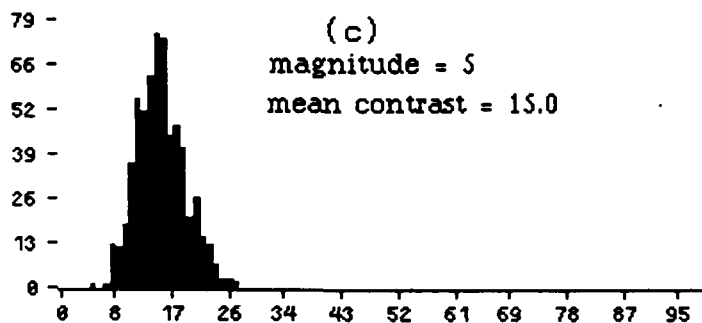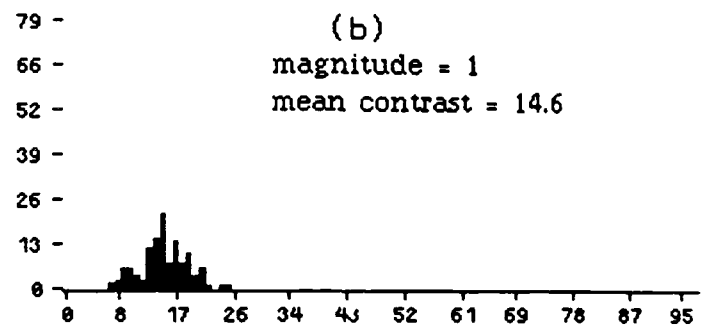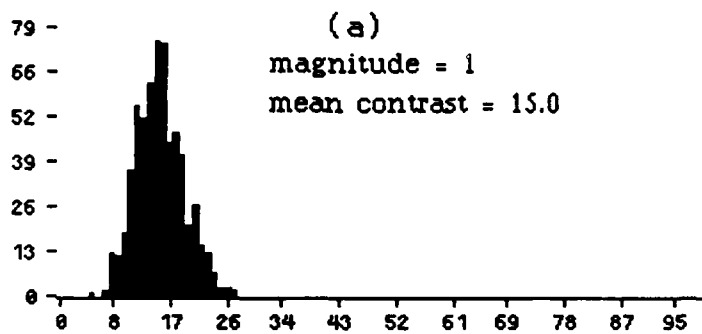
**Figure 17b. Contrast Histograms for Bright CP Line–Like Masks in "White Noise" ($\sigma$=10) Image.**

(a), (c), (e): at pixels where nonlinear detector responds.

(b), (e), (f): at pixels where nonlinear detector does not respond.
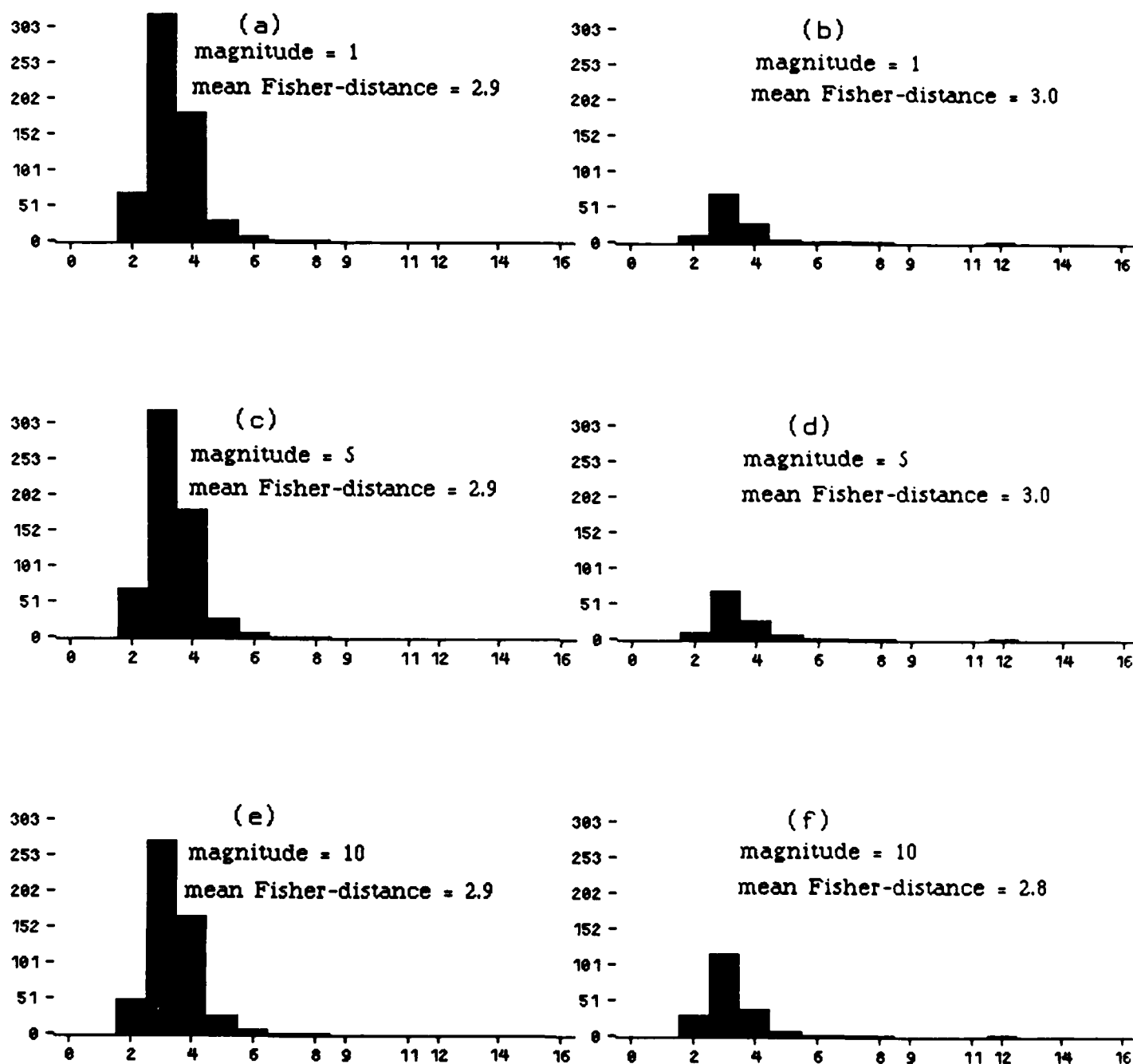
**Figure 17c. Fisher–distance Histograms for Bright CP Line–Like Masks in "White Noise" ($\sigma$=10) Image.**

(a), (c), (e): at pixels where nonlinear detector responds.

(b), (e), (f): at pixels where nonlinear detector does not respond.

### 4.3. Summary of Experimental Results

(1) The statistics tend to be characteristic of images of a given type. However, the statistical properties of the white noise images (of appropriate variance) overlap those of the suburban images.

(2) The frequencies of occurrence of classes of matched masks generally do not depend strongly on the type of the image. (Exceptions are the End and Corner mask classes.)

(3) Images of suburban type can in principle be distinguished from images of homogeneous type by the values of parameters such as the mean and median robustness or contrast of the matched masks.

(4) Images of suburban type may sometimes be distinguished from white noise images by comparing the statistics of bright CP and dark CP matched masks.

## 5. Probabilistic Analysis

### 5.1. Motivation and Problem Definition

The objective of the analysis in this section is to compute the probabilities of certain events (e.g., frequency of occurrence of a given mask, expected robustness of a class of masks, etc.) for a "white noise" image having normally distributed gray levels. These probabilities can be used to identify a real image "window" as "interesting" in the sense of having a high frequency of occurrence of line–like features.

Let $glv$, the image gray level, be a random variable having a Gaussian distribution with mean $\mu$ and standard deviation $\sigma$. Assuming independent pixels, we want to evaluate the following:

- Probability for a $3 \times 3$ neighborhood to satisfy a given mask or class of masks.

- Expected robustness for a given mask/class of masks.

For a continuous random variable $glv$, the normal density function is given by

$$f(glv) = \frac{1}{\sigma\sqrt{2\pi}} e^{-(glv-\mu)^2/2\sigma^2}$$

Since $glv$ takes on integer values only, it is more appropriate to treat it as a random variable of *discrete* type [5]. Assuming a gray scale of 0 to 255, the density function of $glv$ is thus

$$f(glv) = \frac{1}{\sigma\sqrt{2\pi}} \sum_{k=0}^{255} e^{-(k-\mu)^2/2\sigma^2} \, \delta(glv-k)$$

where $\delta$ denotes the Dirac delta or impulse function.

## 5.2. Theoretical Derivation

In deriving the probability of a $3 \times 3$ neighborhood satisfying a given mask, we first observe, based on the assumption that the pixels are statistically independent, that this probability is the same for any $d$ dark pixel mask. Thus we need only derive the probability of satisfying a $\{d, 9-d\}$ mask, without reference to its specific geometric pattern.

Let $F_{glv}(t) = Pr\{glv \leq t\}$ (i.e., the probability of a pixel gray level being less than or equal to $t$ ) denote the distribution function of the random variable $glv$. Obviously, $Pr\{glv \leq t\} = \sum_{k=0}^{t} f(glv=k)$, and $Pr\{glv \leq 255\} = 1$ .

Let $t$, $r$ denote the threshold and robustness of a given $\{d, 9-d\}$ mask matched by some $3 \times 3$ neighborhood, and let $<t,r,d>$ denote this statistical event. The probability of this event is $Pr^d\{glv \leq t\}Pr^{9-d}\{glv \geq t+r\}$, provided there exists at least one "dark" pixel with $glv=t$ and at least one "bright" pixel with $glv=t+r$. Thus

$$Pr\{<t,r,d>\} =$$
$$\left[Pr^d\{glv \leq t\} - Pr^d\{glv < t\}\right]\left[Pr^{9-d}\{glv \geq t+r\} - Pr^{9-d}\{glv > t+r\}\right]$$

or, in terms of the density and distribution functions:

$$Pr\{<t,r,d>\} =$$

$$\left\{ F_{glv}{}^{d}(t) - \left[ F_{glv}(t) - f(glv=t) \right]^{d} \right\} \left\{ \left[ 1 - F_{glv}(t+r) + f(glv=t+r) \right]^{9-d} - \left[ 1 - F_{glv}(t+r) \right]^{9-d} \right\}$$

Summation of this probability over all possible values for $t$ and $r$ (this is legitimate, since it involves addition of probabilities of disjoint events) yields

$$Pr\{<d>\} = \sum_{r>0}^{255} \sum_{t=0}^{255-r} Pr\{<t,r,d>\}$$

where $<d>$ stands for the event that a $3 \times 3$ neighborhood matches a given $\{d, 9-d\}$ mask.

It should be noted that since we require strictly positive robustness, we have $\binom{9}{d} Pr\{<d>\} < 1$ for $d = 1, 2, ..., 8$. In other words, the probability of some $3 \times 3$ neighborhood matching *any* $d$ dark pixel mask is strictly less than 1.

Also, since matching different masks simultaneously in a given $3 \times 3$ neighborhood still involves disjoint events (i.e., $<d_1> \bigcap <d_2> = \emptyset$, provided that *mask_number* $\{d_1, 9-d_1\} \neq$ *mask_number* $\{d_2, 9-d_2\}$ in case $d_1 = d_2$), the probability of a $3 \times 3$ neighborhood satisfying a given *class* of masks is

$$Pr\{<C_j>\} = \sum_{i=1}^{8} n_i(C_j, d_i) Pr\{<d_i>\}$$

where $<C_j>$ denotes the event that the neighborhood matches a mask which is a member of class $C_j$, and $n_i(C_j, d_i)$ is the number of $\{d_i, 9-d_i\}$ mask configurations in class $C_j$ (See Table 1.) For example, the probability of a $3 \times 3$ neighborhood satisfying an edge type mask is

$$Pr\{<Edge>\} = 8\ Pr\{<5>\} + 8\ Pr\{<6>\}$$

Similarly, the probabilities for the rest of the classes can be evaluated.

In evaluating the expected robustness for a given mask, a proper normalization factor should be introduced. This implies expressing the required expected value in the following manner:

$$E(r|<d>) = \frac{\displaystyle\sum_{r>0}^{255} r\ Pr\{<r,d>\}}{Pr\{<d>\}}$$

where $Pr\{<r,d>\} = \displaystyle\sum_{t=0}^{255-r} Pr\{<t,r,d>\}$ denotes the probability that the neighborhood matches a given $d$ dark pixel mask having robustness $r$.

To conclude our analysis, we now extend the above expected value to a given class of masks. The result is evaluated by the following weighted sum:

$$E(r|<C_j>) = \frac{\displaystyle\sum_{i=1}^{8} n_i(C_j,\ d_i)\ Pr\{<d_i>\}\ E(r|<d_i>)}{Pr\{<C_j>\}}$$

### 5.3. Numerical Results

The numerical values shown in the following tables were obtained for $\mu=127.5$ and $\sigma=5, 10, 15, 20, 25, 30, 35$. (Since the random variable is of discrete type, higher values for $\sigma$ are impractical.) Note that $Pr\{<C_{j_1}>\} = Pr\{<C_{j_2}>\}$ and $E(r|<C_{j_1}>) = E(r|<C_{j_2}>)$ for classes of masks consisting of *single* (identical or complementary) partition types. Thus, the results for these cases are given for a combined class entry form.

## Table 13 – Probability of Matching a Given {$d$, 9−$d$} Mask vs. $\sigma$

| $d$ | $\sigma=5$ | $\sigma=10$ | $\sigma=15$ | $\sigma=20$ | $\sigma=25$ | $\sigma=30$ | $\sigma=35$ |
|---|---|---|---|---|---|---|---|
| 1 | .095724 | .103145 | .105738 | .107058 | .107857 | .108374 | .108526 |
| 2 | .021880 | .024633 | .025635 | .026153 | .026470 | .026683 | .026837 |
| 3 | .008889 | .010269 | .010783 | .011052 | .011217 | .011328 | .011409 |
| 4 | .005778 | .006756 | .007125 | .007318 | .007437 | .007518 | .007576 |
| 5 | .005778 | .006756 | .007125 | .007318 | .007437 | .007518 | .007576 |
| 6 | .008889 | .010269 | .010783 | .011052 | .011217 | .011328 | .011408 |
| 7 | .021880 | .024633 | .025635 | .026153 | .026470 | .026683 | .026836 |
| 8 | .095724 | .103145 | .105738 | .107058 | .107857 | .108393 | .108775 |

## Table 14 – Probability of Matching a Given Class of Masks vs. $\sigma$

| Class | $\sigma=5$ | $\sigma=10$ | $\sigma=15$ | $\sigma=20$ | $\sigma=25$ | $\sigma=30$ | $\sigma=35$ |
|---|---|---|---|---|---|---|---|
| Edge | .117337 | .136195 | .143266 | .146962 | .149233 | .150769 | .151877 |
| Line | .106668 | .123222 | .129399 | .132622 | .134600 | .135938 | .136903 |
| Wide–Line | .023113 | .027024 | .028500 | .029274 | .029750 | .030072 | .030305 |
| Right–Ang. Acute–Ang. | .071112 | .082148 | .086266 | .088415 | .089733 | .090625 | .091269 |
| End–Point | .175040 | .197064 | .205082 | .209227 | .211757 | .213464 | .214694 |
| Corner | .581048 | .636667 | .656534 | .666731 | .672935 | .677106 | .680093 |
| L–Line Y–Junction | .046225 | .054047 | .057000 | .058548 | .059500 | .060144 | .060610 |
| T–Junction | .156858 | .179603 | .188041 | .192435 | .195128 | .196948 | .198259 |
| X–Junction | .011556 | .013512 | .014250 | .014637 | .014875 | .015036 | .015152 |

## Table 15 – Expected Robustness of a Given $\{d, 9-d\}$ Mask vs. $\sigma$

| $d$ | $\sigma=5$ | $\sigma=10$ | $\sigma=15$ | $\sigma=20$ | $\sigma=25$ | $\sigma=30$ | $\sigma=35$ |
|---|---|---|---|---|---|---|---|
| 1 | 3.20248 | 5.95157 | 8.71042 | 11.47166 | 14.23372 | 16.98960 | 19.68012 |
| 2 | 2.28344 | 4.06157 | 5.85552 | 7.65334 | 9.45269 | 11.25332 | 13.06100 |
| 3 | 1.98847 | 3.44697 | 4.92478 | 6.40733 | 7.89176 | 9.37728 | 10.86542 |
| 4 | 1.88220 | 3.22365 | 4.58604 | 5.95359 | 7.32318 | 8.69383 | 10.06560 |
| 5 | 1.88220 | 3.22365 | 4.58604 | 5.95359 | 7.32318 | 8.69375 | 10.06437 |
| 6 | 1.98848 | 3.44697 | 4.92478 | 6.40733 | 7.89176 | 9.37697 | 10.86064 |
| 7 | 2.28345 | 4.06158 | 5.85553 | 7.65335 | 9.45270 | 11.25231 | 13.04562 |
| 8 | 3.20247 | 5.95157 | 8.71042 | 11.47166 | 14.23372 | 16.98970 | 19.68163 |

## Table 16 – Expected Robustness of a Given Class of Masks vs. $\sigma$

| Class | $\sigma=5$ | $\sigma=10$ | $\sigma=15$ | $\sigma=20$ | $\sigma=25$ | $\sigma=30$ | $\sigma=35$ |
|---|---|---|---|---|---|---|---|
| Edge | 1.94661 | 3.35835 | 4.79001 | 6.22657 | 7.66507 | 9.10422 | 10.54287 |
| Line Right–Ang. Acute–Ang. | 1.98847 | 3.44697 | 4.92478 | 6.40733 | 7.89176 | 9.37728 | 10.86542 |
| Wide–Line L–Line X–Junction Y–Junction | 1.88220 | 3.22365 | 4.58604 | 5.95359 | 7.32318 | 8.69375 | 10.06437 |
| End–Point | 2.28344 | 4.06157 | 5.85552 | 7.65334 | 9.45269 | 11.25332 | 13.06100 |
| Corner | 2.87310 | 5.25078 | 7.63959 | 10.03116 | 12.42373 | 14.81250 | 17.15832 |
| T–Junction | 2.10608 | 3.68335 | 5.27831 | 6.87763 | 8.47868 | 10.08033 | 11.67890 |

Theoretically, the probability and expected robustness results for a given $\{d, 9-d\}$ mask should be identical to those for a given $\{9-d, d\}$ mask. (Practically, the results are identical within minor inaccuracies for the higher $\sigma$'s examined.)

Also, the agreement between the theoretical results and those obtained in Section 4 for "white noise" images should be noted. For example, for $\sigma=5$, $Pr\{<Corner>\} = 0.581048$, whereas the relative average frequency of occurrence of Corner type masks, in the corresponding white–noise image, is approximately 59% . Similarly, for $\sigma=20$, $E(r|<Line>) = 6.41$, whereas the average mean robustness computed for Line type masks in the corresponding white–noise image is approximately 6.35 .

Finally, the $\sigma$ dependence of $Pr\{<d>\}$ (i.e., $\binom{9}{d} Pr\{<d>\} \rightarrow 1$ as $\sigma$ approaches its maximum possible value) is qualitatively explained by the following argument. The higher $\sigma$, the less probable it is that two pixels have the same gray level value. Thus, the frequency of occurrence of masks having zero robustness decreases, and consequently, the probability of a $3 \times 3$ neighborhood matching any non–zero robustness mask approaches 1.

## 6. Concluding Remarks

In this paper, we have introduced a set of $3 \times 3$ binary masks that can be used to extract linear features from an image. By matching the masks with the image, we assign labels to each pixel, each label corresponding to a particular mask. We also compute confidence measures associated with each label, based on the homogeneity of the foreground and background in each mask, and the difference between them. Several statistical studies, attempting to distinguish suburban images from homogeneous and white noise images, were carried out.

It was shown that suppression of matched masks by thresholding of the confidence measures yields unsatisfactory results. It is preferable to record all the information obtained from the masks, in order to make use of it at the later stages of the linear feature detection process.

## 7. Acknowledgements

# References

1. A. Rosenfeld and A.C. Kak, *Digital Picture Processing* (second edition), Academic Press, New York, 1982, Chapter 10.

2. J.M. Canning, J.J. Kim, and A. Rosenfeld, Symbolic Pixel Labeling For Linear Feature Detection, TR-1761, Computer Vision Laboratory, Center for Automation Research, University of Maryland, January 1987.

3. E.M. Allen, R.H. Trigg, and R.J. Wood, The Maryland Artificial Intelligence Group Franz Lisp Environment, Variation 3.5, TR-1226, Department of Computer Science, University of Maryland, December 1984.

4. D.E. Knuth, *The Art of Computer Programming,* Volume 2, *Seminumerical Algorithms,* second edition, Addison-Wesley, Reading, Mass., 1981, Chapter 3, p. 117.

5. A. Papoulis, *Probability, Random Variables, and Stochastic Processes,* McGraw-Hill, New York, 1965, Chapter 4.

Appendix A – 512  3 × 3  Binary Masks

# Appendix B – Statistics of Additional Images.

Table B-1a – Statistics for Dark Center Pixel Masks in Lower-right Quadrant of Greenbelt1

| Class | # of Masks | Robustness | | | | Contrast | | | | Fisher distance | | | |
|---|---|---|---|---|---|---|---|---|---|---|---|---|---|
| | | Max | Mean | Var | Med | Max | Mean | Var | Med | Max | Mean | Var | Med |
| Edge | 2104 | 127.0 | 8.2 | 174.8 | 4.0 | 163.3 | 25.8 | 502.4 | 20.5 | 24.7 | 3.7 | 4.4 | 3.2 |
| Line | 318 | 49.0 | 5.6 | 62.0 | 2.0 | 112.3 | 21.0 | 403.1 | 15.6 | 16.7 | 2.8 | 3.4 | 2.4 |
| Wide-Line | 79 | 10.0 | 2.3 | 3.4 | 1.0 | 59.4 | 16.4 | 141.2 | 12.6 | 5.4 | 2.6 | 0.8 | 2.5 |
| Right-Angle | 134 | 25.0 | 3.2 | 14.7 | 2.0 | 87.2 | 17.4 | 211.3 | 13.2 | 6.1 | 2.3 | 0.8 | 2.2 |
| Acute-Angle | 300 | 18.0 | 3.2 | 10.5 | 2.0 | 86.2 | 17.7 | 175.8 | 14.8 | 8.0 | 2.4 | 1.0 | 2.2 |
| End-Point | 489 | 27.0 | 3.4 | 12.9 | 2.0 | 97.4 | 18.4 | 260.2 | 14.4 | 8.5 | 2.2 | 0.8 | 2.0 |
| Corner | 3782 | 103.0 | 8.2 | 117.7 | 4.0 | 148.5 | 24.9 | 450.7 | 19.5 | 47.5 | 3.3 | 4.8 | 2.8 |
| L-Line | 187 | 23.0 | 3.9 | 17.1 | 2.0 | 120.6 | 22.1 | 423.3 | 16.8 | 6.1 | 2.8 | 0.8 | 2.7 |
| T-Junction | 504 | 74.0 | 4.1 | 42.6 | 2.0 | 138.3 | 20.7 | 345.8 | 16.5 | 8.1 | 2.9 | 1.1 | 2.8 |
| X-Junction | 12 | 3.0 | 1.8 | 0.5 | 2.0 | 30.2 | 14.7 | 91.5 | 13.2 | 3.2 | 2.4 | 0.2 | 2.4 |
| Y-Junction | 47 | 8.0 | 2.6 | 4.7 | 2.0 | 38.6 | 15.5 | 86.9 | 15.2 | 3.8 | 2.5 | 0.4 | 2.5 |

Table B-1b – Statistics for Bright Center Pixel Masks in Lower-right Quadrant of Greenbelt1

| Class | # of Masks | Robustness | | | | Contrast | | | | Fisher distance | | | |
|---|---|---|---|---|---|---|---|---|---|---|---|---|---|
| | | Max | Mean | Var | Med | Max | Mean | Var | Med | Max | Mean | Var | Med |
| Edge | 2126 | 148.0 | 8.1 | 189.3 | 4.0 | 168.2 | 26.1 | 508.5 | 21.1 | 38.6 | 3.3 | 5.3 | 2.9 |
| Line | 320 | 40.0 | 6.4 | 54.9 | 3.0 | 109.2 | 23.5 | 320.6 | 19.8 | 18.5 | 3.3 | 3.0 | 2.8 |
| Wide-Line | 89 | 23.0 | 3.7 | 19.6 | 2.0 | 62.3 | 19.6 | 195.2 | 16.3 | 8.0 | 2.8 | 1.1 | 2.6 |
| Right-Angle | 164 | 19.0 | 3.2 | 12.2 | 2.0 | 90.0 | 19.4 | 229.9 | 15.9 | 8.7 | 2.6 | 0.7 | 2.5 |
| Acute-Angle | 332 | 61.0 | 3.9 | 31.9 | 2.0 | 113.7 | 20.8 | 310.8 | 16.6 | 6.6 | 2.8 | 0.8 | 2.7 |
| End-Point | 517 | 36.0 | 5.6 | 35.5 | 3.0 | 99.3 | 22.6 | 311.5 | 18.2 | 16.7 | 2.8 | 1.5 | 2.6 |
| Corner | 3830 | 96.0 | 5.8 | 60.5 | 3.0 | 147.1 | 22.8 | 375.9 | 18.1 | 41.3 | 2.5 | 1.9 | 2.2 |
| L-Line | 209 | 27.0 | 3.4 | 12.1 | 2.0 | 115.2 | 21.7 | 368.1 | 18.6 | 5.9 | 2.9 | 0.6 | 2.8 |
| T-Junction | 490 | 35.0 | 3.5 | 17.3 | 2.0 | 125.9 | 19.7 | 295.9 | 16.0 | 6.8 | 2.5 | 0.8 | 2.4 |
| X-Junction | 10 | 4.0 | 1.8 | 1.4 | 1.0 | 50.8 | 18.2 | 212.0 | 16.7 | 4.1 | 2.6 | 0.6 | 2.3 |
| Y-Junction | 42 | 13.0 | 3.6 | 12.4 | 2.0 | 38.1 | 17.3 | 81.8 | 16.7 | 4.3 | 2.8 | 0.4 | 2.8 |

Table B-2a — Statistics for Dark Center Pixel Masks in 16×16 window_1 of Greenbelt1

| Class | # of Masks | Robustness | | | | Contrast | | | | Fisher distance | | | |
|---|---|---|---|---|---|---|---|---|---|---|---|---|---|
| | | Max | Mean | Var | Med | Max | Mean | Var | Med | Max | Mean | Var | Med |
| Edge | 26 | 2.0 | 1.1 | 0.1 | 1.0 | 3.8 | 2.7 | 0.5 | 2.8 | 4.6 | 3.2 | 0.5 | 3.2 |
| Line | 19 | 3.0 | 1.2 | 0.2 | 1.0 | 5.8 | 2.9 | 1.7 | 2.3 | 5.7 | 3.6 | 0.7 | 3.6 |
| Wide-Line | 3 | 1.0 | 1.0 | 0.0 | 1.0 | 2.3 | 1.9 | 0.1 | 2.2 | 3.2 | 2.9 | 0.2 | 3.1 |
| Right-Angle | 2 | 1.0 | 1.0 | 0.0 | 1.0 | 2.2 | 2.2 | 0.0 | 2.2 | 5.3 | 4.4 | 0.8 | 4.4 |
| Acute-Angle | 7 | 2.0 | 1.1 | 0.1 | 1.0 | 3.8 | 2.4 | 0.7 | 2.0 | 4.2 | 3.5 | 0.3 | 3.5 |
| End-Point | 23 | 2.0 | 1.3 | 0.2 | 1.0 | 6.1 | 3.0 | 1.8 | 2.5 | 5.9 | 3.2 | 1.0 | 3.0 |
| Corner | 91 | 3.0 | 1.2 | 0.2 | 1.0 | 4.4 | 2.6 | 0.4 | 2.5 | 5.2 | 2.8 | 0.6 | 2.5 |
| L-Line | 6 | 2.0 | 1.2 | 0.1 | 1.0 | 4.8 | 2.7 | 1.7 | 2.0 | 4.0 | 3.3 | 0.4 | 3.5 |
| T-Junction | 17 | 2.0 | 1.1 | 0.1 | 1.0 | 4.6 | 2.4 | 0.7 | 2.2 | 6.8 | 3.4 | 1.2 | 3.0 |
| X-Junction | 0 | 0.0 | 0.0 | 0.0 | 0.0 | 0.0 | 0.0 | 0.0 | 0.0 | 0.0 | 0.0 | 0.0 | 0.0 |
| Y-Junction | 4 | 1.0 | 1.0 | 0.0 | 1.0 | 3.1 | 2.5 | 0.3 | 2.5 | 6.0 | 4.2 | 1.3 | 4.0 |

Table B-2b — Statistics for Bright Center Pixel Masks in 16×16 window_1 of Greenbelt1

| Class | # of Masks | Robustness | | | | Contrast | | | | Fisher distance | | | |
|---|---|---|---|---|---|---|---|---|---|---|---|---|---|
| | | Max | Mean | Var | Med | Max | Mean | Var | Med | Max | Mean | Var | Med |
| Edge | 29 | 4.0 | 1.3 | 0.4 | 1.0 | 6.2 | 3.3 | 1.2 | 3.2 | 6.5 | 3.5 | 0.8 | 3.4 |
| Line | 11 | 2.0 | 1.1 | 0.1 | 1.0 | 4.0 | 2.5 | 0.7 | 2.2 | 7.1 | 4.0 | 2.7 | 3.5 |
| Wide-Line | 4 | 1.0 | 1.0 | 0.0 | 1.0 | 3.0 | 2.4 | 0.3 | 2.4 | 3.8 | 3.6 | 0.0 | 3.6 |
| Right-Angle | 3 | 1.0 | 1.0 | 0.0 | 1.0 | 2.7 | 2.2 | 0.1 | 2.2 | 2.5 | 2.4 | 0.0 | 2.5 |
| Acute-Angle | 13 | 2.0 | 1.1 | 0.1 | 1.0 | 3.2 | 2.3 | 0.3 | 2.3 | 6.1 | 3.1 | 1.1 | 3.2 |
| End Point | 18 | 2.0 | 1.1 | 0.1 | 1.0 | 4.4 | 2.5 | 0.8 | 2.2 | 6.9 | 3.1 | 2.0 | 2.8 |
| Corner | 109 | 4.0 | 1.4 | 0.4 | 1.0 | 7.0 | 3.2 | 1.6 | 2.9 | 6.6 | 3.1 | 0.9 | 2.9 |
| L Line | 6 | 1.0 | 1.0 | 0.0 | 1.0 | 4.4 | 2.5 | 0.9 | 2.3 | 3.5 | 3.0 | 0.1 | 3.0 |
| T Junction | 16 | 2.0 | 1.1 | 0.1 | 1.0 | 4.6 | 2.5 | 0.8 | 2.3 | 4.3 | 3.1 | 0.3 | 3.0 |
| X Junction | 0 | 0.0 | 0.0 | 0.0 | 0.0 | 0.0 | 0.0 | 0.0 | 0.0 | 0.0 | 0.0 | 0.0 | 0.0 |
| Y Junction | 2 | 1.0 | 1.0 | 0.0 | 1.0 | 1.9 | 1.8 | 0.0 | 1.8 | 6.1 | 5.0 | 1.2 | 5.0 |

Table B 3a   Statistics for Dark Center Pixel Masks in 16×24 window_2 of Greenbelt1

| Class | # of Masks | Robustness | | | | Contrast | | | | Fisher distance | | | |
|---|---|---|---|---|---|---|---|---|---|---|---|---|---|
| | | Max | Mean | Var | Med | Max | Mean | Var | Med | Max | Mean | Var | Med |
| Edge | 170 | 74.0 | 8.7 | 250.1 | 3.0 | 85.0 | 21.1 | 472.5 | 11.1 | 28.5 | 4.8 | 17.1 | 3.4 |
| Line | 26 | 3.0 | 1.3 | 0.4 | 1.0 | 36.8 | 6.1 | 43.9 | 4.5 | 4.1 | 2.7 | 0.9 | 2.9 |
| Wide Line | 3 | 1.0 | 1.0 | 0.0 | 1.0 | 5.1 | 4.3 | 0.9 | 4.8 | 3.7 | 3.0 | 0.3 | 3.0 |
| Right Angle | 4 | 2.0 | 1.3 | 0.2 | 1.0 | 12.3 | 6.0 | 13.5 | 4.2 | 3.5 | 2.8 | 0.7 | 3.2 |
| Acute Angle | 12 | 2.0 | 1.2 | 0.1 | 1.0 | 9.0 | 5.7 | 5.7 | 4.7 | 3.8 | 2.5 | 0.5 | 2.2 |
| End Point | 32 | 4.0 | 1.3 | 0.4 | 1.0 | 35.8 | 7.4 | 67.6 | 4.6 | 4.5 | 2.5 | 0.8 | 2.5 |
| Corner | 310 | 46.0 | 4.6 | 39.6 | 2.0 | 75.2 | 16.3 | 396.6 | 7.1 | 13.6 | 3.1 | 1.7 | 2.8 |
| L Line | 21 | 3.0 | 1.5 | 0.3 | 1.0 | 48.8 | 6.8 | 91.1 | 4.4 | 4.1 | 2.9 | 0.4 | 2.9 |
| T Junction | 21 | 6.0 | 1.4 | 1.2 | 1.0 | 70.3 | 8.5 | 208.0 | 4.5 | 4.3 | 3.1 | 0.3 | 3.1 |
| X Junction | 0 | 0.0 | 0.0 | 0.0 | 0.0 | 0.0 | 0.0 | 0.0 | 0.0 | 0.0 | 0.0 | 0.0 | 0.0 |
| Y Junction | 2 | 1.0 | 1.0 | 0.0 | 1.0 | 4.1 | 2.9 | 1.4 | 2.9 | 3.5 | 3.2 | 0.1 | 3.2 |

Table B 3b   Statistics for Bright Center Pixel Masks in 16×24 window_2 of Greenbelt1

| Class | # of Masks | Robustness | | | | Contrast | | | | Fisher distance | | | |
|---|---|---|---|---|---|---|---|---|---|---|---|---|---|
| | | Max | Mean | Var | Med | Max | Mean | Var | Med | Max | Mean | Var | Med |
| Edge | 164 | 68.0 | 4.3 | 56.9 | 2.0 | 75.8 | 17.7 | 274.2 | 10.5 | 20.5 | 3.3 | 4.7 | 2.8 |
| Line | 23 | 31.0 | 5.0 | 65.9 | 1.0 | 57.7 | 19.6 | 394.2 | 5.5 | 6.9 | 3.2 | 1.8 | 3.1 |
| Wide Line | 0 | 0.0 | 0.0 | 0.0 | 0.0 | 0.0 | 0.0 | 0.0 | 0.0 | 0.0 | 0.0 | 0.0 | 0.0 |
| Right Angle | 6 | 2.0 | 1.2 | 0.1 | 1.0 | 5.0 | 3.7 | 1.0 | 3.9 | 4.9 | 3.1 | 0.7 | 2.8 |
| Acute Angle | 20 | 11.0 | 2.4 | 8.5 | 1.0 | 59.2 | 14.6 | 360.9 | 5.3 | 3.7 | 2.7 | 0.4 | 2.8 |
| End Point | 31 | 29.0 | 3.6 | 34.8 | 1.0 | 58.6 | 16.0 | 386.9 | 5.4 | 5.1 | 2.7 | 0.9 | 2.5 |
| Corner | 234 | 23.0 | 2.3 | 6.2 | 2.0 | 66.1 | 12.7 | 188.9 | 6.5 | 6.9 | 2.5 | 1.0 | 2.4 |
| L Line | 20 | 45.0 | 4.7 | 107.9 | 1.0 | 66.7 | 19.7 | 465.4 | 6.4 | 10.8 | 3.3 | 3.3 | 2.9 |
| T Junction | 31 | 3.0 | 1.5 | 0.3 | 1.0 | 19.7 | 8.9 | 118.2 | 5.3 | 5.0 | 2.9 | 1.1 | 2.7 |
| X Junction | 0 | 0.0 | 0.0 | 0.0 | 0.0 | 0.0 | 0.0 | 0.0 | 0.0 | 0.0 | 0.0 | 0.0 | 0.0 |
| Y Junction | 3 | 2.0 | 1.7 | 0.2 | 2.0 | 4.6 | 3.9 | 0.7 | 4.5 | 4.5 | 3.9 | 0.5 | 4.3 |

Table B 4a Statistics for Dark Center Pixel Masks in 16×24 window_3 of Greenbelt1

| Class | # of Masks | Robustness | | | | Contrast | | | | Fisher distance | | | |
|---|---|---|---|---|---|---|---|---|---|---|---|---|---|
| | | Max | Mean | Var | Med | Max | Mean | Var | Med | Max | Mean | Var | Med |
| Edge | 129 | 71.0 | 5.1 | 7.9 | 2.0 | 104.7 | 20.0 | 450.4 | 13.2 | 11.0 | 3.4 | 1.7 | 3.1 |
| Line | 14 | 6.0 | 1.7 | 1.8 | 1.0 | 22.5 | 7.8 | 34.6 | 5.9 | 3.4 | 2.3 | 0.5 | 2.2 |
| Wide Line | 6 | 25.0 | 5.3 | 77.9 | 1.0 | 99.9 | 19.6 | 1295.4 | 3.0 | 3.8 | 3.7 | 0.0 | 3.7 |
| Right Angle | 6 | 3.0 | 1.8 | 0.8 | 1.5 | 11.0 | 7.6 | 9.6 | 8.4 | 3.9 | 2.6 | 0.9 | 2.7 |
| Acute Angle | 24 | 6.0 | 2.2 | 2.6 | 1.0 | 66.8 | 12.7 | 182.2 | 8.6 | 4.7 | 2.5 | 1.4 | 2.5 |
| End Point | 38 | 7.0 | 2.0 | 2.6 | 1.0 | 59.9 | 9.2 | 105.4 | 6.1 | 4.2 | 2.4 | 0.8 | 2.3 |
| Corner | 289 | 89.0 | 8.8 | 196.8 | 4.0 | 128.8 | 21.1 | 715.1 | 11.4 | 47.2 | 3.9 | 13.3 | 3.2 |
| L Line | 14 | 12.0 | 2.1 | 7.7 | 1.0 | 68.1 | 11.8 | 316.6 | 4.0 | 4.0 | 2.9 | 0.4 | 3.0 |
| T Junction | 29 | 8.0 | 1.8 | 2.2 | 1.0 | 48.9 | 12.2 | 130.7 | 6.5 | 4.6 | 2.8 | 0.6 | 2.5 |
| X Junction | 1 | 2.0 | 2.0 | 0.0 | 2.0 | 5.8 | 5.8 | 0.0 | 5.8 | 3.1 | 3.1 | 0.0 | 3.1 |
| Y Junction | 8 | 1.0 | 1.0 | 0.0 | 1.0 | 6.8 | 3.4 | 1.9 | 3.1 | 4.3 | 2.9 | 0.4 | 2.8 |

Table B 4b Statistics for Bright Center Pixel Masks in 16×24 window_3 of Greenbelt1

| Class | # of Masks | Robustness | | | | Contrast | | | | Fisher distance | | | |
|---|---|---|---|---|---|---|---|---|---|---|---|---|---|
| | | Max | Mean | Var | Med | Max | Mean | Var | Med | Max | Mean | Var | Med |
| Edge | 133 | 31.0 | 3.5 | 20.8 | 2.0 | 92.4 | 17.9 | 358.0 | 11.9 | 7.0 | 2.7 | 1.1 | 2.6 |
| Line | 19 | 15.0 | 2.5 | 12.1 | 1.0 | 34.2 | 7.6 | 53.2 | 4.5 | 5.6 | 3.1 | 1.0 | 2.9 |
| Wide Line | 3 | 10.0 | 6.7 | 11.6 | 8.0 | 78.9 | 40.9 | 878.7 | 37.3 | 3.7 | 3.2 | 0.2 | 3.4 |
| Right Angle | 8 | 25.0 | 11.5 | 109.3 | 6.5 | 94.2 | 30.8 | 787.1 | 25.7 | 6.3 | 4.0 | 1.1 | 4.0 |
| Acute Angle | 29 | 41.0 | 5.8 | 89.2 | 2.0 | 103.7 | 21.7 | 791.3 | 11.3 | 8.6 | 3.4 | 1.9 | 3.0 |
| End Point | 39 | 46.0 | 5.4 | 117.0 | 1.0 | 104.1 | 16.6 | 615.5 | 5.0 | 7.5 | 3.1 | 1.8 | 2.6 |
| Corner | 266 | 19.0 | 2.9 | 6.3 | 2.0 | 80.0 | 14.0 | 217.4 | 8.1 | 8.3 | 2.3 | 1.1 | 2.2 |
| L Line | 16 | 19.0 | 2.8 | 18.9 | 1.0 | 79.2 | 14.4 | 365.5 | 7.1 | 4.0 | 3.1 | 0.3 | 2.9 |
| T Junction | 28 | 9.0 | 2.1 | 3.7 | 1.0 | 70.1 | 12.7 | 227.9 | 7.7 | 5.0 | 2.5 | 0.0 | 2.5 |
| X Junction | 0 | 0.0 | 0.0 | 0.0 | 0.0 | 0.0 | 0.0 | 0.0 | 0.0 | 0.0 | 0.0 | 0.0 | 0.0 |
| Y Junction | 5 | 1.0 | 1.0 | 0.0 | 1.0 | 4.3 | 3.2 | 0.7 | 3.2 | 3.8 | 3.0 | 0.5 | 2.8 |

Table B-5a – Statistics for Dark Center Pixel Masks in 20×20 window_4 of Greenbelt1

| Class | # of Masks | Robustness | | | | Contrast | | | | Fisher distance | | | |
|---|---|---|---|---|---|---|---|---|---|---|---|---|---|
| | | Max | Mean | Var | Med | Max | Mean | Var | Med | Max | Mean | Var | Med |
| End | 121 | 50.0 | 7.5 | 72.6 | 4.0 | 77.0 | 32.6 | 337.0 | 31.9 | 12.1 | 3.1 | 1.6 | 2.9 |
| Line | 40 | 29.0 | 8.0 | 54.0 | 4.0 | 51.0 | 27.6 | 122.2 | 29.6 | 5.1 | 2.3 | 1.0 | 2.0 |
| Wide-Line | 6 | 5.0 | 3.0 | 1.3 | 3.0 | 41.8 | 26.8 | 143.2 | 26.1 | 4.1 | 2.4 | 0.8 | 2.1 |
| Right-Angle | 10 | 14.0 | 3.7 | 14.6 | 2.0 | 52.3 | 25.2 | 187.2 | 22.8 | 3.3 | 2.0 | 0.5 | 1.8 |
| Acute-Angle | 32 | 12.0 | 4.0 | 12.3 | 2.0 | 54.8 | 26.6 | 167.0 | 27.3 | 3.4 | 2.0 | 0.4 | 1.8 |
| End-Point | 52 | 15.0 | 3.7 | 9.7 | 3.0 | 48.4 | 23.9 | 131.7 | 24.6 | 3.3 | 1.8 | 0.4 | 1.7 |
| Corner | 297 | 66.0 | 15.6 | 253.4 | 10.0 | 98.3 | 38.6 | 516.5 | 36.9 | 21.3 | 3.9 | 6.7 | 3.1 |
| L-Line | 32 | 38.0 | 6.2 | 49.8 | 4.0 | 53.6 | 33.9 | 157.0 | 34.1 | 9.4 | 2.5 | 1.8 | 2.3 |
| T-Junction | 40 | 45.0 | 7.8 | 98.2 | 3.5 | 71.4 | 29.7 | 322.1 | 29.9 | 8.0 | 3.2 | 1.8 | 2.8 |
| X-Junction | 1 | 1.0 | 1.0 | 0.0 | 1.0 | 5.6 | 5.6 | 0.0 | 5.6 | 2.4 | 2.4 | 0.0 | 2.4 |
| Y-Junction | 4 | 14.0 | 6.0 | 23.5 | 4.5 | 35.7 | 28.3 | 55.7 | 30.6 | 4.5 | 3.0 | 1.3 | 3.0 |

Table B-5b – Statistics for Bright Center Pixel Masks in 20×20 window_4 of Greenbelt1

| Class | # of Masks | Robustness | | | | Contrast | | | | Fisher distance | | | |
|---|---|---|---|---|---|---|---|---|---|---|---|---|---|
| | | Max | Mean | Var | Med | Max | Mean | Var | Med | Max | Mean | Var | Med |
| End | 144 | 38.0 | 6.3 | 43.6 | 4.0 | 67.6 | 30.1 | 263.5 | 28.9 | 13.2 | 2.6 | 1.7 | 2.5 |
| Line | 43 | 37.0 | 9.5 | 95.0 | 5.0 | 68.0 | 34.9 | 384.6 | 35.2 | 9.3 | 3.4 | 2.8 | 2.8 |
| Wide-Line | 3 | 3.0 | 2.3 | 0.9 | 3.0 | 34.2 | 29.1 | 36.8 | 32.6 | 2.4 | 1.9 | 0.2 | 2.0 |
| Right-Angle | 17 | 20.0 | 6.5 | 31.8 | 6.0 | 57.3 | 36.4 | 183.1 | 40.5 | 4.2 | 2.9 | 0.4 | 3.0 |
| Acute-Angle | 33 | 20.0 | 4.8 | 20.0 | 4.0 | 62.7 | 32.3 | 244.3 | 32.0 | 6.1 | 3.0 | 0.8 | 2.9 |
| End-Point | 65 | 56.0 | 13.2 | 187.2 | 9.0 | 78.7 | 42.5 | 360.8 | 46.8 | 13.1 | 3.8 | 5.0 | 3.3 |
| Corner | 304 | 30.0 | 5.5 | 29.7 | 4.0 | 61.6 | 27.0 | 192.2 | 27.4 | 5.0 | 2.0 | 0.8 | 1.8 |
| L-Line | 39 | 29.0 | 6.3 | 41.7 | 4.0 | 63.3 | 27.8 | 231.1 | 26.8 | 7.0 | 2.8 | 0.9 | 2.7 |
| T-Junction | 49 | 13.0 | 3.6 | 8.0 | 3.0 | 57.9 | 27.7 | 161.9 | 26.5 | 4.8 | 2.0 | 0.8 | 1.8 |
| X-Junction | 0 | 0.0 | 0.0 | 0.0 | 0.0 | 0.0 | 0.0 | 0.0 | 0.0 | 0.0 | 0.0 | 0.0 | 0.0 |
| Y-Junction | 3 | 12.0 | 4.7 | 26.9 | 1.0 | 39.2 | 15.3 | 284.0 | 3.6 | 3.8 | 3.3 | 0.1 | 3.1 |

Table B-6a – Statistics for Dark Center Pixel Masks in 48×64 window_8 of Greenbelt

| Class | # of Masks | Robustness | | | | Contrast | | | | Fisher distance | | | |
|---|---|---|---|---|---|---|---|---|---|---|---|---|---|
| | | Max | Mean | Var | Med | Max | Mean | Var | Med | Max | Mean | Var | Med |
| Edge | 1776 | 69.0 | 8.5 | 98.8 | 5.0 | 125.5 | 28.5 | 367.2 | 25.5 | 32.4 | 3.8 | 4.7 | 3.3 |
| Line | 224 | 29.0 | 4.2 | 24.5 | 2.0 | 90.5 | 19.9 | 254.4 | 16.7 | 11.7 | 2.6 | 1.4 | 2.4 |
| Wide-Line | 24 | 14.0 | 3.3 | 12.2 | 2.0 | 43.3 | 20.1 | 133.5 | 19.1 | 5.5 | 3.0 | 0.7 | 2.8 |
| Right-Angle | 91 | 18.0 | 2.6 | 10.3 | 1.0 | 60.7 | 15.0 | 143.7 | 12.7 | 6.1 | 2.3 | 0.8 | 2.0 |
| Acute-Angle | 240 | 29.0 | 3.5 | 18.1 | 2.0 | 75.5 | 18.5 | 164.5 | 15.8 | 6.2 | 2.5 | 0.9 | 2.4 |
| End-Point | 343 | 38.0 | 3.6 | 19.7 | 2.0 | 81.1 | 16.7 | 175.3 | 13.4 | 6.3 | 2.2 | 0.8 | 1.9 |
| Corner | 3083 | 141.0 | 8.7 | 124.1 | 5.0 | 160.3 | 27.3 | 415.0 | 23.8 | 39.2 | 3.3 | 3.9 | 2.9 |
| L-Line | 182 | 30.0 | 4.1 | 24.5 | 2.0 | 91.1 | 19.9 | 230.5 | 17.3 | 7.1 | 2.8 | 1.0 | 2.7 |
| T-Junction | 391 | 44.0 | 3.8 | 22.4 | 2.0 | 94.2 | 19.8 | 235.9 | 16.7 | 16.9 | 3.0 | 1.8 | 2.8 |
| X-Junction | 1 | 2.0 | 2.0 | 0.0 | 2.0 | 13.7 | 13.7 | 0.0 | 13.7 | 3.3 | 3.3 | 0.0 | 3.3 |
| Y-Junction | 35 | 10.0 | 2.4 | 4.3 | 2.0 | 53.6 | 13.3 | 119.8 | 11.6 | 3.8 | 2.7 | 0.4 | 2.6 |

Table B-6b – Statistics for Bright Center Pixel Masks in 48×64 window_8 of Greenbelt

| Class | # of Masks | Robustness | | | | Contrast | | | | Fisher distance | | | |
|---|---|---|---|---|---|---|---|---|---|---|---|---|---|
| | | Max | Mean | Var | Med | Max | Mean | Var | Med | Max | Mean | Var | Med |
| Edge | 1607 | 80.0 | 7.6 | 80.6 | 4.0 | 135.3 | 27.9 | 322.5 | 26.2 | 23.0 | 3.1 | 2.4 | 2.8 |
| Line | 257 | 69.0 | 6.4 | 57.9 | 4.0 | 128.3 | 24.2 | 272.5 | 21.8 | 10.4 | 3.2 | 1.4 | 2.9 |
| Wide-Line | 40 | 30.0 | 3.9 | 26.4 | 2.0 | 50.7 | 23.1 | 186.2 | 21.7 | 5.9 | 2.7 | 0.9 | 2.7 |
| Right-Angle | 105 | 17.0 | 3.1 | 8.5 | 2.0 | 92.3 | 17.8 | 194.0 | 16.0 | 10.2 | 3.0 | 1.1 | 2.8 |
| Acute-Angle | 267 | 50.0 | 4.8 | 35.0 | 3.0 | 123.2 | 24.2 | 302.6 | 21.3 | 9.9 | 2.9 | 1.1 | 2.8 |
| End-Point | 412 | 111.0 | 6.4 | 96.6 | 3.0 | 157.6 | 24.3 | 350.3 | 21.8 | 12.1 | 2.8 | 1.4 | 2.6 |
| Corner | 2830 | 67.0 | 5.4 | 47.4 | 3.0 | 127.3 | 23.9 | 280.2 | 21.6 | 22.0 | 2.3 | 1.4 | 2.1 |
| L-Line | 232 | 32.0 | 5.6 | 32.7 | 4.0 | 110.5 | 25.0 | 210.6 | 23.7 | 10.8 | 3.3 | 1.7 | 3.0 |
| T-Junction | 377 | 40.0 | 3.8 | 20.7 | 2.0 | 88.9 | 21.6 | 214.5 | 18.9 | 7.9 | 2.5 | 0.9 | 2.4 |
| X-Junction | 5 | 4.0 | 2.0 | 1.2 | 2.0 | 44.4 | 17.0 | 277.5 | 5.0 | 3.4 | 2.4 | 0.2 | 2.2 |
| Y-Junction | 33 | 7.0 | 2.6 | 3.0 | 2.0 | 41.7 | 12.9 | 104.2 | 10.3 | 9.9 | 3.2 | 2.2 | 2.8 |

Table B-7a – Statistics for Dark Center Pixel Masks in a 64×64 "White Noise" Image with $\mu=127$, $\sigma=5$

| Class | # of Masks | Robustness | | | | Contrast | | | | Fisher distance | | | |
|---|---|---|---|---|---|---|---|---|---|---|---|---|---|
| | | Max | Mean | Var | Med | Max | Mean | Var | Med | Max | Mean | Var | Med |
| Edge | 473 | 8.0 | 2.0 | 1.7 | 2.0 | 15.5 | 7.7 | 3.9 | 7.5 | 6.9 | 3.0 | 0.7 | 2.9 |
| Line | 397 | 6.0 | 2.0 | 1.4 | 2.0 | 14.7 | 7.9 | 4.2 | 7.8 | 10.2 | 2.9 | 0.7 | 2.8 |
| Wide-Line | 68 | 6.0 | 1.9 | 1.4 | 2.0 | 11.8 | 7.8 | 3.6 | 7.8 | 5.9 | 3.1 | 0.7 | 2.9 |
| Right-Angle | 251 | 8.0 | 2.0 | 1.7 | 2.0 | 15.7 | 7.8 | 4.0 | 7.5 | 7.5 | 2.9 | 0.6 | 2.8 |
| Acute-Angle | 288 | 7.0 | 2.0 | 1.6 | 2.0 | 15.5 | 7.8 | 4.4 | 7.3 | 7.5 | 2.9 | 0.8 | 2.7 |
| End-Point | 674 | 11.0 | 2.4 | 2.4 | 2.0 | 16.7 | 8.1 | 5.1 | 7.9 | 6.9 | 2.7 | 0.7 | 2.6 |
| Corner | 2282 | 14.0 | 2.8 | 4.3 | 2.0 | 19.8 | 8.4 | 6.9 | 8.0 | 11.0 | 2.6 | 0.8 | 2.4 |
| L-Line | 197 | 6.0 | 1.9 | 1.5 | 2.0 | 15.8 | 7.9 | 3.9 | 7.8 | 5.4 | 3.0 | 0.5 | 2.8 |
| T-Junction | 588 | 9.0 | 2.2 | 2.1 | 2.0 | 15.7 | 7.9 | 4.2 | 7.8 | 8.5 | 2.9 | 0.7 | 2.7 |
| X-Junction | 39 | 8.0 | 1.9 | 1.4 | 1.0 | 11.7 | 7.5 | 3.5 | 7.4 | 6.5 | 3.1 | 0.8 | 3.0 |
| Y-Junction | 179 | 8.0 | 1.9 | 1.7 | 2.0 | 15.3 | 7.7 | 4.2 | 7.8 | 7.4 | 3.0 | 0.7 | 2.9 |

Table B-7b – Statistics for Bright Center Pixel Masks in a 64×64 "White Noise" Image with $\mu=127$, $\sigma=5$

| Class | # of Masks | Robustness | | | | Contrast | | | | Fisher distance | | | |
|---|---|---|---|---|---|---|---|---|---|---|---|---|---|
| | | Max | Mean | Var | Med | Max | Mean | Var | Med | Max | Mean | Var | Med |
| Edge | 482 | 8.0 | 1.9 | 1.3 | 2.0 | 14.8 | 7.9 | 4.1 | 7.7 | 6.6 | 3.0 | 0.7 | 2.8 |
| Line | 403 | 8.0 | 2.0 | 1.6 | 2.0 | 15.8 | 7.9 | 4.3 | 7.7 | 6.2 | 2.9 | 0.7 | 2.8 |
| Wide Line | 78 | 6.0 | 1.7 | 1.0 | 1.0 | 12.9 | 7.5 | 4.1 | 7.2 | 5.1 | 3.0 | 0.6 | 3.0 |
| Right Angle | 276 | 7.0 | 2.0 | 1.6 | 2.0 | 14.8 | 7.9 | 4.3 | 7.7 | 7.3 | 2.9 | 0.7 | 2.8 |
| Acute Angle | 280 | 8.0 | 2.0 | 1.7 | 2.0 | 15.2 | 7.8 | 4.5 | 7.5 | 6.1 | 2.9 | 0.7 | 2.8 |
| End Point | 649 | 10.0 | 2.3 | 2.4 | 2.0 | 15.8 | 8.1 | 5.2 | 7.9 | 7.3 | 2.7 | 0.6 | 2.6 |
| Corner | 2260 | 116.0 | 3.0 | 10.1 | 2.0 | 125.5 | 8.6 | 12.8 | 8.3 | 25.6 | 2.6 | 1.1 | 2.5 |
| L Line | 186 | 7.0 | 2.0 | 1.6 | 1.5 | 13.0 | 7.7 | 4.0 | 7.4 | 5.7 | 3.1 | 0.5 | 3.0 |
| T Junction | 567 | 8.0 | 2.0 | 1.8 | 2.0 | 33.2 | 7.9 | 5.7 | 7.7 | 9.5 | 2.8 | 0.8 | 2.7 |
| X Junction | 35 | 6.0 | 1.7 | 1.0 | 1.0 | 10.8 | 7.9 | 2.5 | 7.5 | 4.7 | 2.9 | 0.4 | 2.8 |
| Y Junction | 188 | 7.0 | 2.0 | 1.5 | 2.0 | 16.6 | 7.6 | 4.1 | 7.4 | 8.8 | 3.1 | 0.8 | 2.9 |

Table B-8a - Statistics for Dark Center Pixel Masks in a 64×64 "White Noise" Image with $\mu=127$, $\sigma=15$

| Class | # of Masks | Robustness | | | | Contrast | | | | Fisher distance | | | |
|---|---|---|---|---|---|---|---|---|---|---|---|---|---|
| | | Max | Mean | Var | Med | Max | Mean | Var | Med | Max | Mean | Var | Med |
| Edge | 608 | 22.0 | 5.0 | 15.7 | 4.0 | 48.1 | 23.1 | 40.5 | 22.7 | 7.8 | 2.9 | 0.7 | 2.7 |
| Line | 476 | 24.0 | 4.9 | 17.8 | 4.0 | 45.8 | 23.4 | 41.4 | 22.8 | 9.6 | 2.7 | 0.7 | 2.6 |
| Wide Line | 130 | 24.0 | 5.0 | 18.5 | 4.0 | 38.3 | 23.4 | 33.1 | 23.0 | 6.8 | 2.9 | 0.6 | 2.8 |
| Right Angle | 342 | 23.0 | 5.0 | 18.2 | 4.0 | 39.5 | 22.9 | 40.0 | 22.5 | 7.2 | 2.8 | 0.8 | 2.6 |
| Acute Angle | 341 | 30.0 | 4.9 | 15.4 | 4.0 | 62.2 | 23.3 | 38.2 | 22.5 | 7.0 | 2.9 | 0.6 | 2.7 |
| End Point | 775 | 28.0 | 6.1 | 23.0 | 5.0 | 48.6 | 24.2 | 44.2 | 23.6 | 8.4 | 2.6 | 0.7 | 2.5 |
| Corner | 2538 | 55.0 | 8.0 | 47.3 | 6.0 | 70.0 | 25.3 | 70.2 | 24.6 | 14.2 | 2.5 | 1.0 | 2.3 |
| L Line | 186 | 19.0 | 4.9 | 14.7 | 4.0 | 36.8 | 23.6 | 33.7 | 24.1 | 5.4 | 2.9 | 0.5 | 2.8 |
| T Junction | 708 | 24.0 | 5.1 | 16.2 | 4.0 | 45.6 | 23.4 | 42.0 | 23.0 | 6.1 | 2.7 | 0.5 | 2.6 |
| X Junction | 62 | 18.0 | 4.9 | 15.1 | 4.0 | 38.7 | 23.6 | 37.6 | 24.1 | 5.1 | 2.9 | 0.6 | 2.8 |
| Y Junction | 211 | 16.0 | 4.1 | 9.9 | 3.0 | 45.4 | 22.4 | 35.9 | 22.3 | 5.3 | 2.8 | 0.5 | 2.7 |

Table B-8b - Statistics for Bright Center Pixel Masks in a 64×64 "White Noise" Image with $\mu=127$, $\sigma=15$

| Class | # of Masks | Robustness | | | | Contrast | | | | Fisher distance | | | |
|---|---|---|---|---|---|---|---|---|---|---|---|---|---|
| | | Max | Mean | Var | Med | Max | Mean | Var | Med | Max | Mean | Var | Med |
| Edge | 570 | 22.0 | 5.0 | 17.8 | 4.0 | 37.0 | 22.9 | 31.3 | 22.7 | 8.6 | 2.9 | 0.7 | 2.8 |
| Line | 489 | 21.0 | 4.7 | 14.5 | 3.0 | 46.5 | 23.0 | 40.0 | 22.8 | 7.6 | 2.8 | 0.6 | 2.6 |
| Wide Line | 108 | 16.0 | 4.9 | 12.9 | 4.0 | 39.9 | 23.3 | 31.2 | 23.1 | 5.3 | 2.9 | 0.5 | 2.8 |
| Right Angle | 326 | 34.0 | 4.7 | 17.9 | 4.0 | 45.8 | 23.1 | 37.7 | 22.7 | 7.9 | 2.8 | 0.7 | 2.6 |
| Acute Angle | 326 | 20.0 | 5.2 | 16.1 | 4.0 | 42.8 | 23.4 | 42.5 | 22.9 | 7.4 | 2.8 | 0.7 | 2.6 |
| End Point | 795 | 35.0 | 6.1 | 26.2 | 5.0 | 51.4 | 24.6 | 51.3 | 24.0 | 8.9 | 2.6 | 0.8 | 2.5 |
| Corner | 2558 | 98.0 | 7.8 | 44.0 | 6.0 | 122.4 | 25.1 | 63.1 | 24.5 | 10.9 | 2.5 | 0.9 | 2.4 |
| L Line | 195 | 20.0 | 4.3 | 11.5 | 3.0 | 40.4 | 21.9 | 35.8 | 21.7 | 7.8 | 2.8 | 0.7 | 2.7 |
| T Junction | 750 | 26.0 | 5.3 | 18.7 | 4.0 | 43.3 | 23.2 | 42.2 | 22.9 | 6.8 | 2.7 | 0.6 | 2.6 |
| X Junction | 57 | 14.0 | 4.9 | 9.7 | 5.0 | 41.1 | 21.8 | 37.5 | 21.4 | 4.7 | 2.7 | 0.5 | 2.6 |
| Y Junction | 194 | 19.0 | 4.7 | 14.3 | 4.0 | 38.9 | 23.0 | 38.3 | 23.1 | 6.4 | 2.9 | 0.7 | 2.7 |

Table B 9a – Statistics for Dark Center Pixel Masks in a 64×64 "White Noise" Image with $\mu=127$, $\sigma=25$

| Class | # of Masks | Robustness | | | | Contrast | | | | Fisher distance | | | |
|---|---|---|---|---|---|---|---|---|---|---|---|---|---|
| | | Max | Mean | Var | Med | Max | Mean | Var | Med | Max | Mean | Var | Med |
| Edge | 571 | 34.0 | 8.0 | 43.2 | 6.0 | 73.7 | 37.6 | 92.1 | 37.2 | 9.8 | 2.8 | 0.8 | 2.7 |
| Line | 504 | 40.0 | 8.4 | 48.6 | 6.0 | 77.8 | 38.1 | 113.5 | 37.3 | 8.7 | 2.8 | 0.7 | 2.7 |
| Wide Line | 118 | 44.0 | 7.8 | 41.6 | 6.0 | 66.2 | 37.2 | 108.9 | 36.2 | 5.7 | 2.9 | 0.6 | 2.7 |
| Right Angle | 337 | 53.0 | 8.2 | 53.9 | 6.0 | 74.2 | 37.9 | 110.0 | 36.2 | 8.6 | 2.8 | 0.9 | 2.7 |
| Acute Angle | 349 | 37.0 | 8.3 | 48.9 | 6.0 | 70.7 | 38.4 | 124.7 | 37.7 | 7.0 | 2.8 | 0.7 | 2.6 |
| End Point | 821 | 46.0 | 9.5 | 61.0 | 7.0 | 86.2 | 39.4 | 133.6 | 38.4 | 11.9 | 2.6 | 0.7 | 2.4 |
| Corner | 2586 | 76.0 | 12.3 | 101.0 | 10.0 | 99.1 | 40.8 | 154.4 | 39.8 | 9.5 | 2.5 | 0.7 | 2.3 |
| L Line | 232 | 47.0 | 7.7 | 50.2 | 6.0 | 76.6 | 38.4 | 120.3 | 37.7 | 5.0 | 2.9 | 0.5 | 2.8 |
| T Junction | 781 | 41.0 | 8.0 | 47.7 | 6.0 | 76.6 | 38.0 | 116.4 | 36.9 | 9.0 | 2.7 | 0.6 | 2.6 |
| X Junction | 60 | 20.0 | 7.6 | 31.9 | 6.0 | 62.5 | 36.9 | 81.6 | 35.3 | 5.4 | 3.0 | 0.7 | 2.8 |
| Y Junction | 223 | 39.0 | 7.6 | 46.0 | 5.0 | 74.9 | 37.5 | 111.0 | 35.9 | 6.6 | 2.9 | 0.5 | 2.9 |

Table B 9b – Statistics for Bright Center Pixel Masks in a 64×64 "White Noise" Image with $\mu=127$, $\sigma=25$

| Class | # of Masks | Robustness | | | | Contrast | | | | Fisher distance | | | |
|---|---|---|---|---|---|---|---|---|---|---|---|---|---|
| | | Max | Mean | Var | Med | Max | Mean | Var | Med | Max | Mean | Var | Med |
| Edge | 605 | 35.0 | 8.0 | 41.3 | 6.0 | 73.3 | 38.0 | 107.9 | 37.0 | 6.0 | 2.8 | 0.5 | 2.7 |
| Line | 506 | 34.0 | 7.7 | 38.0 | 6.0 | 82.8 | 37.9 | 107.6 | 37.3 | 6.4 | 2.7 | 0.5 | 2.6 |
| Wide Line | 101 | 37.0 | 8.7 | 53.0 | 6.0 | 76.1 | 38.7 | 97.5 | 37.4 | 6.5 | 3.0 | 0.9 | 2.8 |
| Right Angle | 358 | 38.0 | 7.6 | 41.8 | 6.0 | 66.3 | 37.2 | 96.5 | 36.7 | 7.3 | 2.8 | 0.6 | 2.6 |
| Acute Angle | 342 | 38.0 | 8.4 | 44.2 | 7.0 | 76.0 | 38.3 | 106.1 | 37.5 | 6.0 | 2.8 | 0.5 | 2.7 |
| End Point | 826 | 65.0 | 9.8 | 70.0 | 7.0 | 99.7 | 39.2 | 128.8 | 38.3 | 8.1 | 2.6 | 0.7 | 2.4 |
| Corner | 2651 | 95.0 | 12.3 | 118.6 | 9.0 | 123.4 | 41.6 | 174.6 | 40.3 | 7.8 | 2.5 | 0.7 | 2.3 |
| L Line | 223 | 32.0 | 7.1 | 33.7 | 5.0 | 66.2 | 37.4 | 103.3 | 36.8 | 5.9 | 2.8 | 0.5 | 2.7 |
| T Junction | 726 | 48.0 | 8.3 | 45.2 | 7.0 | 87.9 | 38.5 | 103.6 | 38.1 | 7.5 | 2.8 | 0.7 | 2.6 |
| X Junction | 58 | 36.0 | 8.3 | 52.5 | 7.0 | 62.3 | 36.2 | 91.8 | 36.2 | 8.7 | 3.2 | 1.4 | 2.9 |
| Y Junction | 220 | 32.0 | 7.5 | 40.3 | 5.0 | 69.4 | 38.6 | 105.3 | 37.4 | 7.0 | 2.9 | 0.6 | 2.8 |

**Table B-10a – Statistics for Dark Center Pixel Masks in a 64×64 "White Noise" Image with $\mu=127$, $\sigma=30$**

| Class | # of Masks | Robustness | | | | Contrast | | | | Fisher distance | | | |
|---|---|---|---|---|---|---|---|---|---|---|---|---|---|
| | | Max | Mean | Var | Med | Max | Mean | Var | Med | Max | Mean | Var | Med |
| Edge | 627 | 50.0 | 8.4 | 58.1 | 6.0 | 83.2 | 44.4 | 148.5 | 43.2 | 9.1 | 2.8 | 0.6 | 2.6 |
| Line | 500 | 50.0 | 9.5 | 72.6 | 7.0 | 88.8 | 45.3 | 149.4 | 44.0 | 7.2 | 2.8 | 0.7 | 2.6 |
| Wide-Line | 92 | 36.0 | 9.2 | 54.0 | 7.0 | 76.9 | 44.4 | 128.8 | 44.2 | 5.5 | 2.9 | 0.6 | 2.7 |
| Right-Angle | 382 | 56.0 | 9.2 | 55.9 | 7.0 | 81.2 | 44.8 | 143.8 | 43.2 | 7.8 | 2.8 | 0.6 | 2.7 |
| Acute-Angle | 358 | 53.0 | 10.2 | 67.1 | 8.0 | 92.5 | 46.0 | 152.5 | 46.3 | 8.9 | 2.9 | 0.8 | 2.7 |
| End-Point | 810 | 55.0 | 11.3 | 93.9 | 9.0 | 103.7 | 47.3 | 177.3 | 46.2 | 9.1 | 2.6 | 0.7 | 2.4 |
| Corner | 2637 | 101.0 | 15.1 | 182.1 | 11.0 | 120.6 | 49.2 | 251.0 | 47.4 | 14.0 | 2.5 | 0.9 | 2.3 |
| L-Line | 223 | 45.0 | 9.0 | 66.3 | 6.0 | 86.3 | 46.0 | 125.5 | 45.8 | 7.9 | 2.9 | 0.8 | 2.7 |
| T-Junction | 779 | 54.0 | 10.0 | 70.9 | 8.0 | 88.1 | 45.7 | 148.9 | 44.2 | 8.5 | 2.7 | 0.7 | 2.6 |
| X-Junction | 69 | 46.0 | 8.3 | 79.4 | 6.0 | 76.6 | 42.7 | 153.2 | 41.1 | 5.9 | 2.7 | 0.7 | 2.6 |
| Y-Junction | 232 | 51.0 | 9.5 | 77.9 | 7.0 | 82.0 | 43.4 | 146.8 | 42.4 | 7.5 | 3.0 | 0.8 | 2.7 |

**Table B-10b – Statistics for Bright Center Pixel Masks in a 64×64 "White Noise" Image with $\mu=127$, $\sigma=30$**

| Class | # of Masks | Robustness | | | | Contrast | | | | Fisher distance | | | |
|---|---|---|---|---|---|---|---|---|---|---|---|---|---|
| | | Max | Mean | Var | Med | Max | Mean | Var | Med | Max | Mean | Var | Med |
| Edge | 579 | 50.0 | 8.8 | 64.1 | 6.0 | 81.8 | 44.1 | 152.8 | 44.0 | 7.4 | 2.8 | 0.7 | 2.7 |
| Line | 528 | 45.0 | 9.2 | 64.4 | 6.5 | 95.3 | 44.7 | 157.3 | 43.5 | 6.6 | 2.8 | 0.6 | 2.6 |
| Wide-Line | 107 | 48.0 | 8.8 | 59.3 | 7.0 | 83.9 | 44.2 | 167.6 | 43.1 | 7.3 | 2.9 | 0.8 | 2.8 |
| Right-Angle | 361 | 46.0 | 9.2 | 61.2 | 7.0 | 84.2 | 45.1 | 162.6 | 43.8 | 6.5 | 2.7 | 0.6 | 2.6 |
| Acute-Angle | 326 | 49.0 | 9.5 | 77.0 | 7.0 | 98.5 | 44.6 | 180.6 | 43.3 | 7.0 | 2.8 | 0.8 | 2.6 |
| End-Point | 824 | 69.0 | 11.1 | 105.8 | 8.0 | 100.3 | 46.4 | 195.2 | 45.1 | 11.6 | 2.6 | 0.9 | 2.4 |
| Corner | 2596 | 86.0 | 14.8 | 160.2 | 11.0 | 123.0 | 48.9 | 239.0 | 47.3 | 19.8 | 2.5 | 0.9 | 2.3 |
| L-Line | 238 | 42.0 | 8.5 | 56.7 | 6.0 | 79.8 | 44.5 | 159.4 | 44.6 | 5.9 | 2.9 | 0.5 | 2.8 |
| T-Junction | 800 | 55.0 | 10.0 | 71.6 | 8.0 | 88.9 | 45.0 | 162.4 | 44.3 | 9.2 | 2.7 | 0.7 | 2.6 |
| X-Junction | 66 | 27.0 | 8.2 | 42.0 | 6.0 | 68.9 | 42.4 | 102.1 | 43.2 | 6.3 | 2.9 | 0.7 | 2.9 |
| Y-Junction | 247 | 48.0 | 8.5 | 56.9 | 6.0 | 86.4 | 43.1 | 144.0 | 42.3 | 6.7 | 2.9 | 0.6 | 2.7 |

**Table B-11a – Statistics for Dark Center Pixel Masks in a 64×64 "White Noise" Image with $\mu=127$, $\sigma=35$**

| Class | # of Masks | Robustness | | | | Contrast | | | | Fisher distance | | | |
|---|---|---|---|---|---|---|---|---|---|---|---|---|---|
| | | Max | Mean | Var | Med | Max | Mean | Var | Med | Max | Mean | Var | Med |
| Edge | 647 | 56.0 | 10.1 | 72.5 | 7.0 | 101.7 | 51.1 | 198.9 | 50.2 | 7.5 | 2.8 | 0.6 | 2.7 |
| Line | 535 | 49.0 | 10.8 | 82.1 | 8.0 | 97.8 | 52.8 | 203.4 | 52.2 | 7.1 | 2.8 | 0.6 | 2.7 |
| Wide-Line | 120 | 43.0 | 9.6 | 57.0 | 8.0 | 88.8 | 51.7 | 166.6 | 49.0 | 5.6 | 2.9 | 0.5 | 2.8 |
| Right-Angle | 334 | 52.0 | 9.9 | 74.1 | 7.0 | 92.7 | 51.0 | 198.4 | 49.1 | 7.6 | 2.8 | 0.7 | 2.6 |
| Acute-Angle | 352 | 58.0 | 10.6 | 100.3 | 7.0 | 103.5 | 53.2 | 233.1 | 52.7 | 6.6 | 2.8 | 0.7 | 2.7 |
| End-Point | 823 | 63.0 | 13.5 | 131.2 | 10.0 | 104.3 | 54.6 | 256.4 | 53.9 | 9.2 | 2.7 | 0.9 | 2.5 |
| Corner | 2657 | 89.0 | 16.7 | 214.2 | 12.0 | 129.9 | 56.0 | 318.7 | 54.2 | 8.2 | 2.5 | 0.8 | 2.3 |
| L-Line | 233 | 43.0 | 10.8 | 75.8 | 8.0 | 99.3 | 51.6 | 208.4 | 49.6 | 7.0 | 2.8 | 0.6 | 2.7 |
| T-Junction | 757 | 67.0 | 11.9 | 110.8 | 8.0 | 119.3 | 53.0 | 238.2 | 51.5 | 7.1 | 2.7 | 0.7 | 2.6 |
| X-Junction | 49 | 27.0 | 7.3 | 26.4 | 6.0 | 84.6 | 50.8 | 176.0 | 50.6 | 3.8 | 2.6 | 0.3 | 2.6 |
| Y-Junction | 224 | 47.0 | 11.4 | 98.3 | 9.0 | 100.1 | 51.2 | 226.5 | 49.8 | 7.8 | 2.9 | 0.8 | 2.8 |

**Table B-11b – Statistics for Bright Center Pixel Masks in a 64×64 "White Noise" Image with $\mu=127$, $\sigma=35$**

| Class | # of Masks | Robustness | | | | Contrast | | | | Fisher distance | | | |
|---|---|---|---|---|---|---|---|---|---|---|---|---|---|
| | | Max | Mean | Var | Med | Max | Mean | Var | Med | Max | Mean | Var | Med |
| Edge | 601 | 58.0 | 11.0 | 89.3 | 8.0 | 98.7 | 53.7 | 198.5 | 52.3 | 7.0 | 2.8 | 0.7 | 2.7 |
| Line | 542 | 61.0 | 10.1 | 87.1 | 7.0 | 95.3 | 52.7 | 189.6 | 51.4 | 9.9 | 2.7 | 0.8 | 2.6 |
| Wide-Line | 127 | 39.0 | 9.1 | 55.1 | 7.0 | 95.4 | 50.6 | 217.7 | 50.8 | 6.5 | 2.8 | 0.5 | 2.7 |
| Right-Angle | 339 | 44.0 | 10.0 | 63.1 | 8.0 | 104.8 | 51.7 | 210.5 | 50.8 | 7.1 | 2.7 | 0.6 | 2.5 |
| Acute-Angle | 351 | 48.0 | 10.5 | 78.9 | 8.0 | 98.3 | 50.4 | 185.6 | 50.3 | 7.4 | 2.7 | 0.7 | 2.6 |
| End-Point | 841 | 66.0 | 12.8 | 121.5 | 10.0 | 115.0 | 53.7 | 254.8 | 52.4 | 11.2 | 2.6 | 0.9 | 2.4 |
| Corner | 2645 | 97.0 | 18.0 | 256.9 | 13.0 | 147.3 | 57.7 | 346.3 | 55.6 | 8.8 | 2.6 | 0.9 | 2.4 |
| L-Line | 235 | 41.0 | 9.9 | 68.5 | 7.0 | 86.1 | 50.5 | 175.8 | 49.1 | 6.6 | 2.8 | 0.6 | 2.6 |
| T-Junction | 730 | 63.0 | 11.6 | 101.6 | 8.5 | 114.3 | 52.6 | 227.1 | 51.2 | 7.7 | 2.7 | 0.7 | 2.6 |
| X-Junction | 62 | 24.0 | 6.8 | 28.7 | 5.0 | 78.7 | 46.5 | 128.9 | 46.4 | 5.0 | 2.8 | 0.5 | 2.7 |
| Y-Junction | 225 | 44.0 | 10.1 | 71.6 | 8.0 | 90.7 | 52.8 | 166.6 | 52.8 | 6.3 | 2.8 | 0.6 | 2.7 |

END

5-87

DTIC